PHASE BEHAVIOUR AND ASPHALTENE ONSET PRESSURE PREDICTION DURING GAS INJECTION IN OIL RESERVOIRS

BY

IFEANYI UCHE ALEX OGUAMAH
(S.I. No: 146841)

B.Sc. Chemical Engineering (FUTO) M.Sc. Petroleum Engineering (Ibadan)

A Thesis in Department of Petroleum Engineering,
Submitted to the Faculty of Technology

in Partial Fulfilment of the requirements for the Degree of

DOCTOR OF PHILOSOPHY

Of the

UNIVERSITY OF IBADAN

JUNE 10, 2019

CERTIFICATION

I certify that this work was carried out by Mr. I U A Oguamah in the department of Petroleum Engineering, University of Ibadan

.

…………………………………………
Supervisor
S. O. Isehunwa
B.Sc., M.Sc. Ph.D. (Ibadan)
Professor and Head Department of Petroleum Engineering
Faculty of Technology
University of Ibadan, Nigeria

DEDICATION

This work is dedicated to the Almighty God, the alpha and Omega, the beginning and the end. I also dedicate it to my late Father Mazi Cletus Abraham Oguamah, may God grant him eternal rest.

ACKNOWLEDGEMENTS

LIST OF TABLES

LIST OF FIGURES

TABLE OF CONTENT

ABSTRACT

Asphaltene Precipitation (AP), a major challenge in the petroleum industry, causes flow assurance issues in reservoirs, pipelines and flow lines. It is therefore important to properly characterise petroleum fluids and predict the conditions under which AP could be prevented. Many of the reported models used for predicting AP to achieve best reservoir and production management practices are rather complex for routine applications. This study was designed to develop a simple but accurate model for characterising petroleum fluids and predicting AP during gas injection into oil reservoirs.

A generalised model for predicting phase behaviour of multiphase systems having different energy states was derived using partition function principle. The model obtained was simplified for routine application to a three-parameter cubic Equation of State (EOS), which was used to characterise selected pure gases, binary mixtures, four crude oil samples (F1, F2, F3 and F4) and n-Pentane+Violanthrone-97 simulated oil (F5), to obtain pressure-temperature phase profiles. The Upper Asphaltene Onset Pressures (UAOP) were estimated under natural gas (0, 15, and 30wt %); carbon dioxide (CO_2) gas (10 and 20wt %) and nitrogen gas (N_2) injections (5wt %). Results were validated using published data, and compared with Soave-Redlich-Kwong (SRK), Peng-Robinson (PR) and the Perturbed Chain Statistical Associating Fluid Theory (PCSAFT) EOS. Data were analysed using ANOVA at $\alpha_{0.05}$.

The developed EOS accounted for the contributions of attractive, repulsive, and non-physical forces in the fluids. Predicted Pressure-Temperature profiles for pure gases compared well to SRK and PR, and matched experimental data with percentage error of 0.04%, 0.13% and 0.05% for nitrogen, carbon dioxide and butane, respectively. The phase envelopes generated for ethanol-benzene, benzene-hexane, hexane-ethanol and methane-propane also matched experimental data. Predicted pressure-temperature envelopes for the crude oils, gave an average deviation of ±0.03%, while the Pentane+Violanthrone-97 rich phase was stable between 16.62 and $65.95kN/m^2$ at 298K and 65.86 and $241.15kN/m^2$ at 338K. These predictions matched experimental data and the results obtained using PCSAFT EOS. Estimated UAOP were 30812.93, 38369.75 and $84947.83kN/m^2$ for F1 at 0, 15, and 30 wt.% natural gas injection, respectively; 52674.81, 59967.88 and $63829.68kN/m^2$ for F2 at 0, 10, 20 wt.% CO_2 gas injection, respectively and $38783.64 kN/m^2$ at 5 wt.% nitrogen gas injection. For F3 and F4 at no gas injection, predicted UAOP were 117094.58 and $63326.02 kN/m^2$, respectively; while 19788.77 and $49051.43kN/m^2$ were predicted for F5 at 10 and 20 wt. % CO_2 gas injections, respectively. Generally, UAOP increased with increasing proportion of injected gases and varied with reservoir fluid and type of injected fluid. There was no significant difference between predicted results and those obtained using the PCSAFT EOS.

A simplified model for characterising petroleum fluids and predicting Asphaltene precipitation was developed. The model achieved faster and better control of Asphaltene precipitation during gas injection operations in oil reservoirs.

Keywords: Asphaltene precipitation, Reservoir fluid modelling, Gas injection operations, Partition function principle.

Word count: 464

CHAPTER ONE

INTRODUCTION

1.1 General Statement

The problems of solids formation in reservoir fluids have been a major challenge in oil and gas production storage and transport. Solids formed in reservoir fluids can be summarized into three categories:

1) Hydrates

2) Wax

3) Aphaltenes

This study shall focus on Asphaltene precipitation in petroleum fluid systems as one of the categories of the solids depositions occurring in crude oil system. Hydrates form when water lighter molecules like Carbon dioxide, Ethane or methane are trapped inside water lattice contained in the reservoir fluid at temperatures close to freezing point of water, thereby forming a stable crystalline solid. Once a stable hydrate is formed, it can exist even at temperature far above freezing point of water. The long distance of travel and the magnitude of changes in pressure and temperature both during transportation of petroleum fluids and shutdown operations can promote hydrate formation. Although a very useful unconventional energy source, Hydrates possess a major problem to petroleum production and transport, the chemical method of inhibition is a widely applied method of mitigating hydrates. Three different types of hydrates identified in reservoir fluids are structure I II and H (Pedersen and Christensen, 2007). Structure I contains guest molecules, which are tiny molecules, contained in the pore cavities of the hydrate, these guest molecules include Carbon dioxide, Methane and Ethane (Ahmed, 2007). Structure II hydrates can contains larger guest molecules, like C3, iC4

and nC4 due to its possession of larger cavities possess larger cavities that can trap heavier gas. Structure H Consists of lighter hydrocarbon and other complex hydrocarbon molecules common in hydrocarbon fluids as guest molecules (Mehta and Sloan, 1996), sH hydrates also show a very high stability at a very wider temperature and temperature conditions than sI and sII. While the structure of sI and sII hydrates consists of cavities of small and large sizes, sH hydrates contains cavities of three different types namely the small, medium size and large sizes. Figure 1.0 indicates the cavity structure of the three different types of hydrates.

Wax are constituents from deposition of heavy paraffinic and branched paraffinic components of reservoir fluids. Similar to Hydrates, they can disrupt the flow of reservoir fluids travelling in pipelines and lower temperature thereby causing operational problems. The components are relatively soluble in liquids. These solubilities are dependent on temperature conditions (Ahmed, 2001). Wax solid precipitation can occur in wells in production facilities and in pipelines.

The behaviour of Asphaltene is difficult to define and study and the challenge Asphaltene precipitation and deposition poses is usually observed in nearly all areas of the petroleum production and storage systems, including reservoir, wellhead, pipelines and process and storage facilities. There has been numerous studies done in areas of Asphaltene thermodynamics, structural characteristics, depositional behaviour, mitigation and economics. These studies however, do not effectively give solutions to the Asphaltene problem, rather more question are generated in oil and gas mixtures
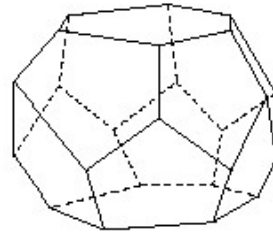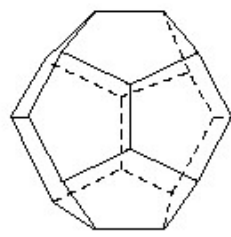
Structure I
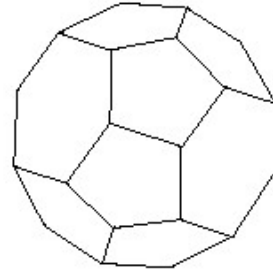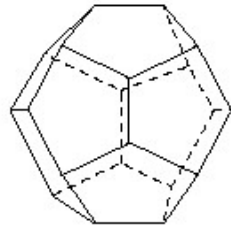
Structure II
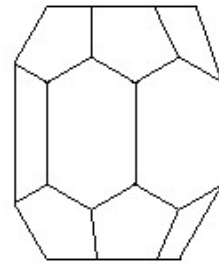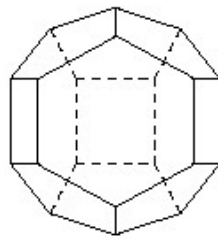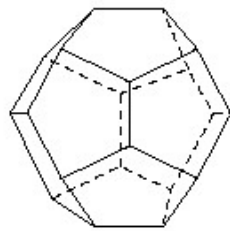
Structure H

Figure 1.1: Cavity Structure for hydrates

This work suggests a method for predicting the thermodynamic behaviour of Asphaltene in petroleum fluid system by determining the Asphaltene Precipitation Envelope (APE).

It is assumed that when phase changes occur in the bulk oil system, the oil mixture can undergo a phase separation precipitating solid Asphaltene phase from the bulk liquid, also, the different states exist in the system at equilibrium with little interaction. The Statistical multistate theory was developed from statistical mechanics, and was used to suggest model equations for studying the behaviour of solid precipitation in petroleum fluids, as temperature and pressure changes occur. The model was further extended to polymer systems to study Asphaltene behaviour during precipitation. In the extension of the model to polymer systems, the fluid is assumed to consist of a pure solvent phase and a polymer phase. Petroleum reservoir fluids consists primarily of hydrocarbons like; Alkanes, which includes; Methane, Ethane, Propane, Cyclo-Butane, Cyclo-Pentane, etc. Alkenes which includes Ethylene Propene and Butene, others include, Alkynes Aomatics, Cyclic-Aromatics and Organometallics. Hydrocarbon fractions containing seven or carbon atoms greater than seven are referred to as C7+ and the bulk of the component of the C7+ are atoms are called the C7+ fraction (Pedersen and Christensen, 2007). Petroleum is usually divided into four classes namely: Saturates, Aromatics, Resins and Asphaltenes.

Alkanes and most cyclo alkanes are referred to as saturates, while Long-chain n-alkanes (C_n >20) are known as waxes and they are the fraction of petroleum that causes the greatest economic losses in oil recovery because they tend to form crystalline structures upon cooling, leading to the clogging of pipelines, (Merino- Garcia, 2004).
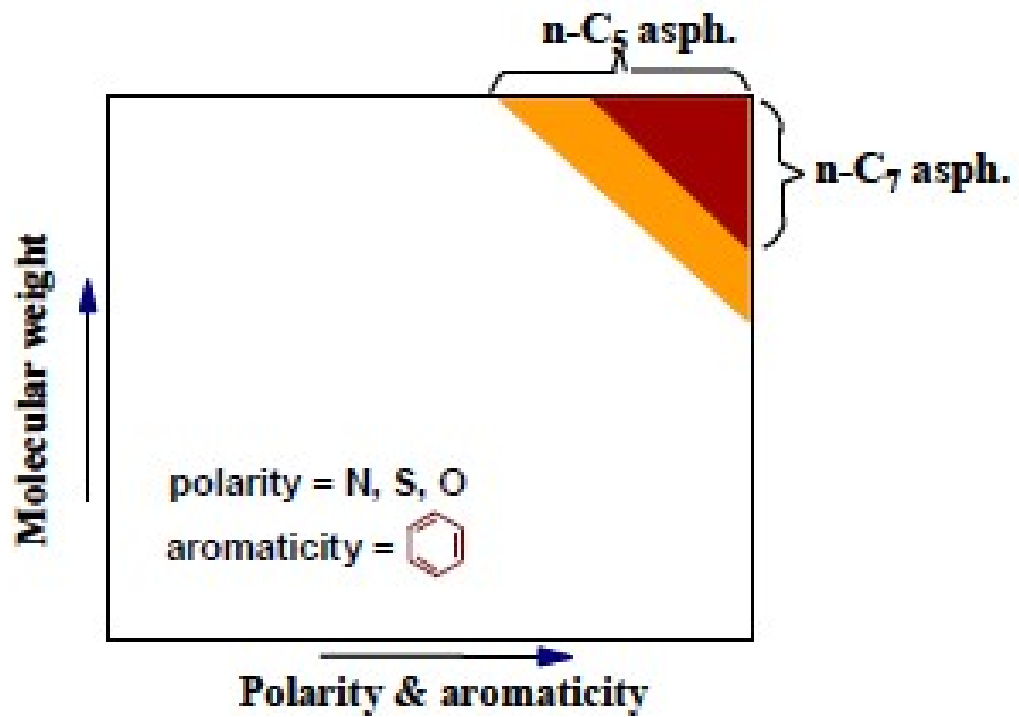
Figure 1.2: "Long Diagram" shows the Relationship Between Molecular weight and Polarity or Aromaticity of Petroleum fluids Fractions. (Long, 1981)

Aromatics contains cyclic structures with double carbon to carbon bonds Benzene C_6H_6 is the most common component of aromatics, other components include toluene and phenol. Saturates and aromatics constitutes the majority in petroleum fluids. The concentration ranges from 50 to 90 wt% (Speight, 1999).

Asphaltenes and resins are very complex solid component of petroleum fluids; they are usually high boiling materials with metals contents and heteroatoms like Nitrogen, Oxygen and sulphur

The most common definition of asphalting is explained by the IP 143 standard (1985) which describes the Asphaltene constituent in a reservoir fluid as the "weight percentage the petroleum material without wax and insoluble in n alkanes like heptane but remains soluble in aromatic solvent (Toluene)". The reason for the high solubility of Asphaltene in toluene is due to the small difference in their solubility parameter, while Asphaltene solubility parameter (δ) is (19-22 Mpa) that of Toluene is estimated at 18.2 MPa, therefore, Asphaltene are insoluble in n-alkanes due to the large difference in solubility parameter (15.2 for n-heptane). This current definition of is somehow incomplete, firstly because little is revealed about the constituent of the Asphaltene structure which is estimated to consist of over 100,000 compounds. (Ting, 2003, Merino-Garcia, 2004). Secondly, Asphaltene deposition may be because of pressure depletion, (Klein *et al.,* 2005). Studies have shown that Asphaltene caused by pressure drop are richer in Sulphur and oxygen containing compounds. (Aquino-Olivos *et al.,* 2003), Studied differences in structures of live oil derived from Asphaltene and that derived by atmospheric titration. The study was based on performing a size exclusion chromatography test to both cases of Asphaltene, Study results showed significant changes in the structures of both cases of Asphaltene it also pointed out that there are structural differences between Asphaltene derived by atmospheric titration derived investigated these differences. FITR tests carried to determine the structures and composition of Asphaltene showed that Asphaltene derived by high-pressure filtration had significant differences in their compositions, it submitted that

Asphaltene obtained by high pressures filtration contains more functional groups than those obtained by normal precipitation (Vaidier, 2000). However, most studies show that Asphaltene molecules are poly dispersed and capable of association under certain conditions, it contains heteroatoms and compounds like PNA, aliphatic and moieties (Strausz *et al.,* 1992). Furthermore, Asphaltene contain large molecular weight when compared to other compounds contained in petroleum fluid mixtures (Aromatics, Resins and Saturates) In general, aromaticity and function group play important role in characterising the nature of Asphaltene, Asphaltenes by their average physical properties (Spiecker *et al.,* 2003). There are different methods for the determination of the composition of Asphaltene; these include IR, NMR, ESR, Spectrometry and X-ray, for the determination of the arrangement of Asphaltene molecular structures, (Mansoori *et al.,* 2001). Other methods include, combustion elemental analysis, for the determination of H/C, N, S containing compounds, inductively coupled mass spectrometry for the determination of V, Ni, Fe, present, Fourier Transform infrared spectroscopy for determining the concentration of polar functional group. The study of solid precipitations and depositions in crude oil has been in focus over the past few decades due to the challenges it poses in the development and production of offshore fields; with growing demand for energy there has been an increase in search for oil at the deep and ultra-deep regions of the world. Therefore, more recent hydrocarbon based energy solution sources face a lot of flow assurance issue of which Asphaltene deposition is one of such; Asphaltene deposition is seen during enhanced recovery by CO_2, this may be as a result of wettability alteration in the reservoir during injection, this will consequently lead to plugging of the reservoir pore spaces, affecting fluid production.

Table 1.1: Some Elements Contained in Asphaltenes and Their Values.

Element	weight%
H/C atom	1.0 - 1.2
Nitrogen	1.0 – 1.2
Sulphur	2.0 – 6.0
Oxygen	0.8 – 2.0
Vanadium (ppm)	100 -300

(Spiecker *et al.,* 2003)

Since Asphaltene are non-crystalline, composed mainly of complex hydrocarbon and the most polydispersed mixture of the heavy, polarizable fraction of reservoir fluid, therefore, Asphaltene precipitation can occur because of changes in reservoir properties due to reservoir depletion or addition of injectant to the reservoir (Mirzayi *et al.*, 2012). Asphaltene deposition involves settling of Asphaltene to the reservoir rock walls or to pipelines during production, it is different from precipitation, which is the separation of solid asphaltene from the liquid phase in the hydrocarbon equilibrium system. Asphaltene precipitates from the liquid phase into solid, Asphaltene precipitation poses little worry to production, their problem lies in their tendency to come together, form colloid, and coagulate into aggregates.

1.1.1. Molecular Weight

Different techniques are used in estimating the molecular weight of Asphaltenes, these includes: light scattering, Osmometric methods, Ebullioscopy, Cryoscopy Spectroscopy, Sedimentation Equilibrium, gel permeation chromatograph, refractive index, Viscometery. The molecular weight of Asphaltenes has been controversial for several decades and largely depends on the experimental method used in the determination. Different methods of molecular weight determination have agreed on the size and structure of Asphaltene, but in recent times further debate on whether Asphaltene are monomeric (single constituent molecule of a polymer) or polymeric (consisting of repeated units) are ongoing, (Mullins, 2005). Although earlier studies on Asphaltene molecular weight showed, it has a molecular weight of about 1000 g/mol, more recent studies suggests a molecular weight values greater than 1000g/mol (Storm and Sheu, 1995). (Groenzin and Mullins, 1999) studied the size of Asphaltene molecules by drawing a strong comparison between Asphaltene molecules and the size of chromophores, further establishing that the bulk Asphaltene molecule consists of one or two chromophores per molecules. (McCaffrey *et al.*, 2003) suggested a molecular weight between

3000-5000 g/mol this was based on the pyrolysis experiment on Asphaltenes, they presented molecules with layered fused sheets connected by alkyl branches

1.1.2. **Dipole Moment**

The dipole moment is a function of the molecular arrangement, composition and size of the Asphaltene molecule. In terms of composition, it is a measure of polarity of the functional groups and metallic element. The amount heteroatom present in a mixture has direct effect on its polarity and the polarity of Asphaltene varies based on the alkane fraction used in its precipitation (Nalwaya *et al.*, 1999), (Goual and Firoozabadi, 2000).

1.1.3. Density

 The density of Asphaltene varies with the experimental procedure used in its determination and the source of the Asphaltene containing fluid. Studies have shown that petroleum and coal based Asphaltenes have a density range of 0.98 - 1.2 g/cm^3 (Panuganti, 2013), the density of Asphaltene also varies with origin and proposed structure of the Asphaltene molecule. (Strausz *et al.*, 1992) calculate the density of Asphaltene in oil sand bitumen to obtain a value 0.98 g/cm^3, while the proposed structure of the Arabian light/ Medium derived asphaltene proposed by (Nomura *et al.,* 1998) gave a density of 1.06 g/cm^3.
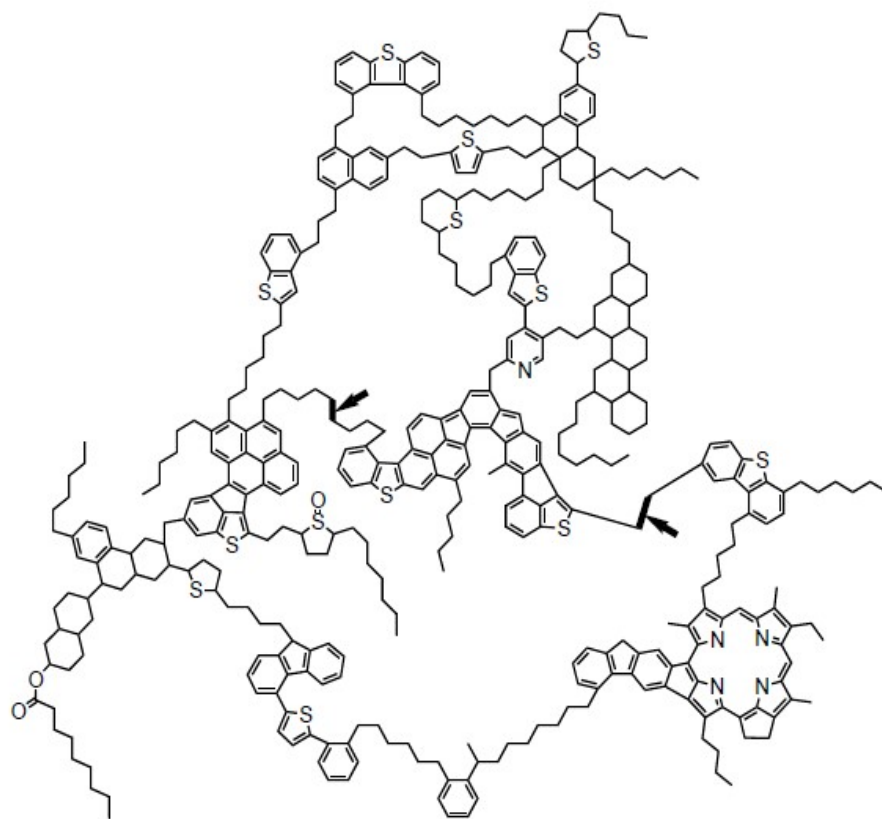
Figure. 1.3a: A model of Asphaltene molecule proposed by (Strausz *et al.*, 1992)
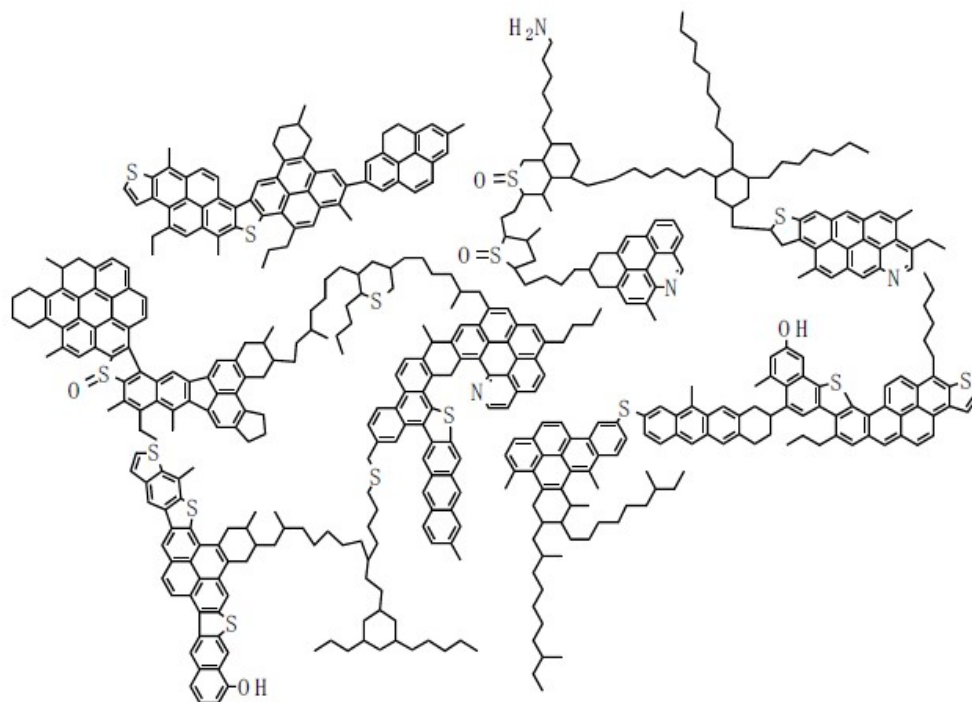
Figure. 1.3b: A model molecule derived by (Nomura *et al.*, 1998) for Arabian Light/ Medium asphaltene

1.1.4. Diffusion

Asphaltene diffusion coefficient is dependent on the size of the Asphaltene aggregates, since they are large molecules, the smaller molecular heteroatoms it contains tend to diffuse faster than the large molecules, (Sane *et. al.*, 1994). Fewer amount of Asphaltene association occurs at lower concentrations, but there is an increase in the levels of association as concentration increases until critical size is achieved. The degree of association also increases with increasing particle size and decreasing diffusion coefficient (Panuganti, 2013).

1.1.5. Interfacial Characteristics

Interfacial Tension (IFT) is very important in determining Asphaltene precipitation onset in reservoir fluids. (Sheu *et al.*, 1992) showed that the discontinuous point observed when, surface tension was plotted against Asphaltene concentration signifies the existence of critical micelle concentration. The appearance of the critical micelle concentration implies that Asphaltene show similar surfactant properties. The CMC is an important characteristic of a surfactant. It is the point in surfactant concentration where additional increase in concentration will cause formation of micelle in an Asphaltene solvent mixture. This also means that Asphaltene will exhibit lower interfacial tension as it approaches the CMC, Varying the concentration of Asphaltene will increase or decrease the interfacial characteristics of the Asphaltene solvent mixture (Maini *et al.*, 1993), (Bauget *et al.*, 2001), (Panugueti, 2013).

Both surfactant and Asphaltene are absorbed to the surface of oil water interface, in an emulsion, with surfactant arriving to the oil water interface first due to its small molecular size.

1.1.6. Viscosity

The viscosity of oil tends to increase during Asphaltene precipitation this creates challenges of transportation and processing of petroleum fluids (Chakma *et al.*, 1994). The presence of solid particles in a reservoir fluid will cause changes in its flow behaviour; in most cases, there is increased resistance to flow of the reservoir fluid (Mousavi-Dehghani *et al.*, 2004). When Asphaltene precipitation occurs, particle interaction further bring about formation of random clusters of varying shapes and sizes, (Luo and Guo, 2007) thereby affecting the viscosity of a reservoir crude oil. As the change in the behaviour of the reservoir fluid occurs due to temperature or pressure changes there can be an increase or decrease in Asphaltene precipitation. In summary, an increase in the portion of precipitated Asphaltene in heavy oils leads to increased viscosity in the oil (Mansoori, 1998).
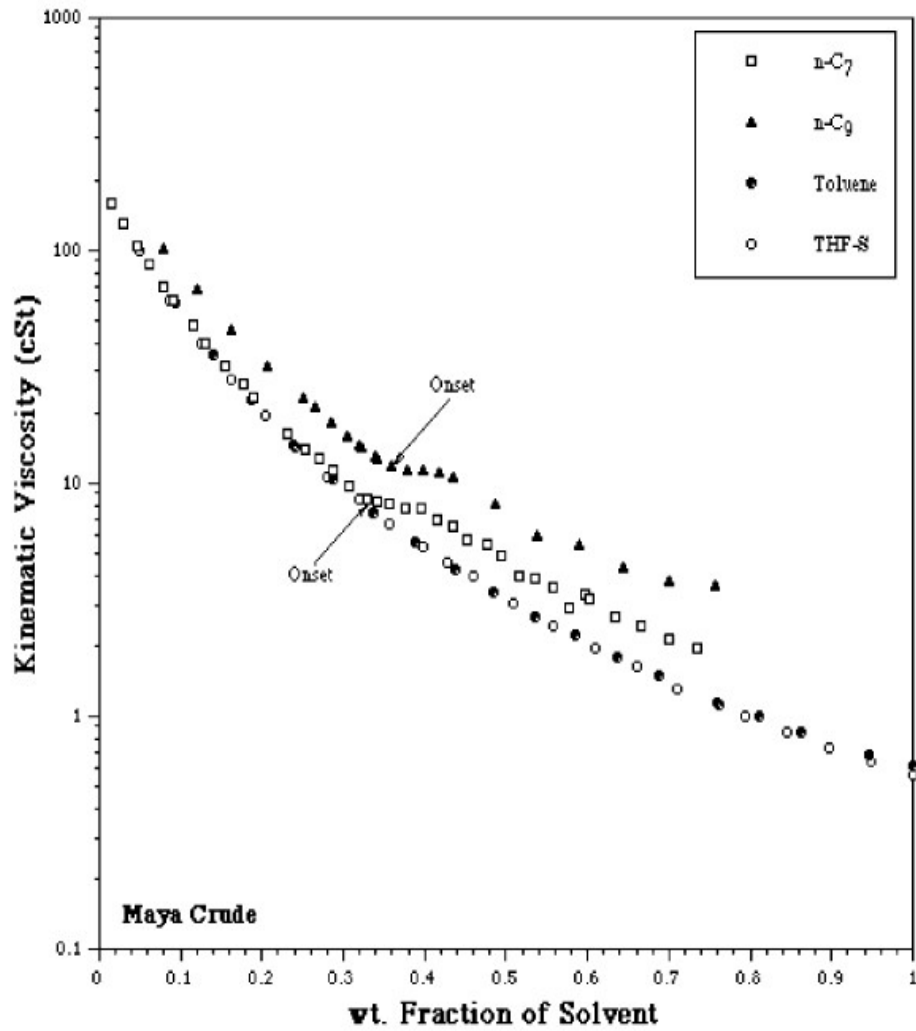
Figure: 1.4 A Plot showing the relationship between viscosity and weight fraction of crude oil dissolved nC7, nC9, Toluene and Tetrahydrofuran. (Mousavi-Dehghan, 2004).

1.1.7. Solubility

When studying the solubility of asphaltene, the solubility parameter becomes an important tool for determining asphaltene solubility characteristics. Scatchard- Hildebrand as defines the solubility parameter, δ as:

$$\delta \equiv c^{1/2} = \left[\frac{\Delta_{vap}u}{v}\right]^{1/2} \quad \text{........ (1.1)}$$

Where $\Delta_{vap}u$ is the change in energy because of isothermal vaporization of the saturated liquid to the ideal gas state and C is the cohesive energy density.

The stability of Asphaltene contained in petroleum fluids is affected by factors including pressure, temperature and composition of oil, largely because of the decrease in the value of the solubility parameter oil during such changes (Panuganti, 2013).

1.1.8. Refractive Index

There is a relationship between the refractive index and the Asphaltene precipitation onset, when London forces is the major force responsible for precipitation and aggregation of Asphaltene. The difference between the value of the refractive index of a sample of petroleum fluid and the value of the refractive index observed for the asphaltene is a measure of the Asphaltene stability in the oil (Buckley *et al.*, 1999). The London dispersion forces are usually weak intermolecular forces and is determined by the relationship between the wavelength and the refractive index, which is mathematically expressed as.

$$\delta = \left(\frac{\sqrt{3}\pi}{384}\frac{hv_c}{\sigma^3}\right)^{1/2}\frac{\sigma}{V/N_o}\frac{n^2-1}{\left(n^2+2\right)^{3/4}} \quad \text{........ (1.2)}$$

Where V is the molar volume and σ is the hard sphere diameter. The refractive index usually lies with a range of 1.54-1.74 when estimated with equation (1.2).The refractive index of a

mixture equals the sum of the individual indexes of compound that constitute the mixture, this rule does not applies to mixture when Asphaltene precipitation occurs (Wattana *et al*., 2007). (Weast, 1987) determined how the solubility parameter relates with the RI for normal alkanes and aromatic hydrocarbon can be determined, (Barton, 1991) by approximating the exponent of ¾ in equation (2) to unity (Buckley *et al*, 1998).

$$F_{RI} = \frac{n^2 - 1}{n^2 + 2} \ldots\ldots (1.3)$$

The stability or instability of Asphaltenes in a solvent mixture depends on its intricate relationship with resins. (Lira-Galeana *et al.*, 2004), gives the definition of resins as the part of petroleum fluid strongly adsorbed to surface-active materials like clay, alumina, or silica while pyridine, carbon disulphide, toluene and methanol mixtures can be used in its desorption. Asphaltene tend to strongly associate with resins, this association determines the extent to which they will remain soluble in petroleum fluids, (Koots and Speight, 1975).

1.1.9. Asphaltene Deposition

Understanding of the depositional process of Asphaltene will result in an improved crude oil production, (Mansoori, 1997). The amount of deposition depends largely on the composition of hydrocarbons present in the oil. (Lin et al, 1954) suggested a predictive model for Asphaltene deposition under turbulent conditions. Many studies have been carried out in other to identify processes responsible for Asphaltene deposition (Newberry and Baker, 1985), (Kim *et al*., 1994), (Pan and Firoozabadi, 1997), numerous studies are still ongoing to further shed light on the mechanism of Asphaltene deposition.

1.1.10. Polydispersivity Effects

Asphatenes remain in equilibrium as heavy organics dispersed in the liquid phase, the degree to which Asphaltene disperses in petroleum fluids relies majorly on the chemical nature of the oil (Kawanaka *et. al.*, 1991). A slight change in the stability of the polydispersed oil mixture will cause deposition of asphaltene (Mansoori, 1996), factors that can contribute to the upset in the stability of the oil mixture include, temperature, pressure and composition. when n-alkane component is added to an Asphaltene containing oil mixture, the resins which stabilises Asphaltene in the mixture dissociates thereby making it possible for the Asphaltenes to self-aggregation (Aske, 2002), (Wu *et al.*, 1998), (Eduardo, 2004). Kokal *et al,* (1992) further stated that as the molecular weight of hydrocarbon in petroleum fluids increases, the quantity of Asphaltene precipitate decreases. The changes in asphaltene precipitation behaviour due to temperature changes has not been clearly defined, while some school of thought hold the degree of aggregation of Asphaltene molecules decreases due to a decrease in the solvation ability of petroleum fluids, other studies have suggested that the aggregate size of Asphaltene will decreases with an increase temperature (Aske, 2002). Pressure depletion alone can cause asphaltene precipitation and maybe the major cause of asphaltene deposition in reservoir and wellhead (Eduardo *et a.l,* 2004), (Verdier, 2006).

1.1.11. Steric Colloidal Effect:

Nellenstyen (1924) proposed the steric colloidal effect by suggesting that asphaltene exists as aggregates peptized by resins and dispersed in a hydrocarbon medium. Asphaltene self-association usually occurs as the n-alkane content of the petroleum fluid increases, thereby separating from the oil phase to form an aggregate (Mousavi-Delghani *et al.*, 2004), the stabilization of Asphaltene aggregates in solution by resins and the stability of the aggregated Asphaltenes relies on the resin concentration in the mixture.

1.1.12. Aggregation effect:

As the concentration of peptizing agent (resins) in oil mixture decreases, the reduction in the concentration of the resins adsorbed to Asphaltene surface, will cause the Asphaltenes to flocculate and form aggregates (Buenrostro-Gonzalez *et al.*, 2004). Study on these aggregates shows that they are irreversible and follow a growth pattern. (Park and mansoori, 1988a);

1.1.13. Electrokinetic Effect

Due to the polar nature of petroleum fluids, (Mansoori, 1997) Suggested that asphaltene deposition is due to the electrical potential developed by the wall of the pipeline and the colloidal heavy organic flowing through it. (Nalwaya *et al.*, 1999) pointed out the relationship between the polarity of Asphaltene particles and the heteroatoms and metal contents. The electro kinetic effect is of great importance during oil transport because while the other effects are considered under static conditions of petroleum fluid, the electro kinetic effect is because of charged particles flow a long a wall (Behruz *et al.*, 2013).

1.1.14. Micellization

The thermodynamic model developed by Victorov and Firoozabadi, (1996) to predict the formation of Asphaltene in petroleum fluids, suggests that micellization which is a self-association procedure, can occur when there is a surface acting agent in crude oil. These surface acting agent known as surfactants assemble into geometric shapes and remain suspended in solution (Priyanto *et al.*, 2001). The experimental investigation done by (Rogacheva *et al.*, 1980) explains certain behaviour of Asphaltene in toluene, suggesting that more Asphaltene micelles will form, as there is an increase in the concentration of Asphaltene present in toluene.

1.2. THEORIES OF ASPHALTENE BEHAVIOUR IN PETROLEUM FLUIDS

There are numerous laboratory investigations on the behaviour of Asphaltenes in petroleum fluids (Hirschberg *et al.*, 1984), (Andersen, 1995), (Ting, 2003). These studies have shown that, in light oils pressure contributes majorly to Asphaltene precipitation especially near the bubble point region, at pressures above the bubble point line, an increase in pressure will cause an increase in the solubility of Asphaltenes in crude oil.

1. In propane-deasphalting process, (Ali and Al-Ghannam, 1981) observed a rise in the quantity of precipitated Asphaltene with temperature increase. However, the reverse is the case for asphaltene dispersed in paraffin solutions, as temperature increases will reduce amount of precipitated asphaltene.

2. Asphaltene molecules undergo self-association or association with resins, while resin-to-resin association is not possible, Asphlatene-Resin association causes asphaltene stability in mixtures. (Prausnitz *et al.*, 1998).

3. The dilution ration can also effect the precipitation of Asphaltene, although Asphaltene precipitation is assumed an irreversible process (Hirschberg *et al.,* 1984), some thermodynamic arguments suggest that asphaltene reversibility is possible in the presence of excess solvent (Prausnitz *et al.*, 1998).

The nature of asphaltene in petroleum fluids is usually described by two opposing views as pointed out by Verdier (2005). the first view (the colloidal theory) suggests that asphaltene exits in the petroleum fluid as colloids dispersed in the liquid phase and stabilized by resins while another view (the solution theory) suggests that Asphaltene exists in crude oil as dissolved solutes and dispersed in the liquid phase. Numerous studies have been done to validate each theory and the solution theory cannot adequately explain the stabilization of asphaltene by resins**.**

The behaviour of asphaltene in solution is best described by the molecular solution theory, which suggests that the stability of Asphaltene in oil as solution and the separation of the oil (solvent) and Asphaltene (solid) phase when Asphaltene precipitation occurs. This approach has found use in different literature, which includes the Flory-Huggins-(FH) theory, Flory-Huggins-Goldstein theory, Scatchard-Hildebrand equation, Statistical Association Fluid Theory (SAFT) and thermodynamic colloidal Theories. Most models in literature are based on a combination of these theories, for instance the micellar approach suggests that Asphaltene in aromatic solvents, crudes and aromatic/alkane mixtures form micelles. This approach suggests that the micelles formed by asphaltene molecules remains stable in crude oil and it can precipitate upon the attainment of a critical concentration when the concentration of asphaltene monomers reaches a critical concentration which causes the solubility of the monomer concentration to be lower than the solubility of the Asphaltene micelles (Wu *et al.*, 1998). Studies have shown that Asphaltene micelles form when crude oil contains excess hydrocarbon. (Priyanto *et al.*, 2001), described different stages in Asphaltene association, suggesting that at concentrations above CMC Asphaltene in solution will self-associate, as concentration further increases the self-associated Asphaltene will form coacervate and a continuous increase in concentration will result in the formation of Asphaltene aggregates. Asphaltene micelle formation shares structural similarity with surfactant systems (Sheu and Mullins, 1995). Thermodynamic Micelle based models or micellar approach, are useful in explaining the relation between resins concentration and Asphaltene precipitation.

1.3. ASPHALTENE AND THE PETROLEUM INDUSTRY.

Asphaltene deposition possess a lot of challenge to the petroleum industry, especially in the area of oil production and refining, the severity of this challenge is worsen by the lack of proper and detail understanding of the behaviour, nature, composition and structure of asphaltenes. Asphaltene deposition causes increase in the cost of petroleum production, transport and processing (Carpentier *et al.*, 2007), (Mansoori, 1998), (Pineda-Flores *et al.*, 2001), (Vadier, 2006) summarised the problems caused by Asphaltene precipitation and deposition as the following:

1.3.1. Extraction/ Recovery: When deposition occur in the reservoir the asphaltene tend to clog the pore space of the reservoir porous rocks thereby reducing recovery and causing wettability alterations in the reservoir. Experimental studies have shown that CO_2 and Natural gas injections into petroleum reservoirs generally tends to promote asphaltene precipitation and deposition by altering the composition of the reservoir fluids. (Escobedo and Mansoori, 1995a), (Mousavi-Dehghani *et al.*, 2004), (Janier *et al.*, 2013).

1.3.2. Transport: Asphaltene deposition in most cases occur in pipes, as a results of blending of different streams of petroleum with different composition (Verdier, 2006) or flow of reservoir fluids under conditions that promotes asphaltene depositions. The effect constitutes problem to flow of petroleum in pipelines and risers

1.3.3. Processing: Asphaltenes cause catalyst deactivation, which causes unstable products and increased laydown of coke on the catalyst. (Bartholdi and Andersen, 2000) also Asphaltene containing petroleum fluids require more specialized and expensive catalytic hydrocracking methods in other to increase petroleum product yield, (Leon, 2012).

1.3.4. Economics: The Desirability of exploiting and producing an oil field is sometimes affected by the presence of asphaltenes its reservoirs. Most crudes with high Asphlatene content are usually referred to as heavy or low quality crude and possess low market demand.

1.3.5. Environment: Asphaltene form stable emulsions in surface separation equipment, making oil water separation difficult, these emulsion has negative impact to the environment when they a discharged. (Stephenson, 1997). Another source of environmental concern is the chemical solvents used in the industry for dissolving Asphaltene, although very effective in treatment of Asphaltene deposition problems, these solvent poses lots of health safety and environmental concerns as a result of the chemical nature. (Okafor *et al.*, 2014), also these solvent inhibitors are non-bio-degradable and highly flammable (Lalit and Achala, 2012). The continual use of these solvent has raised lots of safety compliance issues and environmental agitations. This prompted further research in "Green solvents" in other solves certain environmental and health concerns posed by the solvents.

1.4. Asphaltene precipitation Envelope

The Asphaltene precipitation envelope is a temperature-pressure profile diagram showing the regions of Asphaltene formation in a reservoir. The envelope indicates the relationship between the quantities of precipitated Asphaltene with temperature or pressure changes. The upper Asphaltene onset pressure usually occurs at higher pressure than the saturation pressure and is pressure at which Asphaltene precipitation is first observed. The amount of precipitated Asphaltene reaches a maximum as the saturation pressure gradually decreases beyond the saturation pressure until the pressure reaches the lower Asphaltene precipitation pressure. The Asphaltene precipitation envelope shows the thermodynamic path that must be followed to minimize or avoid Asphaltene precipitation (Ahmed, 2007)
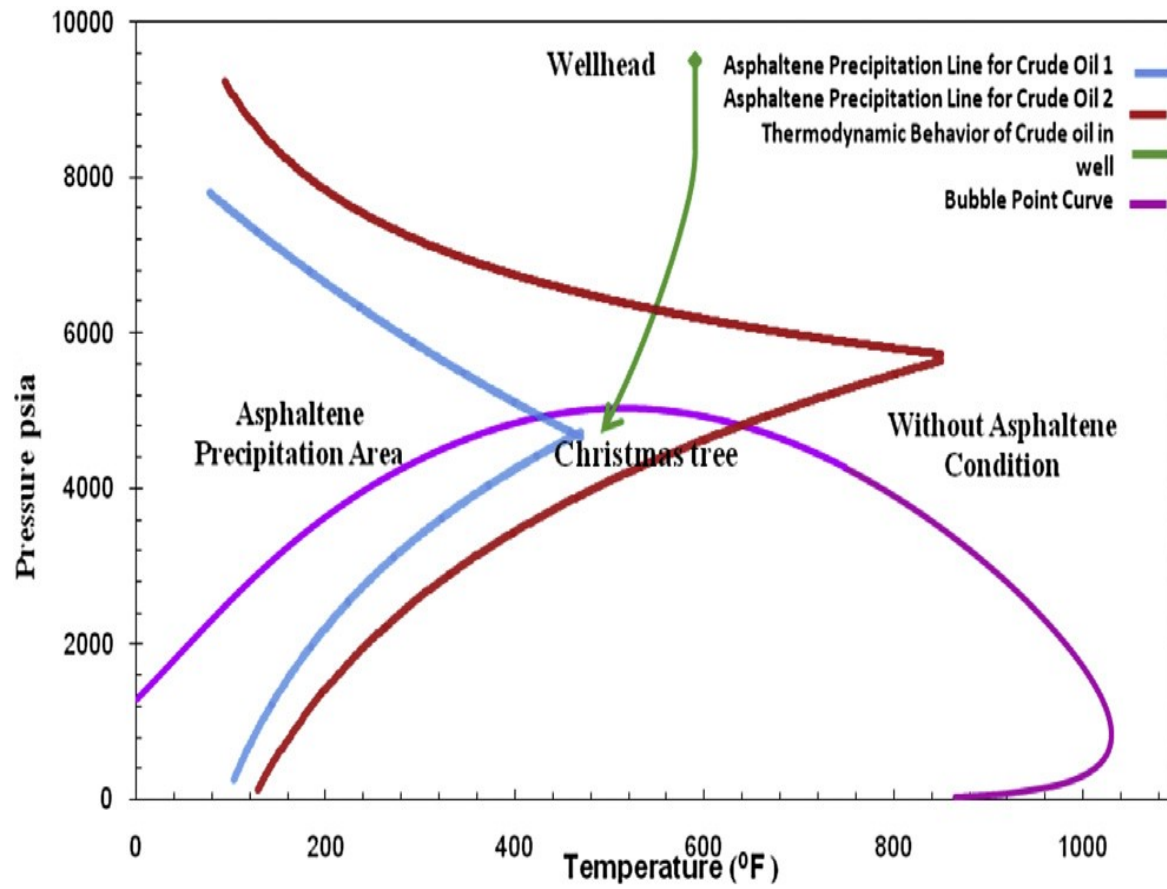
Figure 1.5. Asphaltene Precipitation Envelope (APE) for two oil samples during Production (Hasanvand *et al.*, 2015)

1.5 EQUATION OF STATE FOR SOLIDS

The challenges usually associated with developing equation of state for solids arise from the inability to explicit define a method of solid formation. Solid can form by association, precipitation, crystallization and micellization. Asphlatene exhibit polymer characteristics being derived from association of basic hydrocarbon units. In reservoir, fluids most solid precipitates are usually modelled using mostly equation of state for polymers. There is a number of equation of state for polymers used to model Asphaltene behaviour; the equation of state is broadly classified as:

Cubic Equation of State: These Include (Wenzel and Schmidt, 1980) Yokozeki equation, Sako-Wu-Prausnitz equation, Cubic plus association by Kontogeorgis, Wong Sandler mixing rule, Linear Combination of Vidal and Michelsen (LCVM), etc.

The Cell Models: Prigogine cell model (PCM), Flory-Orwoll-Vrij (FOV), Pertubed Hard Chain Theory.

Lattice fluid models: Flory Huggins (FH), Sachez-Lacombe (SL) Equation, Costas and Sanctuary Equation (C&S), (Panayiotou and Vera, 1982), Mean Field Lattice Gas (MFLG)

Hole model: Sima-Somcynsky EOS (SS), and Tangent Sphere model. Generalised Flory Theory, Statistical Associated Fluid Theory, Perturbed Hard Chain Theory. Some of `these equations shall be discussed briefly in subsequent pages.

The focus of this study will be on formulation of equation of state with ability to study solid-liquid- vapour systems, this will involve a simple operational research analysis procedure, which includes problem definition, model development, problem solution, and data collection, and data interpretation, application of result to the study and discussion of solution.

1.5.1 A Single Equation for a Three Phase Solid -Liquid -Gas System Based on Hole Model

For a system with N-identical non interacting atoms or molecules the total energy of the system can be partitioned based on the contributions from the different energy parameter that determine the different state of the physical system.

$$E_j = \sum_j E_j^i = E_j^{trans} + E_j^{ns} + E_j^{rot} + E_j^{vib} + E_j^{e} ....(1.1)$$

The partition function can be written as:

$$Z = \sum g_i e^{-E_j/K_B T} ....(1.2)$$

Where g_i is the degeneracies of each state.

Therefore, the total partition function of an N- non-interacting system of atoms and molecules may be written in relation to the partition function of the individual state of the molecules as:

$$Z = \prod_i Z^i = Z^{trans} \times Z^{ns} \times Z^{rot} \times Z^{vib} \times Z^{e} ....(1.3)$$

Initially at solid state the molecules rotate about a fixed point until energy introduced to the system causes the molecules to vibrate, thereby causing the one dimensional rotational degree of freedom to become three dimensional vibrational degree of freedom. The energy of solids changes from rotational energy to vibrational energy.

$$E^{solid} = E^{rot} + E^{vib} ....(1.4)$$

Therefore:

$$Z^{solid} = \sum_i \left(Z^{rot} + Z^{vib} \right) ....(1.5)$$

The energy of rotation is

$$E_j^{rot} = \frac{J^2}{2I} = \frac{J(J+I)h^2}{2I} = J(J+1)B........(1.6)$$

$$B = \frac{h^2}{2I} \text{ is called the rotational constant}$$

J is the quantum number

I is the moment of inertia.

For each value of J, the rotational degeneracy $g_i = (2i+1)$

Therefore, the partition function can be expressed as

$$Z_{rot} = \sum_{i=1}^{N} g_i e^{-E_i/K_B T} = \sum_{i=1}^{N} (2i+1) e^{-j(j+1)B/K_B T} ....(1.7)$$

For a vibrating body, we assume that each atom of solid is an independent 3D harmonic oscillator, having same frequency. The Energy of the oscillating atom can be expressed as:

$$E_v = \sum_{n=1}^{\infty} \hbar v_E (n+1/2)........(1.8)$$

Where

$$v_E = \sqrt{\frac{k}{m}} \text{ is the frequency}$$

hv_E = quantum Energy.

h= planck's constant

n= 0,1,2,3….

Therefore, the partition function for a vibrating atom of solid is

$$Z_{vib} = \sum_{i=1}^{\infty} \exp(-BE_v)........(1.9)$$

$$= Z_{vib} = \sum_{i=1}^{\infty} \exp\left[-\beta\hbar v_E\left(n+1/2\right)\right]\dots\dots(1.10)$$

$$Z = e^{-\beta h v_E/2} \sum e^{-\beta n h v_E}\dots\dots(1.11)$$

Since:

$$\sum_{n=0}^{\infty} (-\beta\hbar v_E)^n = \frac{1}{1-\beta\hbar v_E}$$

$$Z_{vib} = \frac{e^{-\beta h v_E/2}}{1-e^{-\beta h v_E}}\dots\dots(1.12)$$

Note: $\beta = 1/k_B T$

1.5.2 The gas phase Contribution

For a gas of N particle in a volume, the total energy can be expressed as

$$E(P,U) = \frac{1}{2m}\left(P_x^2 + P_y^2 + P_z^2\right) + U(x,y,z)\dots\dots(1.13)$$

In the case of an ideal gas, the potential energy is zero, therefore U=0

The equation can be written as

$$E(P,U) = \frac{1}{2m}\left(P_x^2 + P_y^2 + P_z^2\right)\dots\dots(1.14)$$

For an N particle system the Partition function becomes:

$$Z_1 = \frac{1}{N!h^{3N}} \int d^3 q_n \int d^3 p_n e^{-\beta H}\dots\dots(1.15)$$

Therefore a one particle system, the partition function becomes:

$$Z_1 = \frac{1}{h^3} \int d^3q \int d^3 p_n e^{-E(p)/K_B T} \quad \text{........(1.16)}$$

Integrating over momentum P:

$$\int d^3 pe^{-p^2/2mK_B T} = \left(\int dp_x e^{-p_x^2/2mk_B T} \right)\left(\int dp_y e^{-p_y^2/2mk_B T} \right)\left(\int dp_z e^{-p_z^2/2mk_B T} \right) \text{........(1.17)}$$

The integral over position produces volume V

$$Z^{gas} = V \left[\frac{2\pi mk_B T}{h^3} \right]^{3/2} \text{........(1.18)}$$

Where m= particle mass.

1.5.3 Liquid phase Contribution

The following assumption is made:

1. Liquid is a compressed gas.

2. The liquid phase is a transition between solid and gas phase and therefore the thermodynamic properties will be intermediate between its solid and gas component (Eyring, 1977).

3. Molecule sized holes are assumed to be abundant in the solid state which will confer fluid like properties on the solid.

4. An increase in the fluidized vacancies increases the chances of molecules to become less solid.

5. Liquid is a compressed gas and therefore during compression the vacant holes are replaced by molecules, thereby causing gas molecules to act as liquids.

Assumptions: (3) and (4) leads to the identification of three significant structures (Eyring et al, 1977)

1. Molecules with solid like degree of freedom

2. Fluidized vacancies propelled through the solid converting three vibrational degree of freedom to three translational degree of freedom simulating gas behaviour.

3. Positional degeneracies due to the presence of vacant sites for the solid like molecules

While assumption (1) and (3) identifies a fourth structure:

4. Molecules moving to fill vacancies thereby creating intermolecular bonding energy and causing reduced localized loosening of structure and improving liquid like behaviour of structures.

Let

V_g = the total gas volume

V_l = liquid volume.

The degrees of freedom for the liquid system becomes V_l / V_g

and that of gas becomes: $(V_g - V_l) / V_g$

The Energy of compression can be written as:

$$E_s * V_l / V_g$$

E_s = energy of sublimation.

As a molecule fill fluidized vacancy, it exerts a force of attraction a_t on the neighbouring molecules nearest to it. Therefore, the pressure it exerts on the neighbouring molecules becomes:

$$P = \frac{a_t}{n_m}$$

Where:

P= intermolecular pressure

n_m= Number of neighbouring molecules

Since most liquids assume a closed packed structure, n_m should be ≤ 12

Therefore, the partition function of a normal liquid based on the assumptions can be expressed as

$$Z^{liquid} = \left\{1-e^{-E_s/k_BT}\right\}^{-1} e^{-E_s/k_BT/2} \times \left[n_m e^{a_{t/n_m} \times \frac{1}{k_BT}}\right] N\left(V_g - V_l\right)/V_g \times \left[\frac{2\pi m k_B T}{h^3}l\right] \times \frac{V_l}{V_g} \times \frac{\left(V_g - V_l\right)N}{V_g}! \dots\dots(1.19)$$

l= the distance of a molecule to a vacancy.

Therefore the total partition function for a three phase system becomes:

$$\left(Z_{rotational} + Z_{vibrational}\right) + Z^{liquid} + Z^{gas} \dots\dots(1.20)$$

$$Z_N = \sum_{i=1}^{N}(2i+1)e^{-j(j+1)B/K_BT} + \frac{e^{-\beta hk/2}}{1-e^{-\beta v_k}} + \left\{1-e^{-E_s/k_BT}\right\}^{-1} e^{-E_s/k_BT/2}\left[n_m e^{a_t/n_m \times \frac{1}{k_BT}}\right] N\left(V_g - V_l\right)/V_g \times \left[\frac{(2\pi m k_B T)^{3/2}}{h^3}l\right] \times \left[\frac{V_l}{V_g}\right] \times \frac{\left(V_g - V_l\right)N}{V_g}! + V\left(\frac{2\pi m k_B T}{h^3}\right)^{3/2} \dots\dots(1.21)$$

$$Z_n = \left\{Z_1 + Z_2\right\} + Z_3\left(n_m e^{a_t/n_m \times \frac{1}{k_BT}}\right) N\left(V_g - V_l\right)/V_g \times \left[\frac{V_l}{V_g}\right] \times \frac{\left(V_g - V_l\right)N}{V_g}! + Z_4 V \dots\dots(1.22)$$

Where:

$$Z_1 = \sum_{i=1}^{N}(2i+1)e^{-J(J+1)B/K_BT}$$

$$Z_2 = \frac{e^{-\beta h v_E/2}}{1-e^{-\beta h v_E}}$$

$$Z_3 = \frac{e^{-\beta h v_E/2}}{1-e^{-\beta h v_E}}\left(\frac{2\pi m k_B T}{h^2}l\right)^{3/2}$$

$$Z_4 = \left(\frac{2\pi m k_B T}{h^2} \right)^{3/2} V.$$

From the classical definition of energy, the total energy of the system becomes

$$\langle E \rangle = -\frac{\partial \ln Z_n}{\partial \beta} \ldots\ldots\ldots(1.23)$$

The Helmholtz Energy of any system can be expressed as:

$$A = \langle E \rangle - TS = -k_B T \ln Z \ldots\ldots(1.24)$$

Where <E> is the total energy of the system

S is the Entropy of the system.

Combining Equation (1.3) and (1.24)

$$-k_B T \ln Z_n = -k_B T \ln \left(Z_1 \times Z_2 \times Z_3 \times Z_4 \right)\ldots\ldots(1.25)$$

$$-k_B T \ln Z_n = -k_B T \left(\ln Z_1 + \ln Z_2 + \ln Z_3 + \ln Z_4 \right)\ldots\ldots(1.26)$$

$$A_n = A_1 + A_2 + A_3 + A_4 \ldots\ldots(1.27)$$

Where the A_n is the total Helmholtz energy of the system.

1.5.4 The Perturbed Chain Statistical Association Fluid Theory

There are different approaches to describing molecular fluid thermodynamic behaviour, these approaches include, the Perturbation Theory, Tangent Sphere model, Lattice model, Hole model, Molecular simulation, Scaled Particle Theory, Partition function Theory,

The Cell and Lattice Models provide different adaptations of compressible lattice model of solid polymer while incorporating compressibility in a different manner. The hole model combines both methods of incorporating compressibility introduced by cell and lattice fluid, it

assumes that molecular sized holes exist in a solid state and an increased number of holes will confer fluid like properties to the solids, also during compression vacant holes are replaced by molecules, thereby causing gas to act as liquid. Perturbation theory is a useful tool in many branches of physics and statistical mechanics of classical fluids. In perturbation theory, the fluid structure is characterised by a set of distribution functions brought about by expanding a fluid about the same properties of its reference fluid. One of the earliest application of perturbation theory can be seen in the assignment of parameters to VDW EOS in order to account for the two major interacting components namely, the high-density repulsion and the low-density attraction.

$$P = \frac{\rho T}{1 - \rho / \rho_s} - a\rho^2 ....(1.28)$$

Where ρ_s is the saturation density, "a" is the intermolecular attraction, P refers to pressure of the system while T is temperature of the system.

In recent times Perturbation theory have been widely applied to classical associating fluids in other to understand their thermodynamic behaviours (Wertheim, 1983)

Perturbation theory has also found a wider application in both the industry and in research for instance in the thermodynamic perturbation for hard sphere fluids (Baker and Henderson, 1967), or in the thermodynamic modelling of flexible chain by applying Wertheim first order perturbation theory (Wertheim, 1984), (Wertheim, 1986a), (Wertheim, 1986b). Wertheim had previously derived a formulation of statistical thermodynamics based equations, which can model molecular systems with strong directional attractive forces and associating systems (Wertheim, 1984). The Thermodynamic First Order Perturbation theory (TPT1) was later derived based on the calculation of the residual Helmholtz free energy over a reference system at a given temperature and density, assuming that the reference system

consists of molecules with only repulsive potential interaction (Wertheim, 1986). The first order perturbation is applicable to flexible chain molecules and is generalised as

$$\left(\frac{p}{\rho k_B T}\right)_{hsc} = 1 + r^2 b \rho g\left(d^+\right) - (r-1)\left[\rho \frac{\partial \ln g\left(d^+\right)}{\partial \rho}\right] \ldots\ldots(1.29)$$

Where: $g\left(d^+\right)$ radial distribution function of hard sphere at contact and can be calculated from the Canahan-Starlings equation r is the number of tangent sphere and b is the second virial coefficient of hard sphere before chain formation.

Wertheim suggested the Statistical Associated Fluid Theory (SAFT), for describing the thermodynamic behaviour of associating fluid. The basis for the development of the SAFT was the sequential expansion of the Helmholtz energy about an integral molecular distribution function and the inherent association capability (Chapman et. al, 1989). Wertheim considered the perturbation expansion of the monomer and hard sphere liquid volume to determine the free energy contribution due to bonding (Ting, 2003). This resulted in an association between the excess Helmholtz energy of association, the energy formed because of formation of adjacent molecular chains and a function related to the segment-to-segment interaction.

SAFT EOS is usually expressed as the total sum of the systems Helmholtz energies.

$$a^{res} = a^{seg} + a^{chain} + a^{assoc} \ldots\ldots(1.30)$$

Where, a^{seg} is the residual energy contribution as a result of interaction of adjacent segments, a^{chain} refers to contribution due to formation of adjacent chains, a^{res} refers to site-site interaction of segments while a^{assoc} refers to the association energy contribution. Equation (3) can further be expressed for a fluid mixture as

$$\frac{A^{res}}{RT} = \frac{A^{seg}}{RT} + \frac{A^{chain}}{RT} + \frac{A^{assoc}}{RT} = m\frac{A_0^{hs}}{RT} + m\frac{A_0^{disp}}{RT} + \frac{A^{chain}}{RT} + \frac{A^{assoc}}{RT} \ldots\ldots(1.31)$$

$A_0{}^{hs}$ refers to hard sphere (HS) contribution while $A_0{}^{disp}$ represent the dispersion contribution term, m refers to the number of segment and is expressed as:

$$m = \sum x_i m_i \text{.......}(1.32)$$

Where x_i the pure component is segment composition and m_i is the pure component segment number.
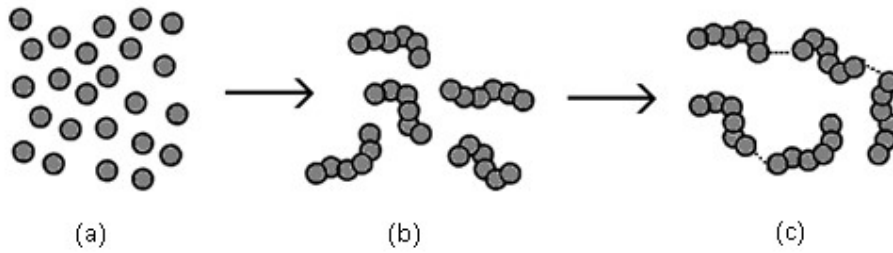
Figure 1.6: The behaviour of spherical Structure as suggested by SAFT EOS (Ting, 2003)

The association energy contribution is defined as:

$$X_A = \left[\sum_j \sum_{Bj} \rho_j X^{B_j} \Delta^{A_i B_j} \right]^{-1} \text{........}(1.33)$$

Where M represents number of sites in a molecule capable of associating, X^A represents number of unbounded molecules to site A , ρ_j is the molar density of molecules $\Delta^{A_i B_j}$ is the association strength, the association strength is defined as

$$\Delta^{AB} = 4\pi F^{AB} d^3 g(d)^{seg} k^{AB} \text{........}(1.34)$$

Where F^{AB} is expressed as:

$$F^{AB} = \exp\left(\varepsilon^{AB} / T\right) - 1 \text{........}(1.35)$$

The Helmholtz energy due to chain formation can be expressed as:

$$\frac{A^{chain}}{RT} = \sum_i X_i \left(1 - m_i\right) \ln\left(g_{ii}\left(d_{ii}\right)^{hs}\right) \quad \text{.......(1.36)}$$

Where m_i refers to the segments number of component i, g_{ii} refers to the radial distribution function (RDF).

Mansoori Canaghan Sterling Equation of State (MCSL-EOS) suggested the HS contribution to Helmholtz energy.

$$\frac{A_0^{hs}}{RT} = \frac{6}{\pi\rho}\left[\frac{\zeta_2^3 + 3\zeta_1\zeta_2\zeta_3 - 3\zeta_1\zeta_2\zeta_3^2}{\zeta_3\left(1-\zeta_3\right)^2} - \left(\zeta_0 - \frac{\zeta_2^3}{\zeta_3^2}\right)\ln\left(l - \zeta_3\right)\right] \quad \text{.........(1.37)}$$

$$\text{Where } \zeta_k = \left(\frac{\pi}{6}\rho\right)\sum x_i m_i d_{ii}^k \quad \text{........(1.38)}$$

And

$$d_{ii} = \sigma_i - 0.12\sigma_i \exp\left(-3\varepsilon_i / kT\right) \quad \text{........(1.38b)}$$

Here σ_i refers to the diameter of segment of component i while d_{ii}^k is the temperature dependent segment diameter, ρ refers to the number density of the segment. (Gross and Sadowski, 2001) in order to account for non-hard chain fluids introduced the dispersion contribution

$$\frac{A^{disp}}{RT} = \frac{A_1}{RT} + \frac{A_2}{RT} \quad \text{........(1.39)}$$

$$\frac{A_1}{RT} = -2\pi\rho I_1\left(\eta, \bar{m}\right) m^2 \varepsilon\sigma^3 \quad \text{........(1.40)}$$

$$\frac{A_2}{RT} = -2\pi\rho\bar{m}C_1 I_2\left(\eta, \bar{m}\right) m^2 \varepsilon^2\sigma^3 \quad \text{........(1.41)}$$

C_1 is the compressibility term and is expressed as:

$$C_1 = \left(1 + \bar{m} \frac{8\eta - 2\eta^2}{(1-\eta)^4} + (1-m)\frac{20\eta - 27\eta^2 + 12\eta^3 - 2\eta^4}{\left[(1-\eta)(2-\eta)\right]^2} \right) \quad........(1.42)$$

$$m^2 = \sum_i \sum_j x_i x_j m_i m_j ....(1.43)$$

Simple mixing rule are used for the determination of component segment diameter σ, and the paired interaction potential ε.

$$\varepsilon^2 \sigma^3 = \left(\frac{\varepsilon_{ij}}{kT} \right) \sigma_{ij}^3 ....(1.44)$$

$$\varepsilon^2 \sigma^3 = \left(\frac{\varepsilon_{ij}}{kT} \right)^2 \sigma_{ij}^3 ....(1.45)$$

$$\sigma_{ij} = 0.5\left(\sigma_i + \sigma_j \right) ....(1.46)$$

$$\varepsilon_{ij} = \left(1 - k_{ij} \right)\left(\varepsilon_{ii} \varepsilon_{jj} \right)^{\frac{1}{2}} ....(1.47)$$

When considering square well interaction I_1 and I_2 become functions of molecular volume and number of segment and functions of temperature when considering soft repulsion interaction (Gross and Sadowski, 2001).

$$I_2 = \frac{\partial}{\partial \rho} \left[\rho \int_1^\infty \tilde{u}(x)^2 \, g^{hc}\left(m; x\frac{\sigma}{d} \right) x^2 dx \right] ....(1.48)$$

A_1 and A_2 refers to the contributions to dispersion energy A_0^{disp}. The dispersion contribution shall further be investigated and a possible modification of equation (4.13) suggested.

1.5.5   The Dispersion Contribution To Perturbed Chain-SAFT Equation Of State

Helmholtz Energy is represented by the equation

$$A = -k_B T \ln Q ....(1.49)$$

In fluids composed of N identical molecules, the potential function Q can be written as

$$Q = \frac{1}{N!}\left(\frac{q}{V}\right)^N_{Z_N} \quad \text{........(1.50)}$$

Therefore, the Helmholtz energy can be written as:

$$A = -k_B T \ln \frac{1}{N!}\left(\frac{q}{V}\right)^N_{Z_N} \quad \text{........(1.51)}$$

V denotes the system volume; q is the molecular partition function, which contains different energy contributions, translation, rotation, etc. of a simple independent molecule. From the first other perturbation theory, a potential energy function can be split into

$$U_N = U_0 + \zeta U_P \text{........(1.52)}$$

Where U_0 is the energy function, which is solvable by statistical mechanics and ξU_p is the perturbation, ξ is the coupling parameter, the partition function can be expressed as;

$$Q(\zeta) = \frac{Z_N(\zeta)}{N!\Lambda^{3N}} = \frac{1}{N!\Lambda^{3N}} \int .... \int e^{-B(U_0+U_P)} dr_1 dr_2 ... dr_N \text{........(1.53)}$$

$$\text{Where: } Z = \sum_{N=0}^{\infty} \exp^{-\beta(U_0+U_P)} \text{........(1.54)}$$

Differentiating the Helmholtz energy function with respect to ξ gives:

$$\frac{\partial A}{\partial \zeta} = \frac{-kT}{Q}\frac{\partial Q}{\partial \zeta} = \frac{T_r\left\{\dfrac{\partial u(\zeta)}{\partial \zeta}e^{-\beta U(\zeta)}\right\}}{Tr_c\left\{e^{-\beta U(\zeta)}\right\}} = \left\langle\frac{\partial U(\zeta)}{\partial \zeta}\right\rangle = \langle U_r \rangle \zeta \text{........(1.55)}$$

Where

$$\text{Tr}_c = \int \partial r_1 \ldots \partial r_N \ldots\ldots(1.56)$$

Integrating of ξ from 0, corresponding from the reference system to 1

$$\langle U_1 \rangle_\zeta = \sum_i \sum_{j>i} \phi\left(\left|\overline{r}_i - \overline{r}_j\right|\right) \to \frac{1}{2} \int d^3 r' \phi\left(\left|\overline{r} - \overline{r}\right|\right) \rho(\overline{r}) \rho(\overline{r}') \ldots.(1.58)$$

The Helmholtz free energy is expressed with respect to perturbation pair potential as:

$$A = A_0 + \frac{1}{2} \int d^3 r \int d^3 r' \phi\left(\left|\overline{r} - \overline{r}\right|\right) \rho(\overline{r}) \rho(\overline{r}') \ldots\ldots(1.59)$$

For homogenous fluids, the first order perturbation can be written thus:

$$A = A_0 + \frac{\rho N}{2} \int dr \phi_1(r) g_0(r) \ldots\ldots(1.60)$$

Where g(r) is the radial distribution function, in order to approximate $g_0(r)$ is introduced as the scaling parameter r to scale the size of the test parameter where r(x)referred to as the test function (Sengers, 2000) such that r(x)=1 for x>0 for the upper limit and r(x)=0 for the lower limit.

Therefore:

$$\beta \frac{A}{N} = \ln\left(\rho \Lambda^3\right) + 4\pi\rho \int_0^1 g(r) r^2 \partial r \ldots\ldots(1.61)$$

Methods for solving the radial distribution function include:

1. Molecular Simulation: Molecular dynamics and Monte-Carlo simulation

2. Integration-differential method

3. Ornstein -Zernike / Percus-Yevick approximations

The equation can be solved by applying Ornstein-Zernike approximation to equation (1.60)

$$h_{ij}(r) = c_{ij} + \sum_{k=1}^{m} \rho_k \int c_{ik}(|\vec{s}|) h_{kj}(|\vec{r} - \vec{s}|) d\vec{s} \ldots\ldots(1.62)$$

Which approximates to

$$h(r) = c(r) + \rho \int c(|\vec{s}|) h(|\vec{r} - \vec{s}|) d\vec{s} \ldots\ldots(1.63)$$

And the Percus-Yevick approximation for radial distribution function

$$g_{ij}(r) = \exp\left[-\frac{U_{ij}(r)}{k_B T}\right] [g_{ij}(r) - c_{ij}(r)] \ldots\ldots(1.64)$$

to yield the compressibility and the virial forms respectively as equations 1.67 and 1.68

$$\frac{PV}{Nk_B T} = \frac{1 + \eta + \eta^2}{(1+\eta)^3} \ldots\ldots(1.67)$$

$$\frac{PV}{Nk_B T} = \frac{1 + 2\eta^2 + 3\eta^3}{(1-\eta)^3} \ldots\ldots(1.68)$$

(Carnahan and starling, 1969) showed that for HS fluids the hard sphere compressibility can be calculated from the equation

$$Z_p^{cs} = (1 + \eta + \eta^2 + \eta^3)(1-\eta)^{-3} \ldots\ldots(1.69)$$

(Mansoori et al, 1971) equation suggested a relationship between the compressibility in both compressible and virial form.

$$Z_p^{cs} = \frac{1}{3}(2Z_p^c + Z_p^v) = \frac{(1 + \eta + \eta^2 + \eta^3)}{(1-\eta)^3} \ldots\ldots(1.70)$$

(Kolafa and Nezbeda, 1987) imposed the second viral term to obtain equation of hard sphere compressibility as

$$\frac{PV}{Nk_BT} = \frac{1+\eta-\eta^2-2\eta^2/3-2\eta^4/3}{(1-\eta)^3} \quad\ldots\ldots(1.71)$$

Applying the equation yields the form

$$\frac{\beta A}{N} = \log(\rho\Lambda^3)-1+\frac{1+\eta-\eta^2-2\eta^3/3-2\eta^3/3}{(1-\eta)^3}+2\pi\rho\beta\int_0^\infty g_0(r)\,dr\,r^2\phi_1\ldots\ldots(1.71)$$

Integrating gives:

$$\frac{\beta A}{N} = \log(\rho\Lambda^3)-1+\frac{1+\eta-\eta^2-2\eta^3/3-2\eta^3/3}{(1-\eta)^3}+2\frac{\pi}{3}\rho\sigma\beta\varepsilon\lambda\ldots\ldots(1.72)$$

$$\lambda = \left(1+\frac{\delta}{\sigma}\right)^3-1\ldots\ldots(1.73)$$

σ = Diameter of the Sphere

δ =Range of attraction

Equation of dispersion can be written as

$$A^{disp} = A_0^{disp} + A_p^{disp}\ldots\ldots(1.74)$$

$$A^{disp} = \frac{2\pi}{3}\sum_i\sum_j x_i x_j \varepsilon_{ij}\sigma_{ij}^3\beta\lambda + \log(\rho\Lambda^3)-1+\frac{1+\eta-\eta^2-2\eta^3/3-2\eta^3/3}{(1-\eta)^3}\ldots\ldots(1.75)$$

1.6 Modelling Of Hydrocarbon Systems Using PC-SAFT

1.6.1 Parameters for PC-SAFT Equation of State

Modelling fluid behaviour using PC-SAFT involves the use of pure component parameters, the pure component parameters include: the segment number (m), Segment diameter σ, and energy interaction parameter ϵ/k, the parameter were initially obtained by regressing the vapour fraction and liquid densities of fluid.

The parameters used in this study were obtained from (Gross and Sadowski, 2001), for alkanes and iso-alkanes; (Ting, 2003) and (kouskoumvekaki et al, 2004), for polymers; (Huang and Radosz, 1990) for polynuclear aromatcs. their studies have shown that the PC SAFT component parameters show similarity with compounds of same structure and can be calculated from their average molecular weight.

Table 1.2 SAFT parameter correlations for different classes of hydrocarbons

	n-Alkane	PNA	Benzene Derivatives
M	$0.0253MW + 0.9263$	$0.0139MW + 1.2988$	$0.0208MW + 0.9136$
σ	$(3.369MW^{0.0271})$	$(0.0597MW + 4.2015)/m$	$(0.0901MW + 3.1847)/m$
ε/k	$132.11MW^{0.1221}$	$119.4\ln(MW) - 230.21$	$40.059\ln(MW) + 101.18$

The correlations makes it possible to develop parameter- molecular weight plots which is useful in determining the parameters of higher molecular weight substance which are largely composed waxy solids at room temperature, and whose vapour pressure and liquid density are difficult to determine.

We therefore test the applicability of PC-SAFT EOS on a range of fluid, we applied the PC-SAFT EOS on model fluid mixtures, and we test the ability of EOS to model short chain hydrocarbon system, long chain hydrocarbon- solvent systems, glyme-solvent system, and polymer-solvent system and crude oil systems.
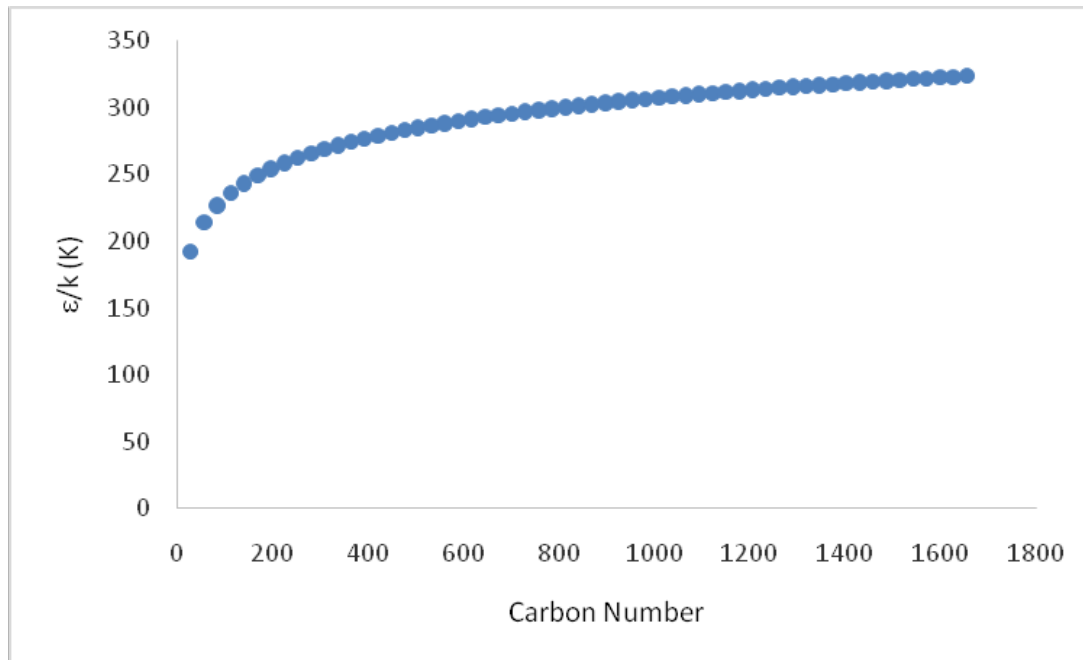
Figure 1.7(a). PC-SAFT Pure Component Energy Interaction Parameters versus Carbon Number for n-alkane Series
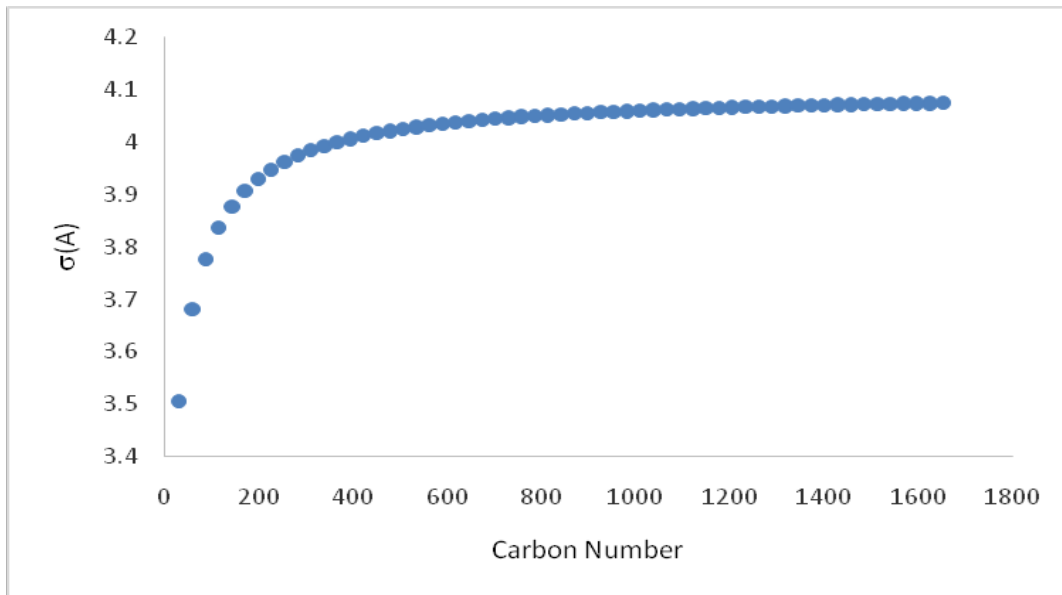
Figure 1.7 (b). PC-SAFT Pure Component Segment Diameters versus Carbon Number for n-alkane Series
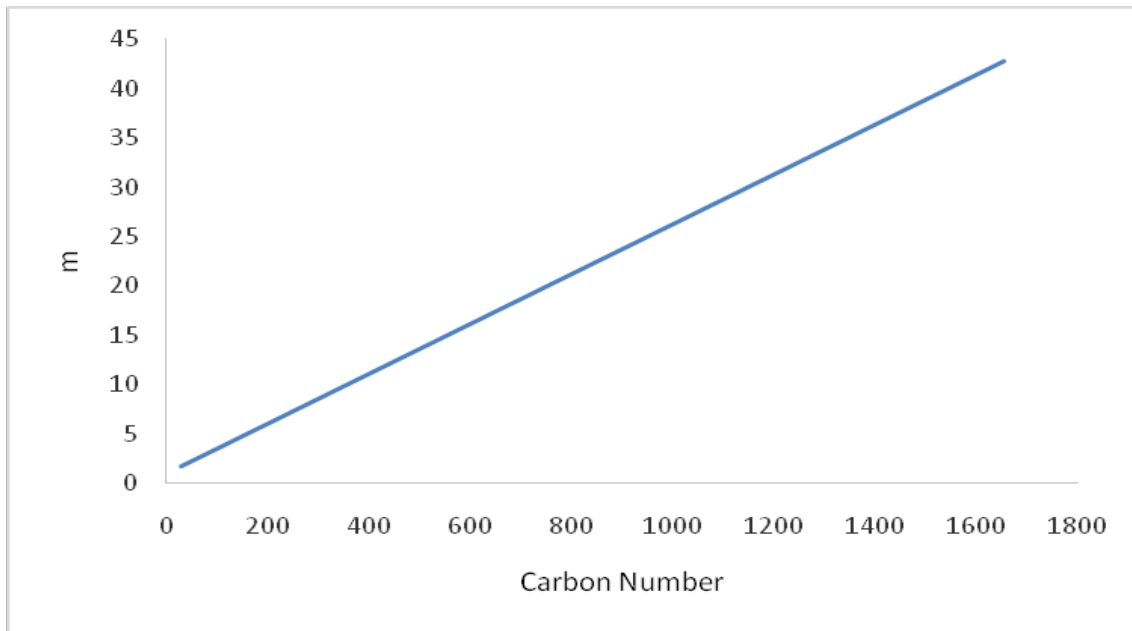
Figure 1.7 (c). PC-SAFT Pure Component segment number versus Carbon Number for n-alkane Series

1.6.2. SHORT CHAIN HYDROCARBON MIXTURES

Short chain normally exists as gaseous or liquid compounds, with simple weak dipole to dipole bond this investigation aims to the determine the ability of PC SAFT to model phase behaviour of short chain alkane mixture, therefore its ability to model lighter ends of hydrocarbon fluids. The UNIQUAC and Soave-Redlich-Kwong equation of states were applied for comparison. The PC-SAFT parameters used in this study were acquired from (Gross and Sadowski, 2001), the tests were conducted at standard conditions. The choice of the UNIQUAC and Soave-Redlich-Kwong (SRK) EOS is because of their frequent application to industrial processes and in describing phase equilibria, consisting of two parts, the UNIQUAC equation of state can be expressed as

$$\ln \gamma_i = \ln \gamma_i^C + in\gamma_i^R \quad ....(1.76)$$

Where:

$$\ln \gamma_i^C = \left(\frac{g^E}{RT}\right)_{Combinatoral} = x_1 \ln \frac{\phi_1^*}{x_1} + x_2 \ln \frac{\phi_2^*}{x_1} + \frac{z}{2}\left(x_1 q_1 \ln \frac{\theta_1}{\phi_1} + x_2 q_2 \ln \frac{\theta_2}{\phi_2}\right) ....(1.77)$$

Is the combinatorial contribution and the residual term is written as:

$$\ln \gamma_i^R = \left(\frac{g^E}{RT}\right)_{residual} = -x_1 q_1 \ln\left(\theta_1 + \theta_2 \tau_{21}\right) - x_2 q_2 \ln\left(\theta_2 + \theta_1 \tau_{12}\right) ....(1.77b)$$

The segment fraction ϕ is given as

$$\phi_1^* = \frac{x_1 r_1}{x_1 r_1 + x_2 r_2} \qquad \phi_1^* = \frac{x_1 r_1}{x_1 r_1 + x_2 r_2} ....(1.78)$$

While the area fractions are given as

$$\theta_1 = \frac{x_1 q_1}{x_1 q_1 + x_2 q_2} \qquad \theta_2 = \frac{x_2 q_2}{x_1 q_1 + x_2 q_2} ....(1.79)$$

Where r, q and q' represent the molecular structure constants for pure fluids. The parameters τ_{12} and τ_{21} are expressed in terms of characteristics energy interaction parameters as,

$$\tau_{12} = \exp\left(-\frac{\Delta u_{12}}{RT}\right) \equiv \exp\left(-\frac{a_{12}}{T}\right) \quad ....(1.80)$$

$$\tau_{21} = \exp\left(-\frac{\Delta u_{21}}{RT}\right) \equiv \exp\left(-\frac{a_{21}}{T}\right) \quad ....(1.81)$$

The SRK Equation of state is expressed as:

$$P = \frac{RT}{v-b} - \frac{\alpha a}{v(v+b)} \quad ....(1.82)$$

The attractive and co-volume parameters are obtained from the relationship

$$a = 0.427480 \frac{R^2 T_c^2}{P_c} \quad ....(1.83)$$

$$b = 0.086640 \frac{RT_c}{P_c} \quad ....(1.84)$$

The constant α is dependent on acentric factor and temperature

$$\alpha = \left[1 + S\left(1 - \sqrt{Tr}\right)\right]^2 \quad ....(1.85)$$

S is a function of acentric factor and can be derived from the regression of vapour pressure data.

The equation can be applied to mixtures by applying the following combination rule

$$\alpha a = \sum\sum x_i x_j \alpha_{ij} a_{ij} \quad ....(1.86)$$
$$b = \sum x_i b_j \quad ....(1.87)$$

The parameter $\alpha_{ij} a_{ij}$ can be expressed as:

$$\alpha_{ij}a_{ij} = \sqrt{\alpha_i\alpha_j a_i a_j \left(1 - C_{ij}\right)}........(1.87)$$

The constant C is zero for the study carried out.

Each of the Equation of State was fitted to mixture of short chain alkane at 273K to determine the VLE properties.

The UNIQUAC model gives a good fit for Toulene+Ethane system, at given pressures and it achieved accuracy even when parameters are set at 1 but fails in butane+ Hexane system. This suggest that the UNIQUAC model may not be effectively predictive in alkane systems, although (Coutinho, 1998) suggested a predictive UNIQUAC model for describing solid liquid equilibria, also the model shows instability at higher pressure. With the SRK EOS a good fit is obtained for n-butane + Hexane system at given pressures, the system interaction parameter k_{ij} was set at 1, and it also achieved a near accuracy even at higher pressures. Therefore SRK EOS does better job for short hydrocarbon liquid systems than, the UNIQUAC model.

Comparison of PC-SAFT with SRK EOS and UNIQUAC in the figures below shows that PC-SAFT clearly gives best fit for VLE equilibrium diagram even at higher pressures. The quantitative behaviour of SRK and PC SAFT are similar and different from UNIQUAC, the UNIQAC critical loci obtained for propane + n-octane system shows a deviation from normal behaviour, since the test was carried out at a higher pressure it may suggest that the model fails at a higher system pressure. Computed temperature-composition critical loci are shown in figures 1.8 to 1.10.

Table 1.3. Interaction Parameters for UNIQUAC

n-Butane/n-Hexane u_{12}	1.0000
n-Hexane/n-Hexane u_{21}	1.0000
Toluene/Ethane u_{12}	1.0000
Ethane/Toluene u_{21}	1.0000

Table. 1.4. PC SAFT Parameters for Some Hydrocarbons.

Component	M	σ	ϵ/k
Ethane	1.6069	3.5206	191.42
Butane	2.3316	3.7086	222.88
Hexane	3.0576	3.7983	236.77
Toluene	2.8149	3.7169	285.69
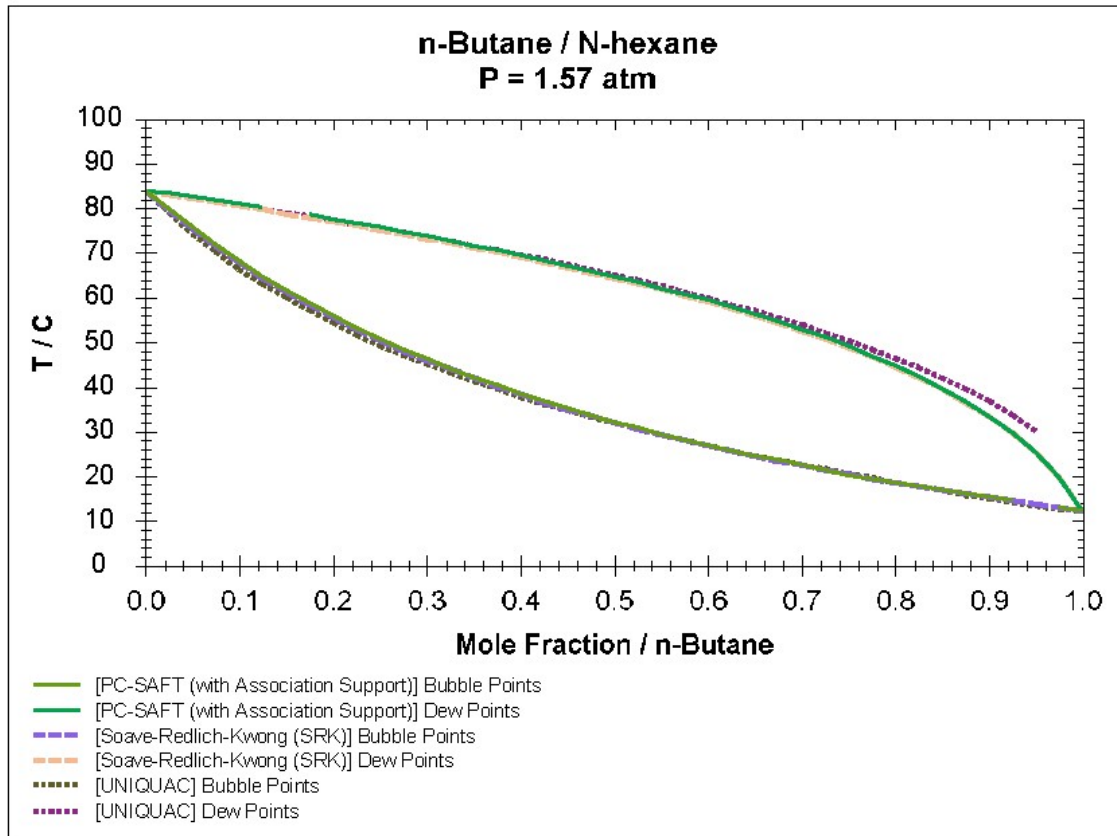
Figure 1.8. Binary Phase envelope n-Butane+ n-hexane system at 1.57 atm comparing PC-SAFT with UNIQUAC and SRK EOS.
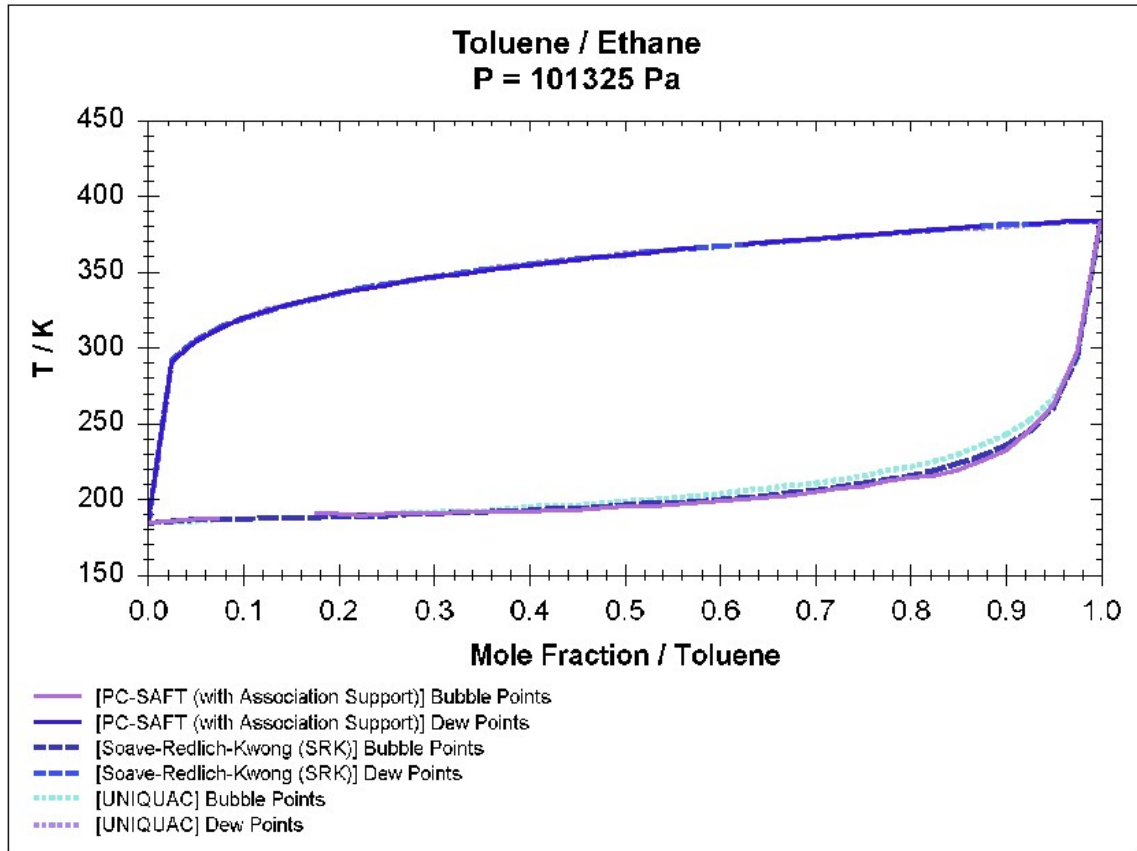
Figure 1.9. Binary Phase envelope n-Toluene+ Ethane system at 273K and 1 atm comparing PC-SAFT with UNIQUAC and SRK EOS.
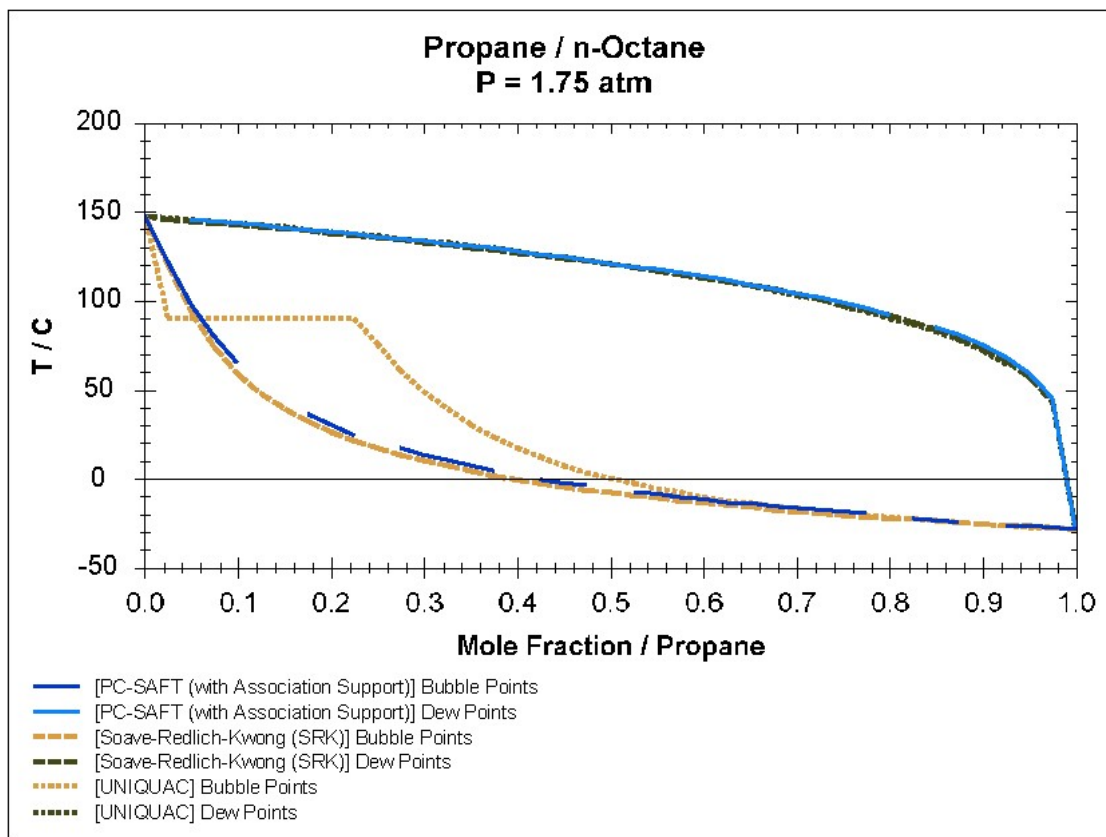
Figure 1.10. Binary Phase envelope Propane + n-Octane system at 273K and 1.75 atm comparing PC-SAFT with UNIQUAC and SRK EOS

1.6.3   LONG CHAIN ALKANE -ALKANOL MIXTURES

This study aims at determining the capacity of PC-SAFT to model homogenous solution consisting of a pure denser liquids/ solid (solute) dispersed in a less dense liquid solvent phase. This can form the basis for modelling Asphaltene solids in reservoir fluids whereby assuming that Asphaltene are monodisperse pseudocomponent in the oil system which during formation separates into a solid rich phase and a solvent rich oil phase. The PC-SAFT was tested for the predictive ability on simulated solid liquid equilibrium data for Ethanol-Eicosane, Ethanol-Tetracosane, and Ethanol-Nonacosane. The solution formed by mixing 30% alkane to 70% ethanol. It is very noteworthy that the long chain alkanes used all exits as solids at room conditions, the tests was carried out at a pressure of 1atm, when done at a higher-pressure say 5 atm the solid phase properties were zero, which indicated that the hydrocarbons did not exhibit solid properties at the pressure. It is therefore arguable that the system does not have a quantifiable vapour pressure; the phase behaviour is expressed in terms of solid-solution system where the solid is miscible in the solution and forms a homogenous mixture.

Table 1.5. PC-SAFT Component Parameters for long Chain Hydrocarbons

Substance	M (g/mol)	M	σ (A)	ϵ/k (K)	Temperature	Source
Ethanol	46.068	1.6000	3.2030	163.2500	273K	Hirahsheh, (2006)
Tetracosane	338.65	9.8220	3.9370	253.1800	217K	Ting, (2003)
Eicosane	282.553	7.9849	3.9869	257.7500	309K	Gross and Sadowski, (2001)
Octadecane	254.500	7.3271	3.9668	256.20	333K	Gross and Sadowski, (2001)
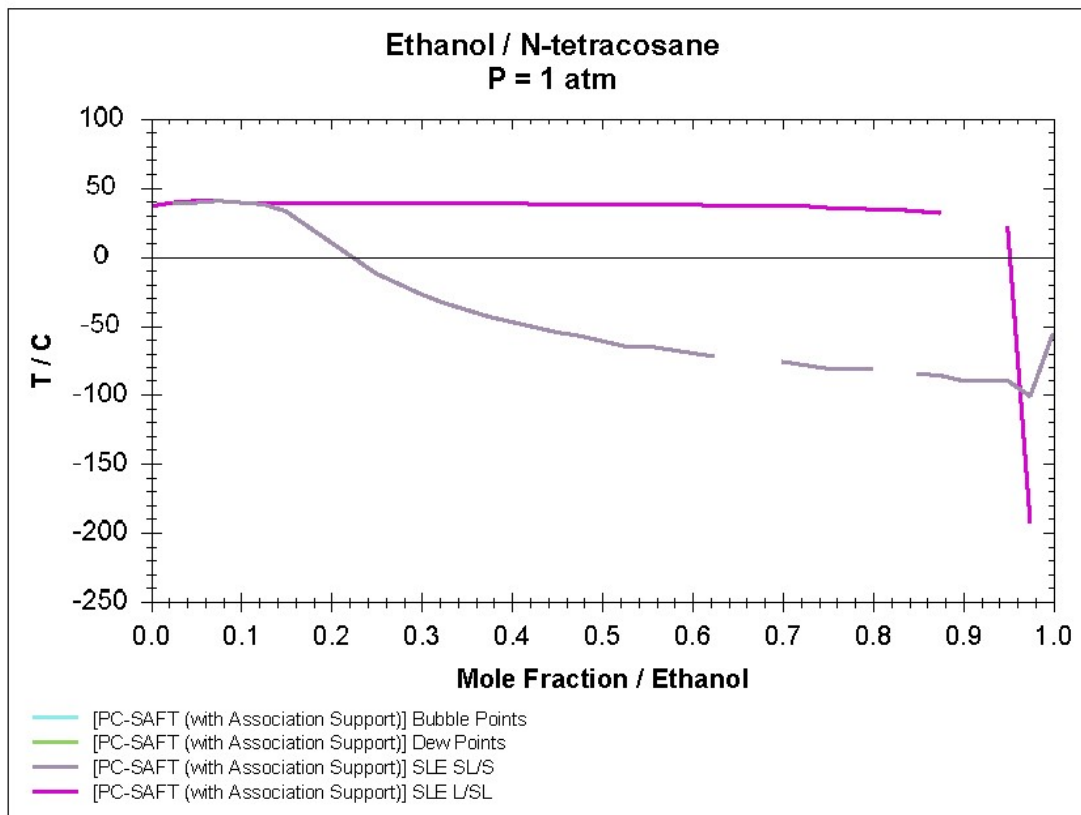
Figure 1.11. Binary Phase envelope Ethanol+ n-Tetracosane system at 273K and 1 atm
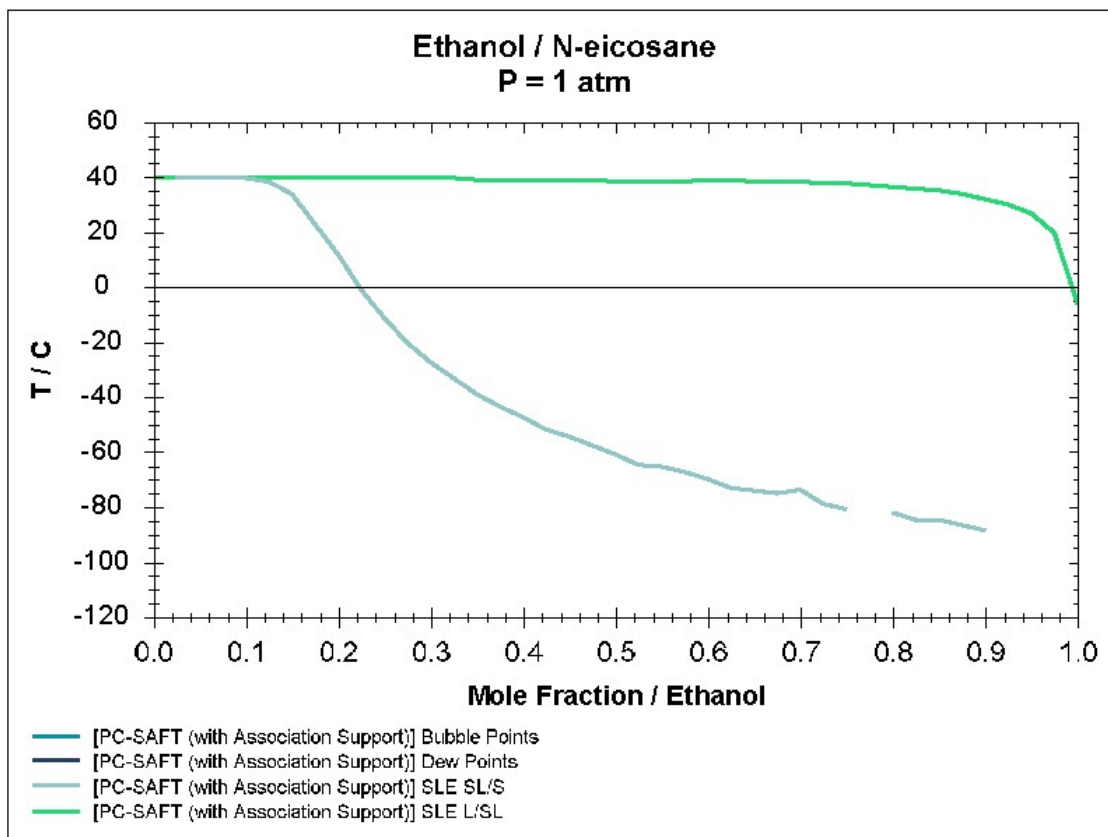
Figure 1.12. Binary Phase envelope Ethanol+ n-Eicosane system at 273K and 1 atm
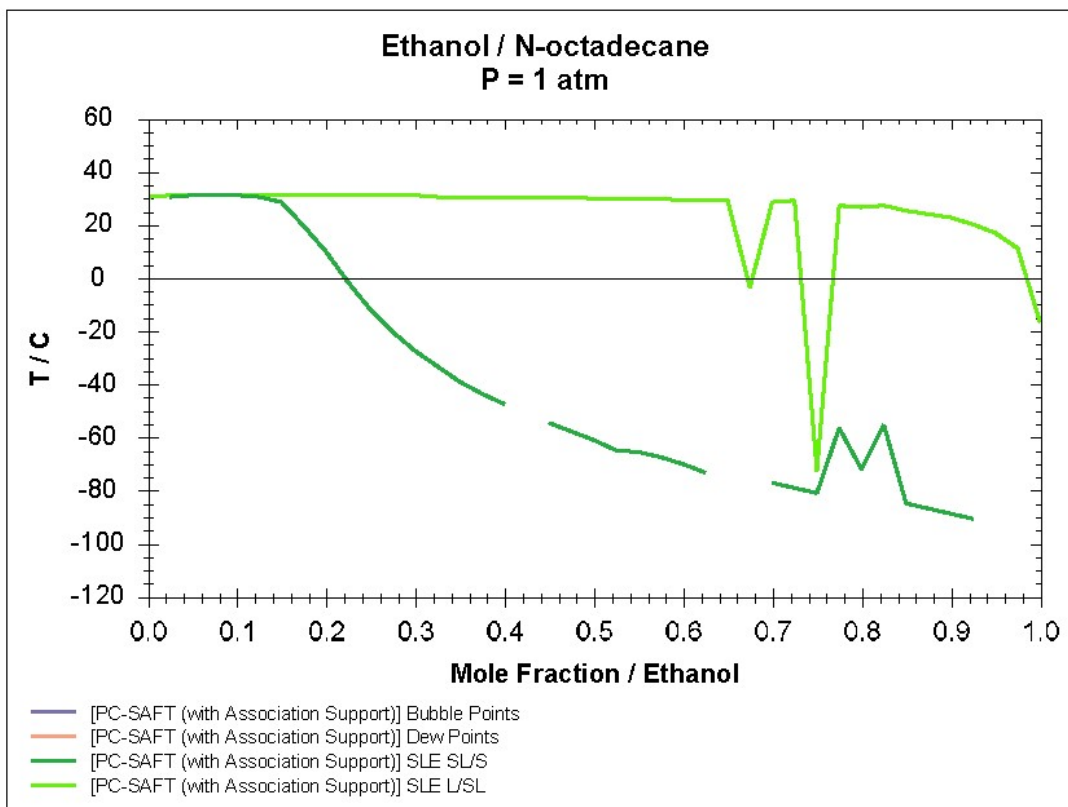
Figure 1.13. Binary Phase envelope Ethanol+ n-Octadecane system at 273K and 1 atm

The capacity of the PC-SAFT to describe solid-liquid and liquid-liquid phase behaviours makes it an excellent equation of state for the study of Asphaltene behaviour in petroleum fluids. Asphaltene has been identified as one of the solids precipitates in crude oil during production or transport, and its deposition poses many challenges in crude oil transport. Studies have shown that the three major factors that contribute to Asphaltene precipitation includes, pressure temperature and compositional changes. Therefore understanding the phase behaviour of Asphaltene is a necessary step to predicting the overall behaviour of the crude oils during production and/or transport. Since the Asphaltene in this case is homogenously distributed throughout the crude oil phase, it becomes vital to first consider the crude oil constitutents and properties. When considering the constituents of the crude oil, it is noteworthy that crude oil consists of hundreds of components at a given temperature and pressure conditions; this makes it imperative to consider methods for classification of the numerous components, and it advisable to classify the components into sub fractions with similar behavioural properties (pseudo components). In other to carry out compositional simulation on the crude oil, it is important to consider how the number of reservoir fluid component in the crude oil mixture will affect the computational time. Therefore one of the major challenges becomes how best to characterise the reservoir fluid. Different authors have suggested different characterization method, (Firoozabadi, 1978) suggested physical properties for petroleum Fractions between C6, and C_{45}, (Whitson, 1983) further suggested a modification to (Katz and Firoozabadi, 1978) by employing the (Riazi and Daubert, 1980) method. (Pedersen et al, 1983) presented an equation that relates Carbon numbers above C_5 and the corresponding logarithm of their molecular weight Z_N

$$C_N = A + B \ln Z_N ....(1.88)$$

While (Peng and Robinson, 1978) proposed a detailed procedure for characterizing heavy hydrocarbons fractions based on PNA, (Bergman et al, 1977) studied extensively experimental

data on gases and condensates and suggested a procedure for characterisation of undefined fractions of hydrocarbon based on their PNA content. In other to study solid precipitation in hydrocarbon fluids it is obvious that PNA characterisation method may not be the best procedure to use because solid organic deposits constitute the heaviest fraction of reservoir fluids which may not be adequately captured by PNA distribution.

The generalised correlation in Table 1.2. for determining PC-SAFT parameters of n-Alkanes was used to determine the parameters for the characterised heavy gas, while the parameters for N_2, CO_2, C_1, C_2, and C_3 were obtained from (Gross and Sadowski, 2001)

TABLE 1.6 PC-SAFT CORRELATIONS USED FOR THE DETERMINING PARAMETERS OF AROMATIC RESINS $\gamma = 0$

PARAMETER	CORRELATION
M	$\gamma\left(0.0139MW + 1.2988\right) + \left(1-\gamma\right)\left(0.0208MW + 0.9136\right)$
Σ	$\gamma\left(0.0597MW + 4.2015\right)/m + \left(1-\gamma\right)\left(0.090MW + 3.14847\right)/m$
ϵ/k	$\gamma\left(119.41\ln(MW) - 230.21\right) + \left(1-\gamma\right)\left(40.059\ln(MW) + 101.18\right)$
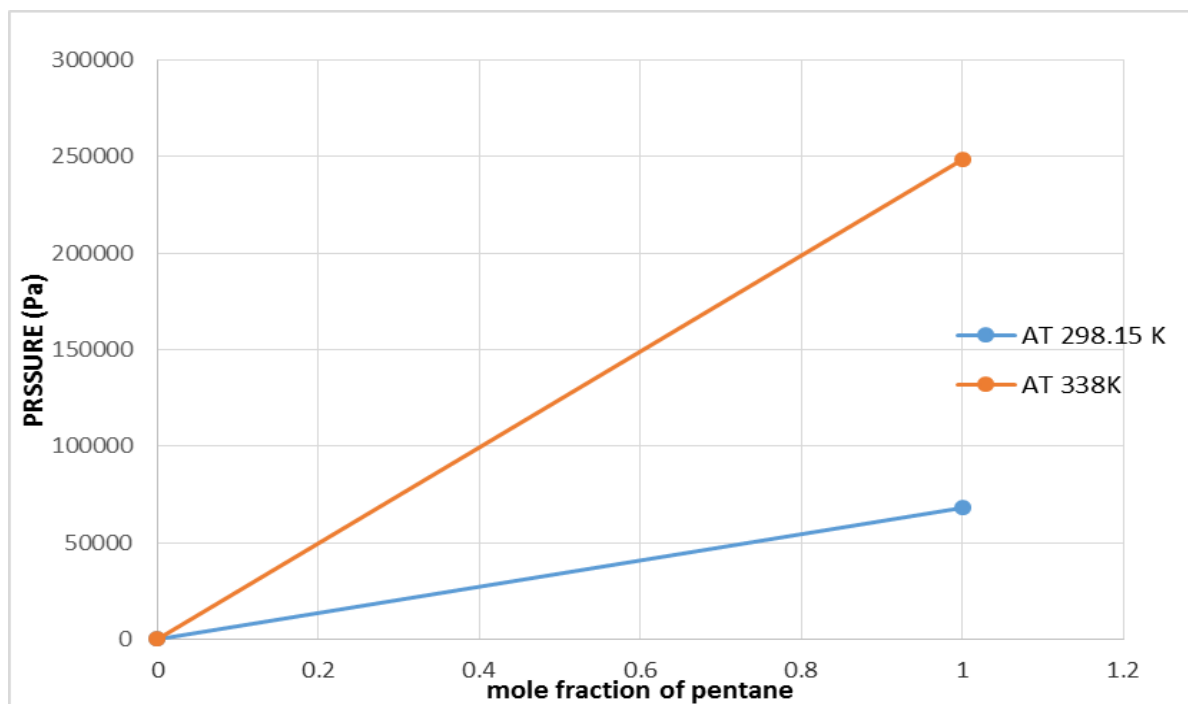
Figure 1.14: PC SAFT Predicted Asphlatene+Pentane Phase Behaviour at 298 and 338K

1.7 PROBLEM STATEMENT

Asphaltene Precipitation (AP), a major challenge in the petroleum industry, causes flow assurance issues in reservoirs, pipelines and flow lines. It is therefore important to properly characterise petroleum fluids and predict the conditions under which AP could be prevented. Many of the reported models used for predicting AP to achieve best reservoir and production management practices are rather complex for routine applications and require long computational time.

1.8. AIM OF STUDY

This study was designed to develop a simple but accurate model for characterising petroleum fluids and predicting AP during gas injection into oil reservoirs.

1.9. OBJECTIVE OF STUDY

The objective of this study is to develop a procedure that will obtain a faster and better control of Asphaltene precipitation during gas injection operation in oil reservoirs.

CHAPTER TWO

LITERATURE REVIEW

2.1. The Behaviour and Structure of Asphaltene

Solids are molecular structure found in crude oils, they can be Asphaltene wax or hydrates along with resins, aromatic hydrocarbons and saturates. They are usually formed petroleum in fluids when n-alkane or a guest molecule is added. The amount of solid organic depositions in petroleum depends on different factors including, depth, physical characteristics and composition of the petroleum fluid (Agrawala, 2001). Asphaltenes usually consist of carbon, hydrogen, nitrogen, oxygen and sulphur including vanadium and nickel. Asphaltene are generally defined as that part of reservoir fluid or coal which does not dissolve in n-alkanes but is soluble in Toluene. Numerous research have been carried out to explain on the nature and behaviour of Asphaltene in petroleum fluids, but there have been challenges in accurately defining the structure and constituent of Asphaltene in petroleum mixtures, the studies notwithstanding are gradually giving explanation to certain aspects of Asphaltene, which so far was unknown. On the struture of Asphaltene, studies have shown that Asphaltene consist of ringed systems with aromatic nuclei and atoms of Hydrogen, Oxygen, Nitrogen and Sulphur (Koots and Speight, 1975). Asphaltene and resins also co-exist in a petroleum crude system with resins have a smaller size than Asphaltene. (Strausz *et al.*, 1992) studies on Alberta Asphaltene, revealed that the presence of condensed percyclic aromatic molecules and aromatic structures in minimal quantities. These studies suggest that petroleum asphaltene undergoes different stages of formations in carboxylic fatty acid precursors including catalytic formation of chain rings, formation of aromatic systems and condensation. To understand the fractal structure of Asphaltene precipitates, (Nazmul *et al.*, 2005) used a photographic technique to determine the size and volume of Asphaltene aggregates in toluene-heptane

mixtures, they concluded that the bulk of Asphaltene formed are characterised by high porosity, high compactions and low space filling capacity. Based on spectroscopic studies, (Dickie and Yen, 1967) suggested a more concise aromatic cluster model with extensive aromatic systems condensed into layers of wide sheets and connected with side chains. Different modifications of the Yen model was later introduced, for instance, recently (Mullins, 2010) suggested a Modified Yen model, which is successful for understanding fundamental observations in oil reservoirs. The Modified Yen model, suggests that most parts of the asphaltene molecule consist of large, lone polycyclic aromatic constituent structure, which is surrounded by alkyl structures. Asphaltene molecules also aggregate with aggregation number approximately 6, further conditions can cause the aggregates to cluster and form larger aggregates with number approximately 8, (Panuganti, 2013). Studies have also show that the Asphaltene deposited due to composition changes vary from Asphaltene deposited because of alterations in physical properties namely temperature and pressure. Studies done on the structure of Asphaltene, Studies have shown the presence of heteroatom O and S functionality, while Nitrogen exists in various heterocyclic types including Pyridine, Aniline, Quinolin and Pyrrole, (Zuo and Shen, 2017). Mass spectroscopic studies carried out by (Moscopedis and Speight, 1976), showed that Carbazole Nitrogen exist in Asphaltene. The application of X-ray absorption near-edge structures (XANES) spectroscopy to the study of Asphaltene, suggested that Asphaltene Nitrogen existing mainly in aromatic form. The Pyrrolic form is in abundance more than the Pyridinic forms. Despite these substantial works by numerous researchers on the topic of Asphaltenes depositions, numerous questions still remain unanswered in these studies, most researchers have studied the behaviours of solids precipitates in other to have a better understanding of how to they can be mitigated. (Leontaritis, 1989) changes in constituent of the oil system as one of the major causes of asphaltene precipitation. During secondary or tertiary recovery fluids are injected into the reservoir, to maintain the production pressure or alter the

characteristics of the reservoir fluid, these result in the change in the composition of the reservoir fluid and has potential of resulting in asphaltene precipitation. (De Pedoza, 1996), (Shedid and Zekri, 2006), (Mousavi-Dehghani, 2007) all showed that the increase of Asphaltene content of the crude oil causes alteration in the wettability of reservoir rocks, damages the absolute permeability and reduces effective porosity. (Shedid, 2001), (Mirzayi, *et al.*, 2008), (Khanifar and Demiral 2011) all suggested that an increase in Asphaltene precipitation causes alteration in the reservoir rock properties while (Arciniegas and Babadagli 2014) concluded that high Asphaltene precipitation improves oil properties and increases the occurrence of porous plugging and permeability reduction. (Cimino *et al.*, 1995) held a different view on Asphaltene precipitation, suggesting that the challenge of Asphaltene precipitation usually a problem in lighter oils with lower Asphaltene content, (up to 4 %wt.). It can therefore be inferred that heavier oils with higher Asphaltene content do not pose greater risk.

Table 2.1: Values of the Composition in n-heptane asphaltenes (Cimino et al., 1995)

H/C Ratio	Sulphur (wt. %)	Nitrogen (wt. %)	Oxygen (wt. %)
0.8-1.4	0.5 - 10.0	0.6 - 2.6	0.3 – 4.8

(Monger and Fu, 1987), (Monger and Trujillo, 1991), studied the behaviour of Asphaltene in porous media. The results of the study suggested that Asphaltenes precipitation during CO_2 injection was also due to many other factor apart from the injected CO_2 gas since it was possible that some Asphaltene dispersed in solvent can precipitate by other heavy organics, therefore precipitation usually occur during development of miscibility. (Dong *et. al.*, 2014) Studied the effect of CO_2 flooding pressure on a drill core displacement apparatus and found that the permeability of test cores decreased with increased CO_2 flooding pressure due to

Asphaltene precipitation. (Burke et al., 1990) reported that oil composition and Asphaltene concentration in petroleum fluids possess remarkable influence on Asphaltene stability Broseta et al., (2000) investigated asphaltene deposition on petroleum fluids using pressure drop measurement across a capillary tube, the study observed that as the distance from the deposition onset point increased, the asphaltene deposition rate also increased. Abdolhossein et. al., (2018) studied the aggregation behaviour of petroleum Asphaltenes dissolved in toluene and showed that Asphaltene aggregate size increases with an increase in Asphaltene concentration, and that the size is very much dependent on Asphaltene composition and structure. Broseta et al. (2000), Wang et al. (2004) and Lawal et al. (2012) further suggested models for the hydrodynamic characteristics of a deposited Asphaltene, assuming that the deposited Asphaltene is uniform. Rayes et al. (2003) conducted tests to determine adsorption of Asphaltene from different categories of crude oils on reservoir rocks, the tests concluded that the quantity of Asphaltenes adsorption on reservoir rocks depended on the mineralogical composition of the reservoir rocks. Mansoori (1997) proposed a model which considered four different effects (mechanisms) on Asphaltene depositions in well heads, these include polydispersivity, steric colloidal, aggregation, and electrokinetic effects. Ramirez-Jaramillo et al., (2006) investigated the Asphaltene deposition in production pipelines via a multiphase multicomponent hydrodynamic model, results indicated that the wells presented the formation of Asphaltene deposit located at various depths. Lin et. al., (1954) proposed the velocity distribution by for generalized turbulent flow in pipe. The model predicted the particle deposition speed with respect to different turbulent flow regimes. It further showed an inverse relationship between deposition rate and particle size, similar view was held by Escobedo and Mansoori (1995) on studies to show how diffusion affects the speed of deposition of solid particles during turbulent flow, the study also revealed that the effect of diffusion was minimal on the rate of solid particle deposition. Hashmi et. al., (2013) investigated the deposition and

clogging of Asphaltenes in pipelines during flow and further suggested a dynamic model for asphaltene deposition during fluid transport in pipelines. The model suggested by Eskin et al. (2011) for Asphaltene deposition in pipelines the model was based on experimental data and consists of factors; Particule size distribution evolution with time in a couette device and along a pipe and particle transport to the walls of device. The results showed that only particles with smaller in critical size will deposit.

On the structure of the deposited asphaltene particles, Gmachowski and Paczuski (2015) studied the depositional behaviour of asphaltene when the petroleum fluid is subjected to turbulent flow. The studies observed that the deposited aggregates possessed a uniform fractal size of 1.75 and are created by micro aggregates of radius 1.2μm and alsphaltene structure plays a key role in modelling its deposition in pipelines. Andersen, (1994) concluded from his experimental studies that Asphaltene consists of the associating and the non-associating species, the non-associating species in asphaltene consists of the part that usually dissolve in the solvent and constitute 60% of the total mass of the asphaltene.

2.2. THE BEHAVIOUR OF ASPHALTENE

The behaviour of asphaltene in petroleum can be classified into for main categories namely: Self-association, flocculation, precipitation, deposition. Asphaltene tend to associate with themselves to form aggregates and with resins to form a stable compound. The degree at which asphaltene undergoes self-association depends on the concentration in the organic solution. Concentrated asphaltene solutions exhibit some degree of colloidal behaviour (Sachanen, (1945), therefore aspahltenes are said to exhibit surfactant properties Waarden, (1958), Neumann, (1965), and stabilize water-in-oil emulsions, this also suggest that they remain in monomeric state in the solution until a certain Critical Micelle Concentration is reached. Above that concentration, asphaltenes arrange themselves into aggregates Merino-Garcia (2004). Sheu et al (1992) carried out the estimation of the surface tension of the Ratawi vacuum resides, in

other to determine how asphaltene concentration in pyridine solution was affecting the critical micelle concentration, the study showed that the point of critical micelle was observed as a discontinuity in the plot of surface tension vs concentration curve.

2.3. THEORIES ON ASPHALTENE STRUCTURES

Experimental studies carried out by Ho and Briggs (1982) studied the size of asphaltene particles in petroleum fluids their and their similarity with micelles. However, Taylor, (1992) pointed out that in the case of nitrobenzene solution there was lack of consistency in the discontinuity for surface tension vs. Logarithm of concentration (log C) plot as would normally be expected in line with the Gibbs isotherm. This raise serious questions about the presence of a CMC in these solutions Studies carried out by the recent data of Loh et al.(1999) and Mohamed et al. (1999a) have demonstrated the persistence of these discontinuities in the surface tension curve even when data were presented on a semi-log scale. Yarranton et al. (2000) could not find a CMC for asphaltenes in toluene and 1, 2- dichlorobenzene by surface tension measurements, while Christensen and Andersen (1999) claimed that the observed changes in the CMC-region may be due to the association of small aggregates into bigger ones. Hydrogen bonding, acid-base interactions, dipole-dipole interactions and n-n stacking of aromatic ring clusters have been suggested as possible mechanisms. Agrawala (2001). Kontogeorgis, (2005), suggested a generally small contribution of induction force during self-association, this contribution does not exceed 7% occurs in the absence of ions or charges

particles in the system, which is the case in Asphaltenes aggregates.
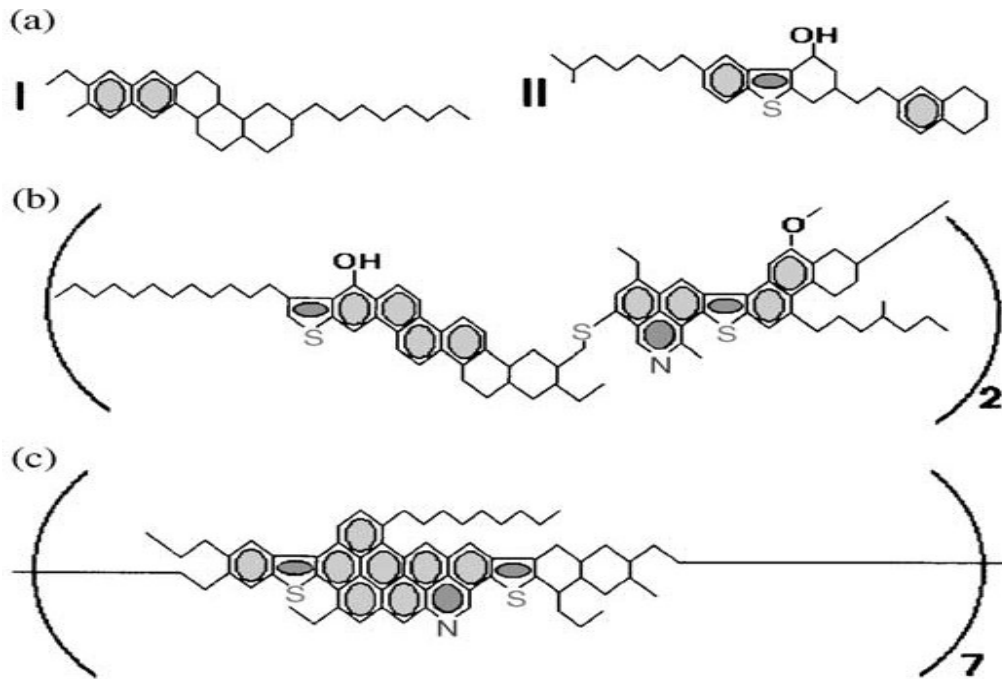
Figure. 2.1: Model Structures for Athabasca tar Sands and Bitumen (a) Resins Structure (b) Asphaltene Structure for tar sand bitumen and (c) Asphaltene Structure for Bitumen. Suzuki et al., (1982).

Leon et al (1998) performed compositional and structural studies, in other to understand the effect of different characteristics Asphaltene factors on stability. Results showed that crude oil was influenced by the structural behaviour of the Asphaltene the study further showed that in particular, the composition and structure of Asphaltenes have great influence on its self-association capability, also, Asphaltene contained in unstable oils tend to form aggregate at lower concentrations in contrast to stable oil Asphaltenes. However, the study did to investigate the role of heteroatom on Asphaltene stability. On the influence of resins on asphaltene stability Leon et. al., (2001) suggested that stabilization of Asphaltene by resins is due to the penetration of the Asphaltene micropores by resin molecules. Brandt et al. (1995) used a computer based molecular modelling tool to determine the parameters of an association

model for Asphaltene solvent mixtures. The presence of stacked aromatics formation as a precursor to aggregation process was observed; the study further suggested that in poor solvents, there increased arrangement of aromatics compound. This occurs at decreased Asphaltene concentration although, when Asphaltene concentration is increased aromatic arrangement decreases. Maruska and Rao (1987), applied dielectric spectroscopy to determine the electrical properties and dielectric behaviour of crude oil based Asphaltenes as a measure of concentration and temperature. Results of the study showed that as concentration of Asphaltene increased the dielectric constant showed negative deviation, indicating the start of molecular interaction. Increases in temperature showed an increase in dielectric constant, which indicates an increase in dissociation of aggregates. On the finite nature of self-association, Roux et al. (2001) studied the structure of asphaltenes using (SANS), studies showed that temperature changes the quality of solvent, also found that Asphaltenes forms monomeric clusters which grows in size with temperature decrease. Porte et al (2003) studied the process of aspahltene aggregation and precipitation and suggested that aggregation and precipitation are not the same but distinct reversible step. While aggregation involves strong specific site interaction, precipitation occurs because of van-der-waals attraction between aggregates during equilibrium shifting. Carbognani, (2003) suggested that steric hindrance caused by alkyl chains has a limiting effect on self- association as the presence of alkyl aggregates reduces the number of sheets contained in an aggregate. Resins and Asphaltenes usually exhibit different characteristics, the structure of resins can be described as usually containing polar end groups with long alkane tails consisting of heteroatoms like oxygen, sulphur, and nitrogen, and ring structure namely aromatic and naphthenic, and they are also insoluble in excess light alkane liquids including Pentane, butane, and heptane and also alcohols and some esters. Therefore, different options available for the determination of the quantity of Asphaltene and resins in crude oils and most of these options are based on defining the compositions of the Asphaltenes

71

and crude oil fractions. Asphaltenes on the other hand are consists of aromatic and naphthenic rings which are bounded by heteroatoms like Nitrogen oxygen and sulphur. Goual and Firoozabadi (2002).). In their recent studies showed that Asphaltene contain oxygen containing compounds including phenol oxygen, polyhydroxyphenol and amide oxygen, this recent observation causes a slight deviation in the structure of Asphaltene originally agreed upon by most researchers. Speight (2014)

2.4 ASPHALTENE PRECIPITATION MODELS

The different precipitants used for Asphaltene precipitation has varying effect on the Asphaltene-Resin interaction, while addition of propane causes separation of asphaltene and resins from the bulk fluid, precipitation by pentane or heptane causes separation between Asphaltene and resin. Tissot and Welte, (1984), When light alkane constituent is added to an Asphaltene containing solution, the alkane constituent reduces the solubility parameter of the Asphaltene in the solution. This causes the resins to desorb from the Asphaltene surface; in order to maintain the thermodynamic equilibrium of the system as a result; there will be an occurrence of Asphaltene-Asphaltene self-aggregation at sight vacated by the desorbed resins Hammami et al., (2000). Therefore, resins being more polar aromatic species play significant role in maintaining the stability of Asphaltenes in petroleum fluids by adsorbing to specific interaction sites of Asphaltenic molecules and preventing further site-specific asphaltene aggregations. Resins do not stabilize effectively in water-oil-emulsions systems despite their surface active behaviour, this reality is in contrast to the view that resins and Asphaltenes combine to form a repeated structural chain, Mclean and Kilpatrick (1997) But resins can cause solvation of asphaltene in oil-water emulsion as a result bring about asphaltene stability stability, Gafonova (2001). Recent studies have further shed light into interaction between asphaltene and resin. Marques et al., (2014) has shown that despite the presence of resins adsorbed to Asphaltene surface in an Asphaltene solvent mixture, there huge possibility of

Asphaltene deposition and flocculation, this is because although resin-Asphaltene interaction occurs by weak van-der-Waals interaction, there is still possibility of Asphaltene-Asphaltene interaction in the same mixture. This notion opposes the well-accepted school of thought that resins stabilizes asphaltenes. Anisimov et al., (2014) studied the stabilization effect of resins on asphaltene contained in petroleum fluids, using dynamic light scattering method. The study revealed that resins inhibit the formation of asphaltene aggregates in petroleum fluids, and reported the dependence on the resin to keep shifting the asphaltene onset; the study further suggested the possibility of defining the aggregation onset and the growth in aggregation size on time basis. Janaina et al., (2015) investigated the nature of relationship existing between asphaltene and resins, by determining the solubility parameter and enthalpies between asphaltene and resins of resins using ultra visible spectrometry (UVS) and microcalorimetry. The study concluded that the strong interaction between Asphaltenes and resins is responsible for Asphaltene stability. Due to changes in their solubility parameter of water, the PH of oil water emulsion also affect Asphaltene stability, sandrine and Jean-François (2005) showed that when the PH value of water oil emulsion increases, the functional groups in Asphaltene molecules acquire charges, thus causing Asphaltene molecules to become surface active.

To describe asphaltene precipitation by use of thermodynamic model and equation of states, Cimino et al., (1995) as described by Verdier (2006), identified the two broad classification of models:

i. "The lyophobic colloidal models: Asphaltenes behaviour is similar to lyphobic colloids since peptization occur in the presence of resins resulting in a two phase system namely the solvent and the asphaltene phase, therefore the lypophobic colloidal model has a great impact in understanding of asphaltene micelles behaviour. In this case, asphaltene, micelle consists of an insoluble aromatic core and the adsorbed micelle that act as

amphiphilic molecules, this structural arrangement results in the formation of stable asphaltene micelles which are usually assumed to be irreversible.

ii. The lyophilic colloidal model suggests that asphaltene momomers remains soluble in the liquid (solvent) medium under reversible conditions as a single stable solution due to the high force of attraction existing between the asphaltene monomers and the solvent and because of the stabilizing power of the resins in the liquid medium. The lyophilic model suggests a very high level of asphaltene-solvent stability, which further implies that at the stability conditions, there is less tendency of asphaltene precipitation.

Leontaritis and Mansoori (1997) developed the steric colloidal model for predicting the onset of flocculation of colloidal asphaltene in oil mixtures Leontaritis and Mansoori (1992). The model is based on two verifiable phenomenon namely

a) Resin particle are very important in Asphaltene stability and play a part in colloidal Asphaltene peptization

b) A streaming potential develops during oil flow, this contains charged colloidal particles which causes the flocculation and precipitation of asphaltene particles
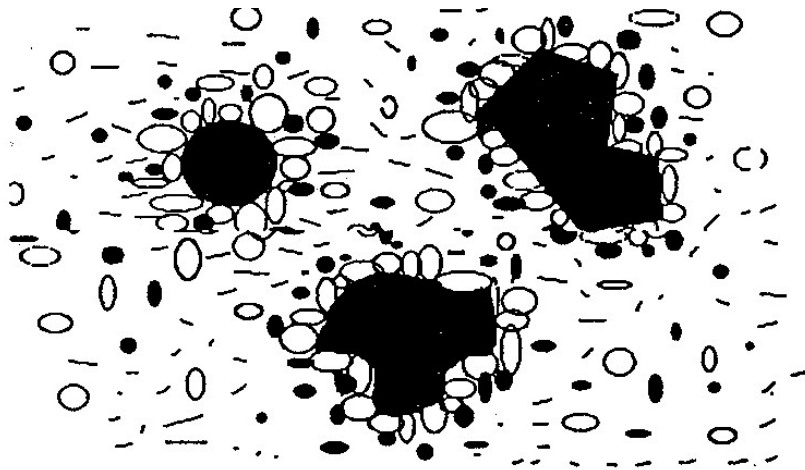
NOTES

1.0 ◯ represents resin molecules

2.0 ● represents aromatic molecules

3.0 — represents oil molecules of different size and paraffinic nature

4.0 ⬛ represents asphaltene particles of different sizes and shapes

Fig 2.2: Asphaltene particle peptization Leontaritis and Mansoori (1992)

They noted since oil phase is in equilibrium with asphaltenes phase, the condition for equilibrium holds.

$$\mu^{\text{oil phase Resin}} = \mu^{\text{Asphlatene phase Resin}} = \Delta\mu_R \ldots (2.1)$$

2.5. FLORY HUGGINS THEORY

Flory Huggins statistical mechanics theory is used to solve for $\Delta\mu_R$ through the following equation

$$\Delta\mu_R / RT = \left[\mu_R - \left(\mu_R \right)_{ref} \right] / RT = \ln\left(\phi_R \right) + 1 - v_R / v_m + \chi_R \ldots(2.2)$$

where $\Delta\mu_R$ is the difference between the chemical potentials of the resins in solution and in their reference state, R the gas constant, T the temperature, ϕ_R the volume fraction of the resins,

$$\chi_R = \left(v_R / RT \right)\left(\delta_m - \delta_R \right)^2 \ldots (2.3)$$

Equation (2.2) is the Flory Huggins interaction parameter between resins and solvents and v_R/v_m the ratio between the molar volumes of the resins and the solvent. Leontaritis and Mansoori defined the point at which there is adequate concentration of resins to keep the colloidal asphaltene particle completely covered as the critical resin point and the concentration of resin in the liquid phase as the critical resin concentration $(C_R)_{\text{crit.}}$ The critical chemical potential $(\Delta\mu R)$ of the resin can be calculated at this concentration. Furthermore, the concepts behind this model still poses a question of whether resins are physically present at the Asphaltene micelles and the crude oil interface Verdier (2006) (Cimino et al., 1995) suggested the possibility of Asphaltenes to remain stable in some solvent, and further suggested that the presence of resins may not be absolutely responsible for Asphaltene stability in solution.

2.6. THERMODYNAMIC MICELLIZATION MODEL

The development of the thermodynamic micellization model on the premise that the precipitated phase remains in the liquid phase and the minimization of the liquid-liquid Gibbs free energy gives the equation for the whole system. The system consists of two liquids phases namely, the precipitated liquid phase (asphaltene) L_1 and the liquid phase containing the precipitated liquid phase L_2. The equation is expressed as:

$$G = G^{L1} + G^{L2} \quad \ldots\ldots \quad (2.4)$$

Where:

$$G_L = \sum_{i=1}^{N_c} N_i^L \mu_i^0(T) + kT \sum_{i=1}^{N_c-2} N_i^{L_1} \ln f_i^{L_1} + kT\left(N_{a1}^{L_1} \ln x_{a1}^{L_1} + N_{r1}^{L_1} \ln x_{r1}^{L_1} + N_m^{L_1} \ln x_m^L\right) + N_m^{L_1}\Delta G_m^{00} + kT(N_a^{L_1} \ln \varphi_a^{L_1} p + N_r^{L_1} \ln \varphi_r^{L_1} P)$$

…… (2.5)

From the equation N_C is the total number of component, the component indices for asphaltene and resin are N_C and N_C-1 respectively. ΔG_m^{00} is the change in Gibbs free energy during the formation of a micelle it is expressed as;

$$\Delta G_m^{00} = n_1\left[\Delta g_a^0 / kT + \ln(\varphi_a^l / \varphi_{a1}^\infty) + \frac{1}{2}\left(\frac{R^2}{m_a L^2} + 2\frac{m_a^{\frac{1}{2}}L}{R} - 3\right)\right] +$$

$$n_2\left[\sigma\left(A - A_0\right)/kT + \left(\Delta h_r^0\right)_{Adp} / kT - \ln(1 - \frac{A_p}{A}) + \ln\left(\varphi_{r,s}^l x_{r,s} / \varphi_r^\infty\right)\right] + \frac{1}{2}\left(\frac{D^2}{m_r L^2} + 2\frac{m_r^{1/2}L}{D} - 3\right) \ldots\ldots(2.6)$$

Where:

$$x_{r,s} = n_2 / \left[n_2 + \left(V_{sh} - n_2 V_r\right)/V_s\right]$$

$$V_{sh} = \frac{4\pi}{3}\left[\left(R + D\right)^3 - R^3\right]$$

$$R = \left(\frac{3}{4\pi} n_1 V_a \right)^{1/3}$$

$$m_a = V_a / V_s$$

$$A = 4\pi R^2 / n_2$$

Thermodynamic Micellization model assumes that the miceller shell contain resin and deasphalt oil the resins is adsorbed at the micelle core, the model was used to describe precipitation resulting from temperature, pressure and compositional changes.

The Flory Huggins polymer theory (FH) (Flory 1942) is a solubility model, which describes polymer stability in relation to reversible equilibrium solution. It involves performance of both VLE and LLE calculations; the former calculation was carried out to get the vapour thermodynamic properties and equilibrium compositional values, while the latter calculation is done by applying the Flory-Huggins theory to get the proportion of asphaltene constituent present in the system. The theory suggests that asphaltene molecules in oils are similar in composition and behaviour with polymer molecules. In applying the Flory Huggins theory to petroleum, systems, it is assumed that only two phases exist in the solution namely, the polymer phase, which consists of the asphaltene dissolved in the solution, and the liquid phase, which consists of the bulk remainder of the oil. This acts as solvent to the polymer phase, it does not consider the effect of resin on asphltene stability. Mousavi-Dehghani (2000) and Kokal et al., (1992) based their studies on this approach. The Flory Huggins model expressed the solubility asphaltenes in as:

$$\phi_a^L = \exp\left[-1 + \frac{v_a}{v_L} - \frac{v_a}{RT}(\delta_a - \delta_L)^2 \right] \quad \ldots\ldots(2.7)$$

Where v is the molar volume, δ the solubility parameter, R the gas constant and T the temperature. The subscripts a and L respectively refer to the asphaltenes and the liquid

medium. The solubility parameter of the liquid is usually determined using a cubic equation of state after the fluid was characterized and the asphaltene properties can be estimated from titration experiments. The study reported a quiet impressive result and the effect of pressure, gas injection and temperature were examined. This is the reason why the Flory Huggins theory remains as a reference. Veidier (2006). The Flory Huggins interaction parameter is determined from intermolecular forces and is assumed independent of composition. It is determined by the energies that characterise the interactions between pairs of polymer segments, between pairs of solvent molecules and between one polymer segment and one solvent segment Wu et al., (1999). When expressed in terms of interchange energy, χ becomes:

$$\chi = \frac{w}{kT} \ldots\ldots(2.8)$$

2.7. THE SCOTT MAGGAT THEORY

Similar to the the Flory-Huggins polymer- solution theory The Scott- Maggat theory suggests that both asphaltenes and polymers contain similar heterogenous structures and show polydiversity and it also suggests an oil system consisting of three phases; the precipitated asphaltene phase, the solvent phase containing the precipitated asphaltene and the asphaltene free oil phase (Maltene phase). Mohammadi and Richon (2008). The chemical potential change of the maltene (Asphaltene free oil) relative to a reference value, and the chemical potential change of the ith asphaltene fraction relative to a reference value ($\Delta\mu_i$) are calculated using the following equations.

$$\Delta\mu_m = RT\left[\ln\phi_m + (1-\phi_m)(1-\frac{1}{M}) + \chi(1-\phi_m)^2\right]\ldots\ldots(2.10)$$

$$\Delta\mu_i = RT\left[\ln\phi_i + (1-\phi_m)(1-\frac{M_i}{M}) - M_i\phi_m + \chi M_i\phi_m^2\right]\ldots\ldots(2.11)$$

Where ϕ_i is volume fraction of the ith Asphaltene fraction. M and M_i represent the average molecular weight of Asphaltene and the molecular weight of the ith Asphaltene fraction, respectively. χ is given by equation (2.8)
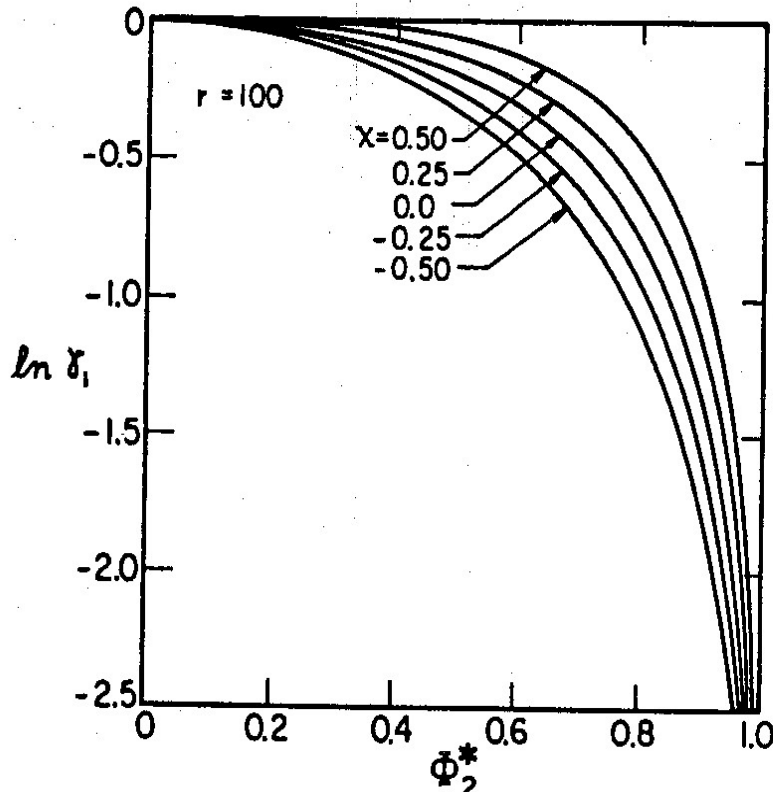
Figure 2.3: Solvent activity coefficient in a real polymer solution according to the equation of flory and Huggins. Paremeter χ depends on the intermolecular force between the solvent and the polymer Prautnitz et al., (1999)

2.8. CUBIC EQUATION OF STATE

Cubic equations of state are very useful for studying the thermodynamic characteristics and phase behaviour of gases, Liquids and mixtures. The quest to extend equation of state to polymer and other complex liquids has thrown different challenges. These challenges include defining the pure component parameters of the equation of the Cubic Equations of State and the application of a suitable mixing rule to the polymer mixture. The classical mixing rules of

van der Waals (vdW) has been tested for polymer solvent mixtures; however, it has been observed that, in order to fit the experimental data, some unrealistic values are necessary for the binary interaction parameters (BIP). Guerrieri et al., (2012). Numerous attempts have been successfully made in the application of a cubic equation to polymers. One example of such attempt is the application of Modified Sako-Wu-Prausnitz Equation of State in polyethylene-Ethylene system at high pressure by Gharagheizi and Vatani (2006). the Equation of State was used to calculate the flash point and cloud point for the polyethylene-ethylene system, the study involved fitting two new pure component parameters using pure component saturated vapour pressures, liquid volumes and the van-der-waals on fluid theorem as mixing rule, the study obtained a correlation for binary polymer-solvent systems existing below critical points. The SWP (Sako-Wu-Prausnitz) equation is a member of the cubic family:

$$P = \frac{R.T.(V - b + b.c)}{V.(V - b)} - \frac{a(T)}{V.(V + b)} ....(2.12)$$

Where T is temperature, V is molar volume, P is pressure and R is the universal gas constant. The parameter a is a measure of the attractive forces between molecules, and the parameter

b is the co-volume occupied by these molecules. Kontogeorgis et al. (1994) used the van der Waals equation of state to correlate vapour-liquid equilibrium data of polymer solutions. The authors further suggested a procedure for calculating the attractive parameter a and co-volume b in the equation of state for polymers from two volumetric datasets at low pressure. Both parameters a and b (assumed to be independent of temperature) can be analytically expressed from two experimental molar volumes, each one at a different temperature. An equation for solid phase fugacity was presented by Gupta (1980) for the Peng Robinson Equation of State, the parameters used for the equation where acquired from a combination of NMR data and the SRK EOS data. Although easy to use Cubic EOS are limited by their poor prediction of Asphaltene properties.

2.9. CUBIC PLUS ASSOCIATION

The Cubic plus Association Equation of state CPA EOS was developed by kontogeorgis et al (1996) combines the Soave Redlich Kwong equation of state with an equation of association

$$\frac{A^{chain}}{RT} = \sum_A \left[\ln X^A \frac{X^A}{2} \right] + \frac{M_i}{2} \dots\dots(2.13)$$

It is generally expressed as:

$$P = \frac{RT}{V-b} - \frac{a(T)}{V(V+b)} - \frac{1}{2}\frac{RT}{V}\left(1 + \rho\frac{\partial \ln g}{\partial p}\right)\sum_i x_i \sum_{A_i}(1 - X_A) \dots\dots(2.14)$$

Where ρ is the molar density.

The term X_A represents the number of association site of the fraction of A on molecule i that does not form bond.

$$X_A = \left[\sum_j \sum_{B_j} \rho_j X^{B_j} \Delta^{A_i B_j} \right]^{-1} \dots\dots(2.15)$$

The CPA Eos is capable of describing complex mixture (Multicomponent, multiphase) containing hydrocarbons, polymers and other associating fluids, like alcohol, water and organic acids.

Wenzel and Schmidt (1980) suggested an equation of state for solids based on van der waal equation of state. The assumption made was that the adjustable parameter c is additional attraction due the solid phase, therefore it is assumed positive and contains a higher value than the repulsive parameter b. it will also contribute to increase the attractive parameter of the system, the equation is expressed as:

$$P = \frac{RT}{V-b} - \frac{a}{V(V+b)} - \frac{c}{(V - 0.97b)^6} \dots\dots(2.16)$$

By regressing the experimental vapour pressure and liquid density the parameters a, b, and c were determined.

2.10 STATISTICAL ASSOCIATED FLUID THEORY

The Statistical Associated Fluid Theory (SAFT), developed by chapman et al., (1989, 1990) is the most recent model based on the perturbation theory family, the basis of this model is the thermodynamic Perturbation Theory (TPT) by Wertheim (1983, 1984, 1986a, 1986b). Wertheim derived his theory by expanding the Helmholtz energy in a series of integrals of molecular distribution function and the association potential. Here molecules are regarded as individual distinct species in line with the number of bonded sites and each possible bonded state of the molecules is assigned a distinct density. The result is a relationship between the residual Helmholtz energy due to association and monomer density. Chapman et al., (1988a, 1988b) extended the Wertheim's theory to mixtures of spheres and chain molecules and compared the results to Monte Carlo based simulation. The PC SAFT model usually assume that the molecules are a mixture of spherical segments of similar size, interacting according to a square-well potential. Also there is the possibility of bond formation between spheres the bonds formed are usually of two types namely: covalent bonds to form chains and association bonds for specific interactions Huang and Radosz (1990a, 1990b). The equation is derived in terms of the residual Helmholtz free energy a^res as:

$$a^{res} = a^{hs}(T,\rho) + a^{chain}(T,\rho) + a^{assoc}(T,\rho). + a^{disp}(T,\rho).......(2.17)$$

The contribution from repulsive hard-sphere interactions among all particles to the Helmholtz energy is obtained from the equation of Mansoori et al. (1971)

$$\frac{A^{hs}}{kT} = N_t^s \left\{ \left[\frac{\zeta_2^3}{\zeta_0 \zeta_3^2} - \zeta_0 \zeta_3^2 \right] \ln(1-\zeta_3) + \frac{1}{\zeta_0} \left[\frac{3\zeta_1 \zeta_2}{(1-\zeta_3)} + \frac{\zeta_2^3}{\zeta_3(1-\zeta_2)^2} \right] \right\} \quad \ldots\ldots\ldots (2.18)$$

Where:

$$\zeta_n = \frac{\pi}{6} \sum x_i m_i \sigma_i^n \qquad n = 0,1,2,3$$

σ_i is the diameter of the spherical segment of chain i, and ζ is the reduced density, x_i is the specific volume of the spherical segment. The Helmholtz energy due to association is given by (Wertheim, 1986; Chapman et al., 1988)

$$\frac{a^{assoc}}{kT} = 2N_A \left(\ln x_\alpha + \frac{1-x_\alpha}{2} \right) + N_R \left(\ln x_\beta + \frac{1-x_\beta}{2} \right) \ldots\ldots(2.19)$$

Where X_α is the fraction of association sites a (at asphaltene molecule) that are not bonded; x_β is the fraction of association sites β (at resin molecule) that are not bonded. X_α and X_β are given by (Chapman et al., 1990)

$$x_\alpha = \left(1 + 2\rho_A \Delta^{\alpha\alpha} x_\alpha + \rho_R \Delta^{\alpha\beta} x_\beta \right)^{-1} \ldots\ldots(2.20)$$

$$x_\beta = \left(1 + 2\rho_A \Delta^{\alpha\beta} x_\alpha \right)^{-1} \ldots\ldots (2.21)$$

The resin chain contribution of the hard sphere chain to the Helmholtz Energy is given by the equation of Chapman et. al (1989) as

$$\frac{A^{chain}}{kT} = N_R (1 - l_R) \ln g_{22}^{hs}(\sigma_{22}) \ldots\ldots (2.22)$$

Where

$$g_{ij}^{hs}(\sigma_{ij}) = \frac{1}{1-\xi_3} + \frac{2\sigma_i \sigma_j}{(\sigma_i + \sigma_j)} \frac{\xi_2}{(1-\xi_2)} + 2\left(\frac{\sigma_i \sigma_j}{\sigma_i + \sigma_j} \right)^2 \frac{\xi_2^2}{(1-\xi_3)^3} \ldots\ldots (2.23)$$

Other modifications of SAFT include PC-SAFT; developed by Gross and Sadowski (2002) based on the Baker Henderson perturbation theory, this modification gives an improved result

when polymeric systems are simulated, Guerrier et al., (2012). Blas and Veja (1998) used the Lennard- Jones fluid, which brought about the soft-SAFT equation. The chain and association terms remained similar to those in the original SAFT formulation. The soft-SAFT equation was successfully applied to pure n-alkanes, 1-alkenes, 1-alcohols and binary and ternary mixtures of n-alkanes including the critical region. The SAFT-VR is a new approach to the SAFT theory of variable attractive range Mc Cabe and Jackson (1998). The differences between SAFT-VR and PC-SAFT is due to the choice of reference fluid used. The SAFT-VR takes as reference the hard-sphere fluid, while PC-SAFT takes the hard sphere- chain fluid.

CHAPTER THREE

METHDOLOGY

3.1. DEVELOPMENT OF A GENERALISED EQUATION

Consider a fluid system with energy levels, such that it changes state under different energy levels and each state is partitioned and has minimal interaction with the previous state. It is possible to develop a simple equation to show the behaviour of the change of state of the system using the partition function principle

Given different states of the systems, as $S_i = \pm 1$

Assuming $S_1 = 1$; $S_2 = 1$; ….. $S_N = 1$

The partition function can be written as

$$Z = \sum_{S_i} \exp\left(\beta \mu_B \sum_{i=1}^{N} s_i B \right) \text{.......(3.1)}$$

Where

μ_B is the Bhor Magneton

B = the volume of the system

$E_{\{S_i\}} = \mu_B \sum_{i=1}^{N} s_i B$ is the energy of each state

Where:

The generalised equation can be re written as:

$$\sum_{S_1 = \pm 1} \sum_{S_2 = \pm 1} ….. \sum_{S_N = \pm 1} \exp\left(\beta \mu_B \sum_{i=1}^{N} S_i B \right) \text{……. (3.2)}$$

Expressing in canonical form,

$$\sum_{S_1=\pm1} \sum_{S_2=\pm1} \ldots \sum_{S_N=\pm1} \prod_{i=1}^{N} \exp(\beta\mu_B s_i B) \ldots\ldots (3.3)$$

Therefore:

$$\sum_{S_1=\pm1} e^{\beta\mu_B S_1 B} \sum_{S_2=\pm1} e^{\beta\mu_B S_2 B} \ldots \sum_{S_N=\pm1} e^{\beta\mu_B S_N B} \ldots\ldots (3.4)$$

Introducing the density operator

$$\rho = \frac{1}{z}\exp(-\beta H)$$

Where: $z = \sum_i \exp(-\beta E_i)\ldots\ldots(3.5)$

And

$$\beta = \frac{1}{K_B T} \ldots\ldots (3.6)$$

Therefore $Z = tr\exp(-\beta H)$ at

$trp = 1$

$$Z = \sum_n \exp(-\beta E_n)\ldots\ldots (3.7)$$

Where:

$$E_n = \frac{E_i}{v}\ldots\ldots (3.8)$$

E_i is the energy of the state

v = volume of partition

Consider an isolated assembly of subsystems, with minimal interaction to energy and matter. The partition function can be written as

$$Z = \sum_n \exp(-\beta E_n) = \sum_{S_{i=1}} \exp\frac{E_i}{vk_BT} + \sum_{S_{i=2}} \exp\frac{E_i}{vk_BT} + \sum_{S_{i=3}} \exp\frac{E_i}{vk_BT} + \ldots \quad \ldots (3.9)$$

Assuming that the number of molecules is not fixed Equation (3.9) becomes

$$\sum_n \exp(-\beta E_n) = \sum_{S_{I=1}} \exp\frac{E_i}{Nk_BT} + \sum_{S_{i=2}} \frac{E_i}{Nk_BT} + \sum_{S_{i=3}} \frac{E_i}{Nk_BT} + \ldots \quad \ldots (3.10)$$

$$\sum_n \exp(E_n) = \sum_{S_{i=1}} E_i + \sum_{S_{i=2}} E_i + \sum_{S_{i=3}} E_i \ldots \quad \ldots (3.11)$$

But PV=nRT

Since $Z = \exp \beta E_i$

$$\log Z = \beta E_i$$

$$E_i = \frac{\log Z}{\beta} = PV \ldots (3.12)$$

Since the entire system is partitioned, we assume it is isothermal, therefore equation (10) can be expressed in terms of pressure as:

$$PV_n = (PV)_1 + (PV)_2 + (PV)_3 + \ldots \ldots (3.13)$$

Where 1, 2, 3 represent the different phases in the system.

Equation (3.12) becomes the equation of states for a coexisting multistate fluid. It is note worthy that S is the energy level of each partition; B also refers to the volume of clusters or number of clusters.

3.2 APPLICATION OF GENERALISED EQUATION TO THE DEVELOPMENT OF EQUATION FOR PHASE EQUILIBRIA BETWEEN SOLID LIQUID AND GAS PHASE.

For a solid, the attractive contribution is assumed to be more pronounce due to an increase in density of the system. This chapter proposes a methodology for developing an equation of states for solid by modifying the repulsive contribution and further introducing an attractive parameter for the solid phase. Equation (3.12) forms the basis for you of perturbation in equation of state development.

Isehunwa (2004) suggested that for a thermodynamically closed system containing multicomponent fluids,

$$P = f(\rho, T, n) \ldots\ldots\ldots(3.2.1)$$

Therefore expanding gives:

$$P = a_0 + a_1\rho + a_2T + a_3n + a_1a_2\rho T + a_1a_3\rho n + a_2a_3Tn + a_{11}\rho^2 + a_{22}T^2 + a_{33}n^2 \ldots\ldots..(3.2.2)$$

The equation introduced the concept of non-physical forces in the development of the equation of states development, which is responsible for solid phase development. If we consider their interaction, we assume that forces act to bring about these phase changes.

Therefore, each molecule contributes an attractive and repulsive pressure on the total system. In terms of the perturbation theory, the total compressibility can be expressed as

$$Z = 1 + Z_0 + Z_1 + Z_2 + \ldots (3.2.3)$$

Where the first term is the contribution of the ideal gas to the rigid sphere. Z_0 is the hard sphere compressibility due to the repulsive term or the unperturbed chain (Vafaie-Sefti et al, 2003). Where Z_1 and Z_2 are the contribution due to the attractive term, Z_1 being the stronger short

range contribution and Z_2 being the long weak range contribution. Carnahan and Starling (1972) suggested that a system consists of a rigid sphere contribution, a soft repulsive, and a cohesion pressure term.

$$P = P_{rs} + \phi(T,V) ....(3.2.4)$$

Where P_{rs}= rigid sphere pressure

$\phi(T,V)$= Soft repulsive and cohesion pressure term.

For a system of n molecules, the pressure contribution to the system can be expressed as:

$$P = P_1 + P_2 + P_3 + ...(3.2.5)$$

From equation (3.2.3)

$$PV = Zk_B T ....(3.2.6)$$

Substituting in equation (3.13)

$$Zk_B T = Z_0 K_B T_0 + Z_1 K_B T_1 + Z_2 K_B T_2 ....(3.2.7)$$

Therefore, if we consider the ideal and non-ideal contributions to the system equation (3.2.7) can be written as:

$$\frac{P}{k_B T} = 1 + \frac{P_1}{k_B T_1} + \frac{P_2}{k_B T_1} + ...(3.2.8)$$

Where the first term accounts for the ideal term. Therefore, the equation of compressibility for a system can be generalised as:

$$Z = Z_1 + Z_2 + Z_3 + ...(3.2.9)$$

The first term in the equation is called the hard sphere compressibility or the hard sphere repulsive term and can be represented by the equation

$$Z_{rep} = \frac{1}{1-b\rho} \text{........}(3.2.10)$$

Equation (3.2.8) identifies three major contributions to the system of hard sphere; the attractive terms, Z_2; the repulsive term Z_1 and other contributions to the attractive hard sphere attractive term. Z_3+... it is similar to the suggestion of Elliot *et. al.*, (1990) for equation of state for hard sphere, as the sum of the attractive and repulsive parameters,

$$Z= 1+Z_{rep}+Z_{att}\text{...........}(3.2.11)$$

While Isehunwa,(2004) described a generalized cubic equation of pure fluids as the sum of the different forces that describe the system.

$$P = P_{\text{repulsive forces}}+ P_{\text{attractive forces}} + P_{\text{non-physical forces}} \text{ .... } (3.2.12)$$

Equation (3.2.11) also show the possibility of having a continuous addition of the attractive forces in a system as it changes phase. It also show the possibility of these additional terms becoming more or less significant in the system.

In describing equation formulation for a gaseous system we may refer to the first and second terms of the cubic equation of state while for a liquid system both second and addition terms will be considered the first term also refers to the contribution of pressure due to repulsive term Shah (1992). By the addition of the repulsive parameter b. Carnahan-Starling generalised the repulsive term of the hard sphere based on expansion of the rigid hard sphere as:

$$Z_{hs} = \frac{1+\eta+\eta^2+\eta^3}{1-\eta^3}\text{........}(3.2.13)$$

Where y is the packing fraction represented as:

$$\eta = \rho \frac{N_A \pi d^3}{6}\text{........}(3.2.14)$$

3.2.1 Development of the Repulsive Term

The van der Waals equation represented the repulsive term contribution to pressure by the equation:

$$P_R = \frac{RT}{V-b} \dots\dots(3.2.15)$$

This contribution does not agree to the Monte-Carlo simulation for hard-sphere, by introducing the hard sphere compressibility Z_{hs} as.

$$Z_{hs} = \frac{1}{1-b\rho} \dots\dots(3.2.16)$$

We can therefore re-write equation (3.2.15) as

$$PV = \frac{RT}{1-b\rho} \dots\dots(3.2.17)$$

We consider the generalised real gas equation of state for a system

$$PV = ZnRT \dots\dots(3.2.18)$$

Assuming n=1

For the First term in equation (3.2.9)

$$Z_1 = \frac{P_1 V_1}{RT_1} \dots\dots(3.2.19)$$

But:

$$\rho = \frac{1}{V}$$

Therefore:

$$Z_1 = Z_{hs} = \frac{1}{v\left(1-\frac{b}{v}\right)} = v\left(1-\frac{b}{v}\right)^{-1} \quad ....(3.2.20)$$

From the Viral Equation

$$Z = \frac{PV}{RT} = 1 + \frac{B}{V} + \frac{C}{V^2} + \frac{D}{V^3} ....(3.2.21)$$

And

$$z = \frac{PV}{RT} = \frac{1}{1-\eta} ....(3.2.22)$$

Expanding gives equation (3.2.21) gives:

$$Z = 1 + \eta + \eta^2 + \eta^3 + \eta^4 + ...(3.2.23)$$

In terms of density

$$Z = 1 + b\rho + b^2\rho^2 + b^3\rho^3 + b^4\rho^4 + ...(3.2.24)$$

This forms the basis for the development of the virial expression for the van der waals repulsion term as expressed by Isehunwa (2004)

$$P_R = RT\rho\left(1 + 4\eta + 16\eta^2 + 64\eta^3 + 256\eta^4....\right)........(3.2.25)$$

By considering the Virial form of equation (3.2.21) is expressed as

$$Z = \frac{PV}{RT} = \left(1 + \frac{b}{V} + \frac{b}{V^2} + \frac{b}{V^3} + ...\right) - \frac{a/RT}{V} ....(3.2.26)$$

Therefore, equation (3.2.25) can be written as

$$V^{-1}\left(1-\frac{b}{V}\right)^{-1} = \left(1 + \frac{b}{V} + \frac{b}{V^2} + \frac{b}{V^3} + ...\right) ....(3.2.27)$$

For an ideal system,

$$\rho = \frac{1}{V} \text{.......(3.2.28)}$$

Equation (3.2.26) becomes

$$\rho\left(1-\frac{b}{v}\right)^{-1} = \rho\left(1+\frac{b}{V}+\frac{b}{V^2}+\frac{b}{V^3}+....\frac{b}{V^{n-1}}\right)\text{........(3.2.29)}$$

(Elliot *et al.*, 1990) based on simulation data suggested a generalised equation of sphere for the hard sphere repulsive term

$$P_R = \frac{c\left(4\eta - 2\eta^2\right)}{1-\eta^3}\text{........(3.2.30)}$$

Where c is density dependent parameter

Substituting equation (3.2.27) into equation (3.2.30) gives

$$P_R = \frac{4\rho\left(1+\frac{b}{V}+\frac{b}{V^2}+\frac{b}{V^4}+....\right)}{1-\left(1+\frac{b}{V}+\frac{b}{V^2}+\frac{b}{V^3}+....\right)^3} - \frac{2\rho\left(1+\frac{b}{V}+\frac{b}{V^2}+\frac{b}{V^3}\right)}{1-\left(1+\frac{b}{V}+\frac{b}{V^2}+\frac{b}{V^3}+\right)^3}\text{........(3.2.31)}$$

Because of the mathematical complexities of solving Carnahan we propose a combination of the approach of the virial form of hard sphere compressibility with the equation suggested by Elliot et. al. (1990)

$$P_R = \frac{4RT\gamma}{\left(1-\eta\right)^r} - \frac{2RT\theta}{\left(1-\eta\right)^r}\text{........(3.2.32)}$$

Where r is a positive integer and γ, θ are density dependent parameters.

Further simplification gives:

$$P_R = \frac{RT(1-\theta)}{(1-\eta)^r} \ldots\ldots(3.2.33)$$

Assuming $\theta = 0$ and r=1 equation (3.44) can be written as

$$P_R = \frac{RT}{(v-b)} \ldots\ldots(3.2.34)$$

3.2.2 Development of the attractive term

The attractive term of Redich-Kwong Equation of state is used in this study and is expressed as:

$$P_{att} = -\frac{a(T)}{V(V+b))} \ldots\ldots(3.2.35)$$

Where a (T) the temperature dependent attractive parameter defined as:

$$a(T) = a_c \alpha(T) = 0.45724 \frac{R^2 T_c^2}{P_c} \alpha(T) \ldots\ldots(3.2.36)$$

3.2.3 Development of the Transition term

The invariant energy of a system can be expressed as the summation of the individual energies of a system and can be expression from equation (3.11) as:

$$E_i = E_1 + E_2 + E_3 + E_4 + \ldots + E_n \ldots\ldots(3.2.37)$$

In terms of attractive and repulsive and the contribution of other terms equation (3.2.37) can be expressed as

$$E_i = E_{attractive} + E_{repulsive} + E_3 + E_4 + \ldots + E_N \ldots\ldots(3.2.38)$$

The energies $E_3 + E_4 + \ldots + E_n$ are undefined but contribute to the system; we can express their summation as:

$$E_N = E_3 + E_4 + ... + E_n.....(3.2.39)$$

Neglecting the ideal gas contribution, equation (3.2.38) becomes

$$E_i = E_{attractive} + E_{repulsive} + ... + E_N.....(3.2.40)$$

E_N is the summation of all undefined energies acting on the system.

Equation (3.2.40) can be expressed in terms of equation (3.12) as:

$$(PV)_i = (PV)_{attractive} + (PV)_{repulsive} + (PV)_N ....(3.2.41)$$

Let:

$$(PV)_N = c ...... (3.2.42)$$

The parameter c is the transition parameter that describes the additional pressure contribution to the system, and tends to increase relatively with a decrease in the co volume parameter b.

Expressing in terms of pressure, and considering the additional effect of molecules on the total system volume:

Equation (3.2.41) becomes:

$$P = \frac{c}{V+b} ....(3.2.43)$$

Where a (T) and c are substance dependent parameters and a(T) is a function of temperature. The equation of state can be expressed as the sum of the attractive and repulsive and transition contributions to pressure, but combining equations (3.2.34) and (3.2.35) may not give a positive equation of state. We therefore assume that $r = \phi = 1$ this will give the equation:

$$P = \frac{RT}{(V-b)} - \frac{a(T)}{V(V+b)} - \frac{c}{(V+b)} ....(3.2.44)$$

This work has the modified form of the equation of state suggested by Isehunwa (2000), by replacing the temperature dependent attractive term $\dfrac{c(T)}{V}$ with a more general term $\dfrac{c(T)}{(V+b)}$,

Where the temperature dependent attractive parameter a is defined as:

$$a = a_{fit}\, a(T) \ldots\ldots (3.2.45)$$

The temperature dependency of the attractive parameter $\alpha(T)$ is taken into account with the help of a modified α function.

$$\alpha(T) = T_r^{2(m-1)} \times e^{\frac{L\left(1-T_r\right)^{MN}}{2N^2}} \ldots\ldots (3.2.46)$$

The α function suggested in equation (3.2.46) was based on a combination of the twu-modified alpha function and normal alpha distribution equation this leads to better results especially at highly reduced temperatures. The L, M, N in equation are determined by fitting to pure component vapour pressures and liquid densities.

The co-volume parameter b is defined as:

$$b = b_{fit}\, b_p \ldots\ldots (3.2.47)$$

Where:

$$b_p = 0.0778 \frac{RT_c}{P_c} \ldots\ldots (3.2.48)$$

The transition parameter c is defined as:

$$c = c_{fit}\, c_p \ldots\ldots (3.2.49)$$

c_p is defined from the equation:

$$c_p = 0.252 \frac{RT_c}{P_c}(1.5448Z_c - 0.4024)........(3.2.50)$$

a$_{fit}$, b$_{fit}$ c$_{fit}$ is are fitted to vapour pressures and liquid densities.

3.2.4 Method Cubic Equation of state parameter Estimation by Line Fitting

The parameters are fitted to the vapour pressure and PVT data using the Generalised Reduced Gradient (GRG) non-linear minimization program, the objective function minimized in this study is the root sum of squares errors function defined by the expression:

$$\text{Objective function} = \sqrt{\sum_{i=1}^{k}\sum_{j=1}^{m}\left(x_{ij}^{\exp} - x_{ij}^{est}\right)^2}........(3.2.51)$$

Where;

i=Data point number with a group

j=Measured variables for a data point

k=Total Number of point in a data group

m=Number of points in a data group.

x is the measured or calculated variable.

3.2.5 Cubic Form of Equation

Equation (3.2.42) can be re-arranged to give the cubic form as follows:

$$V^3 - \left[\frac{RT}{P} + \frac{C}{P}\right]V^2 - \left[b^2 - \frac{RTb}{P} + \frac{a}{P} - \frac{Cb}{P}\right]V - \frac{ab}{P} = 0........(3.2.52)$$

Letting

$$A = \frac{aP}{R^2T^2}..........(a)$$

$$B = \frac{bP}{RT} \ldots\ldots(b)$$

$$C = \frac{cP}{RT} \ldots\ldots(c)$$

Equation (3.2.52) can be expressed in terms of compressibility factor as:

$$Z^3 - [1+C]Z^2 - Z\left[B^2 + B + A + BC\right] - AB = 0 \ldots\ldots(3.2.53)$$

The critical volume can be determined by solving equation 3.2.44 as a quadratic method and assuming that at the critical point,

$$P = \frac{RT}{(V_c - b)} - \frac{a(T)}{V_c(V_c + b)} - \frac{c(T)}{V_c + b} \ldots\ldots(3.2.54)$$

Using the expression suggested by Ikoku (1984):

$$\frac{P}{P_c} = \left(\frac{Z}{Z_c}\right)\left(\frac{V_c}{V}\right)\left(\frac{T}{T_c}\right) \ldots\ldots(3.2.55)$$

The compressibility factor can be written as:

$$Z = Z_c\left[\frac{P_r V_r}{T_r}\right] = \frac{V_r}{V_r - b_r} + \frac{a_r}{(V_r + b_r)T_r} + \frac{c_r V}{Z_c(V_r + b_r)T_r} \ldots\ldots(3.2.56)$$

Where;

$$Z_c = \frac{P_c V_c}{RT_c} \ldots\ldots(d)$$

$$P_r = \frac{P}{P_c} \ldots\ldots(e)$$

$$T_r = \frac{T}{T_c} \ldots\ldots(f)$$

$$V_r = \frac{V}{V_c} \ldots\ldots(g)$$

$$a_r = \frac{a}{V_c} \ldots\ldots(h)$$

$$b_r = \frac{b}{V_c} \ldots\ldots(i)$$

$$c_r = \frac{c}{V_c} \ldots\ldots(j)$$

3.2.6 Extension of Cubic Equation to Mixtures

 The van der waals one fluid mixing rule are used for determining the mixture parameters of the equation:

$$a = \sum_i \sum_j x_i x_j a_{ij} \ldots\ldots(3.2.57)$$

Where:

$$a_{ij} = \left(1 - k_{ij}\right)\left(a_i a_j\right)^{\frac{1}{2}} \ldots\ldots(3.2.58)$$

$$b = \sum_{i=1}^{N} b_i x_i \ldots\ldots(3.2.59)$$

$$c = \sum_{i=1}^{N} c_i x_i \ldots\ldots(3.2.60)$$

3.2.7 Fugacity Expression:

The first step to determining the solid liquid behaviour of mixtures is to define an expression for fugacity, the fugacity coefficient of a component at any given phase is calculated from the thermodynamic equation of Danesh, (1998)

$$\phi_i = \frac{1}{RT} \int_v^\infty \left[\left(\frac{\partial P}{\partial n_i} \right)_{T,n,V,n_j} - RT/V \right] dV - \ln Z \text{........(3.2.59)}$$

The derivation of the fugacity equation for the equation of state formulation is achieved by incorporating, equation (3.2.44) in equation (3.2.59) to obtain.

$$\ln \phi = (z-1) - \ln Z + \frac{1}{RT} \left[-\frac{1}{RT} \ln \frac{V}{V-b} + \frac{a}{b} \ln V(V+b) + c \ln(V+b) \right]_b^V \text{........(3.2.60)}$$

Simplifying further gives:

$$\ln \phi = (Z-1) - \ln Z - \ln(Z-B) + \frac{A}{B} \ln \left(1 + \frac{B}{Z} \right) + C \ln(Z+B) \text{........(3.2.61)}$$

The phase liquid-solid phase equilibrium is given in terms of fugacity as

$$\phi_i^L = \phi_i^V \text{.........(3.2.62)}$$

Where L, V indicate the liquid and vapour phases respectively and i represent the specie. For a liquid- solid phase formulation at equilibrium, the fugacity of the ith component in the liquid and solid phase can be expressed as.

$$\ln \left(\frac{\theta_V}{\theta_L} \right) = Z_V - Z_L - \ln \left(\frac{Z_V}{Z_L} \right) - \ln \left(\frac{Z_V - B}{Z_L - B} \right) - \frac{A}{B} \left(\frac{Z_V + B}{Z_L + B} \right) \left(\frac{Z_V}{Z_L} \right) - C \ln \left(\frac{Z_V + B}{Z_L + B} \right) \text{........(3.2.63)}$$

For each n component in a mixture, the equation of state can be expressed in terms of fugacity as:

$$\ln \phi_i = (Z-1)B' - \ln Z - \ln(Z-B) + \frac{A}{B}(A_i - B_i) \ln \left(1 + \frac{B}{Z} \right) + C_I \ln(Z+B) \text{........(3.2.64)}$$

Where,

$$A' = \left(1/2 \sum_{i,j=1}^{N} \left(1 - k_{ij}\right)\left(a_i a_j\right)^{\frac{1}{2}} \right) \ldots\ldots(3.2.65)$$

$$B' = \frac{b_i}{b} \ldots\ldots(3.2.66)$$

<center>**CHAPTER FOUR**</center>

<center>**RESULTS AND DISCUSSION**</center>

4.1 Application of Equation of State to Pure Component Fluids

The parameters a, b and c in equation (3.2.44) were obtained by fitting to vapour pressures and liquids densities of the pure components used in this study and expressing the parameters in terms of critical temperatures and pressures. The vapour pressures and densities of nitrogen were obtained from the works of Von Siemens (1913), Friedman and White (1950), Yang (1991), Giauque and Clayton (1933) and Dortmund Data Bank. carbon dioxide, methane propane, ethane, butane pentane hexane and hexadecane data were obtained from Chemical Engineering and Materials Research Centre (CHERIC) and Dortmund Data Bank (DDBST). The temperature dependent attractive parameters of the equation were determined at temperatures of 190.0K, 305.3K, 514K, 369.8K, 425K, 469.7K, 723K, 507.6K, 562K for methane, ethane, ethanol, propane butane, pentane, hexadecane, hexane, benzene, respectively. The Generalised Reduced Gradient method of nonlinear optimization was used in the data fitting. The objective function minimized in the study is the root sum of squares errors function defined in equation (3.51). The average absolute deviation in percentage (AAD %) is calculated as

$$ADD\% = \frac{1}{N} \sum_{1}^{N} \left| \frac{X_i^{est} - X_i^{\exp}}{X_i^{\exp}} \right| *100 ....(4.1)$$

The results of the fitted parameters for the α-function, estimated parameters obtained using the critical properties for the model and the fitted equation of state parameters a, b, c parameters are shown in tables (4.1), (4.2) and (4.3). The temperature dependent α function used in this study was a modification of the Twu alpha function predicted at reduced temperatures <0.7 when applied to the equation used in this study. The Function was used to derive a temperature

<center>103</center>

dependent attractive parameter a (α) of the study equation, the parameters of the α function was

obtain by fitting equation to vapour pressure.

Table 4.1: Pure Components and Fitted L, M, N Parameters for the α Function used

Component	T_c (K)	L	M	N
Methane	190.0	0.180787	1.564285	0.845343
Ethane	305.3	0.200716	1.564869	0.839857
Propane	369.8	0.212854	1.565919	0.836344
Butane	425	0.197939	1.564697	0.840636
Pentane	469.7	0.199012	1.565035	0.840302
Hexane	507.6	0.863192	1.526228	1.532501
Hexadecane	723	0.183575	1.564527	0.844522
Ethanol	514	0.367192	1.584014	0.649084
Benzene	562	0.179273	1.564281	0.485727

Table 4.2: Parameters for the Proposed Model

Component	T_c (K)	P_c (atm)	a(T)	b	c
Methane	190	45.388	1446232	1.1221	3.7365
Ethane	305.300	48.083	3889361	1.5841	5.0877
Propane	369.800	41.925	6294171	56.306	0.511
Butane	425	37.464	14841495	3.6817	5.1617
Pentane	469.7	33.259	886113	5.1724	0.862
Hexane	507.6	29.850	17567415	4.783455	2.211
Hexadecane	723	13.820	83255792	289.811	-64.980
Ethanol	514	60.567	100800	54.173	-3.276
Benzene	562	48.310	20125495	2.905	4.1382
Nitrogen	126.2	33.8	1463907	4.9786	2.285
CO2	304.19	72.8	3912711.3	0.6342	1.817

Table 4.3: Fitted Pure Component Parameters

Components	a	b	c	Normalization Error
Nitrogen	1.000099	0.207034	1.143209	$9.56000*10^{-10}$
Carbon dioxide	1.000041	0.023770	1.022507	$5.58985*10^{-7}$
Ethane	1.000041	0.039083	1.036064	$4.88850*10-8$
Propane	0.98595	0.000190	0.013510	0.0000016
Hexane	1.000021	0.044067	1.040660	$4.73471*10^{-14}$
Hexadecane	1.00000	0.867815	1.000000	$5.20765*10^{-14}$
Butane	1.000029	0.050842	1.046427	$1.1327*10^{-8}$
Pentane	1.000026	0.005737	1.051317	$1.87*10^{-9}$
Ethylene	0.99959	-0.00084	0.999601	0.000023
Hexane	1.000018	0.017547	1.018892	$7.80395*10^{-10}$
Benzene	1.000022	0.039123	1.039735	$1.22*10^{-7}$

The equation (3.2.44) represents the final equation for this study, and was validated by applying it to pure component hydrocarbons under varying conditions of pressure and temperature. The vapour pressure curves for the pure component fluid used in this study are show in figures 4.1- 4.10; it was observed that for that. The equation modelled the temperatures and pressures of pure components both above and below their triple points. The study was compared with Van der waals Equation of States, Peng Robinson Equation of states (PR EOS) and Redlich-Kwong Equation of State (RK EOS). From the results, the VDW EOS, PR EOS and RK EOS under predicted at higher-pressure values while the model Equation gave a better prediction when compared to experimental results. The study also has a strong agreement between Van-der-Waals equation of states (VDW EOS), Peng-Robinson of states (PR EOS) and Redlich-Kwong Equation of State (RK EOS). The Parameters obtained from estimation of the critical properties for pure gases and fluids using the model equation are shown in Table (4.2). The compressibility factors of the gases and pure fluids were obtained by solving equation (3.2.53), at temperatures lower than the critical temperature of pure gases and fluids, the results were compared with PR EOS as shown in table (4.4). The model was used to calculate the pressure mole fraction phase envelope for ethanol + benzene, benzene + hexane, hexane + ethanol and methane + propane mixtures, using the Van-der-Waals one fluid mixing rule, equation (3.2.57) to (3.2.60).

Table 4.4: Pure component Z factors for some Pure Hydrocarbons PR EOS Versus model Equation

Component	T(K)	P(atm)	PR EOS			Study		
			Z1	Z2	Z3	Z1	Z2	Z3
Methane	112.65	1.085	0.967	0.026	0.00363	1.021	0.01	0.0031
Ethane	197.885	1.955	0.94	0.039	0.0063	1.033	0.027	0.001
Propane	230.15	0.954	0.967	0.025	0.0035	1.019	0.020	0.0035
Butane	280.15	1.315	0.955	0.034	0.0053	1.029	0.023	0.0056
Pentane	286.96	0.57	0.973	0.021	0.0026	1.003	0.002	0.0020
Hexane	303.15	0.158	0.991	0.0074	0.00083	1.005	-	0.00085
Hexadecane	515.15	0.344	0.970	0.025	0.003	1.017	0.015	0.0027
Ethanol	201.94	$9.8*10^{-6}$	0.999	$9.0*10^{-7}$	$3.3*10^{-8}$	0.990	$2.7*10^{-5}$	$8.8*10^{-6}$
Benzene	363.72	1.345	0.963	0.029	0.0043	1.023	0.019	0.0034

Table 4.5: Model Parameters Used for the Mixtures

n	m	a_{mn}	b_{nm}	c_{nm}
C_2H_5OH	C_6H_8	2794456	75	1.487
CH_4	C_3H_8	16871129	158.272	21.314
C_2H_5OH	C_6H_6	21197543	333	17.890
C_6H_6	C_6H_{14}	79364888	630.39	33.79

Figure 4.1: Pressure Temperature diagram for CO2 comparing the suggested equation of State with PR EOS, VDW EOS, RK EOS and experimental data

Figure 4.2: Pressure Temperature diagram for nitrogen comparing the suggested equation of state with PR EOS, VDW EOS, RK EOS and experimental data

Figure 4.3: Pressure Temperature diagram for methane comparing the suggested equation of state with PR EOS, VDW EOS, RK EOS and experimental data
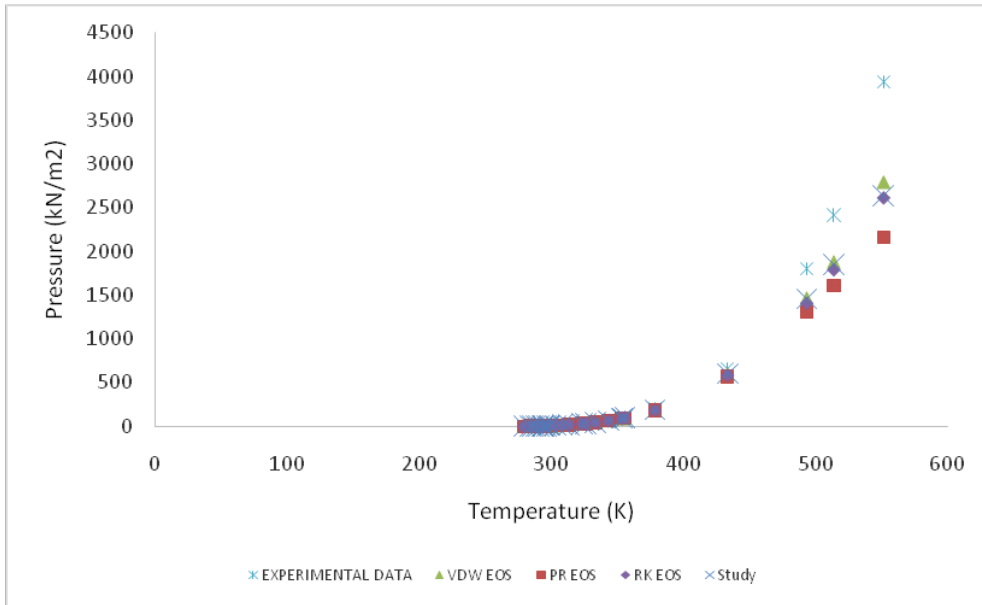
Figure 4.4: Pressure Temperature diagram for hexane comparing the suggested equation of state with PR EOS, VDW EOS, RK EOS and experimental data
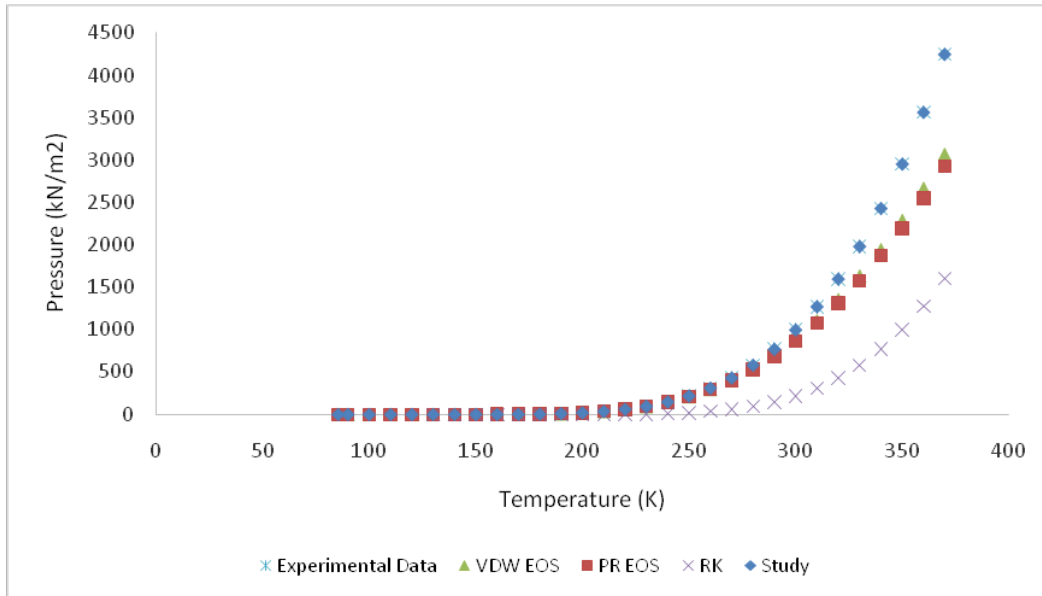
Figure 4.5: Pressure Temperature Diagram for Propane Comparing the suggested equation of State with PR EOS, VDW EOS, RK EOS and Experimental Data
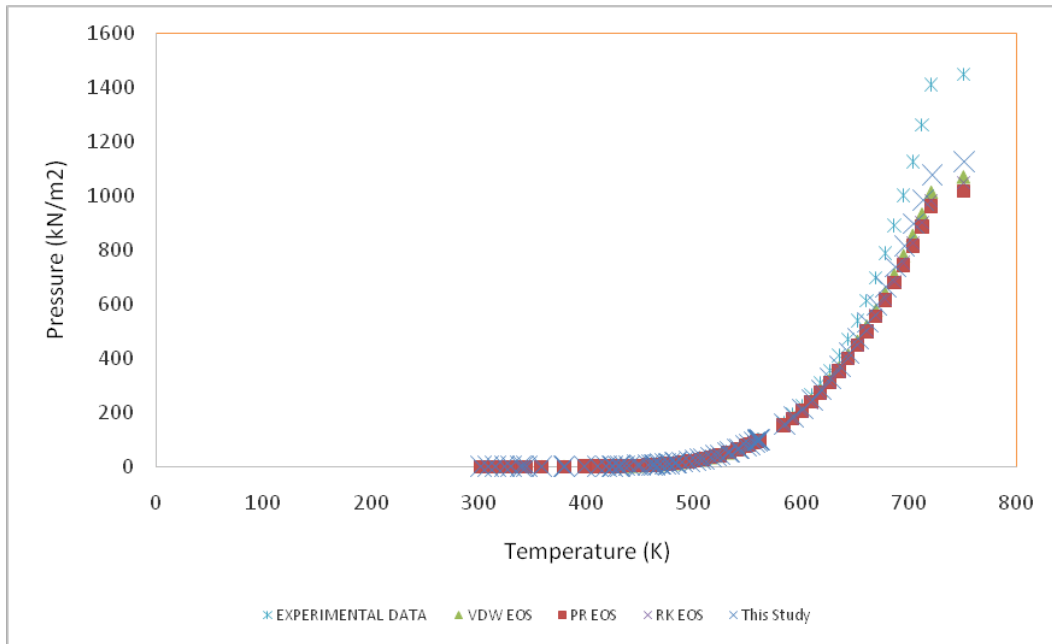
Figure 4.6: Pressure Temperature diagram for hexadecane comparing the suggested equation

of state with PR EOS, VDW EOS, RK EOS and experimental data
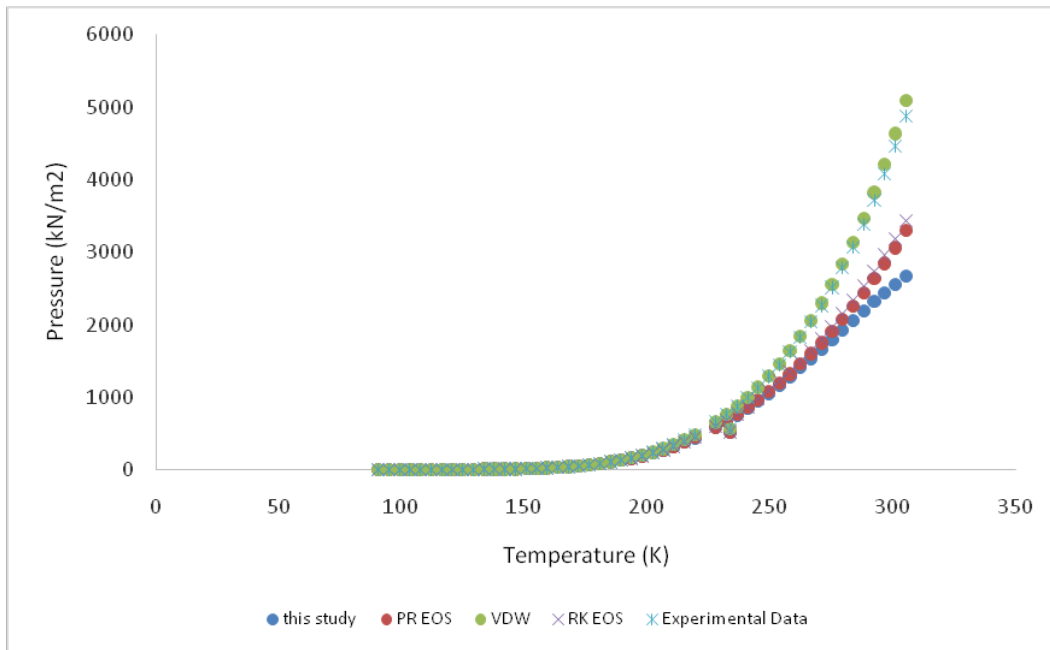
Figure 4.7: Pressure Temperature diagram for ethane comparing the suggested equation of dstate with PR EOS, VDW EOS, RK EOS and experimental data
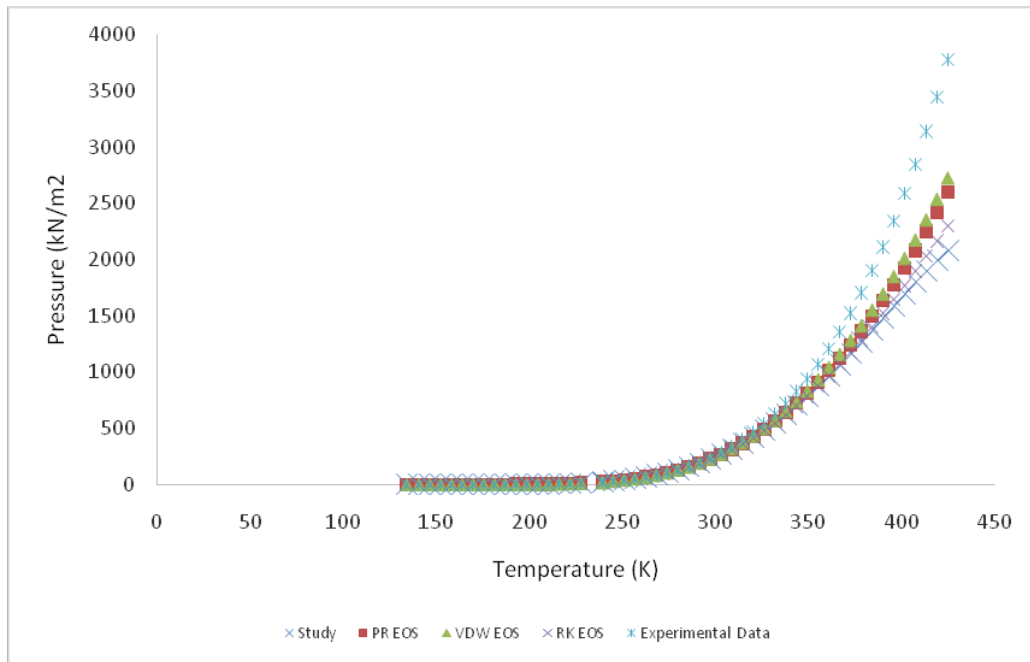
Figure 4.8: Pressure Temperature diagram for butane comparing the suggested equation of state with PR EOS, VDW EOS, RK EOS and experimental data
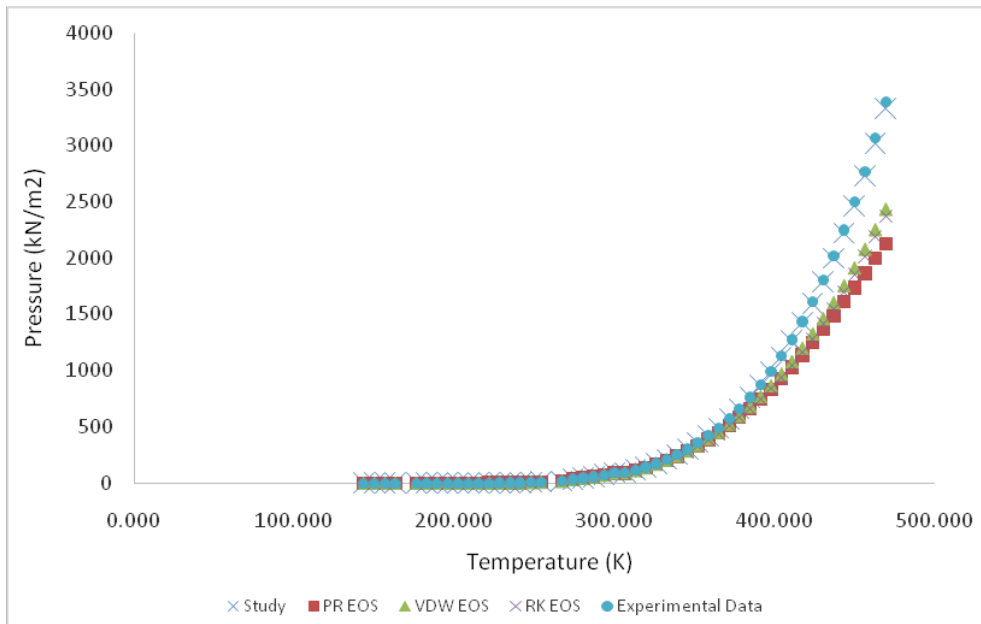
Figure 4.9: Pressure Temperature diagram for pentane comparing the suggested equation of state with PR EOS, VDW EOS, RK EOS and experimental data
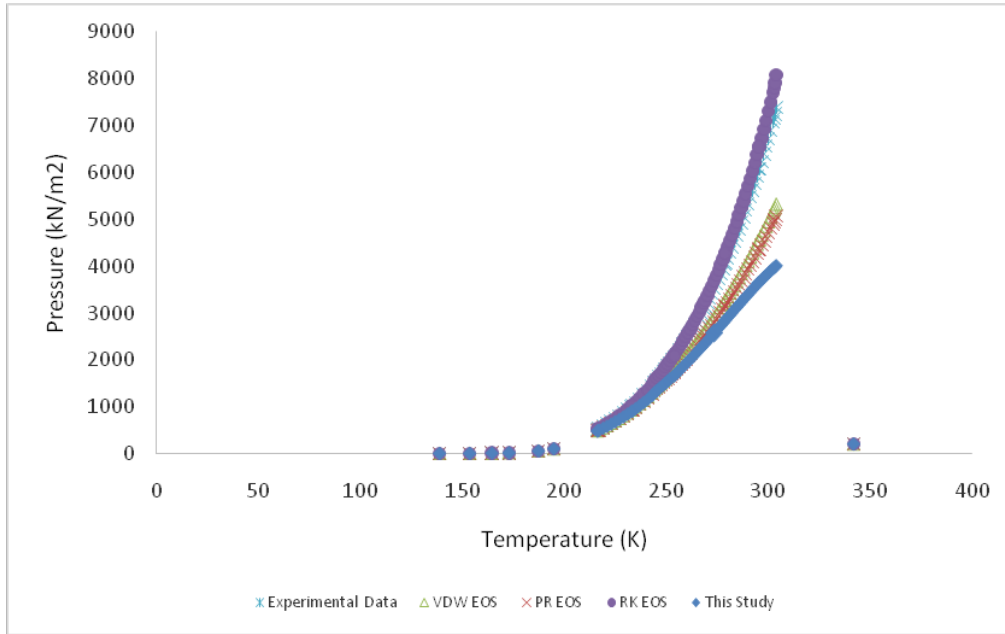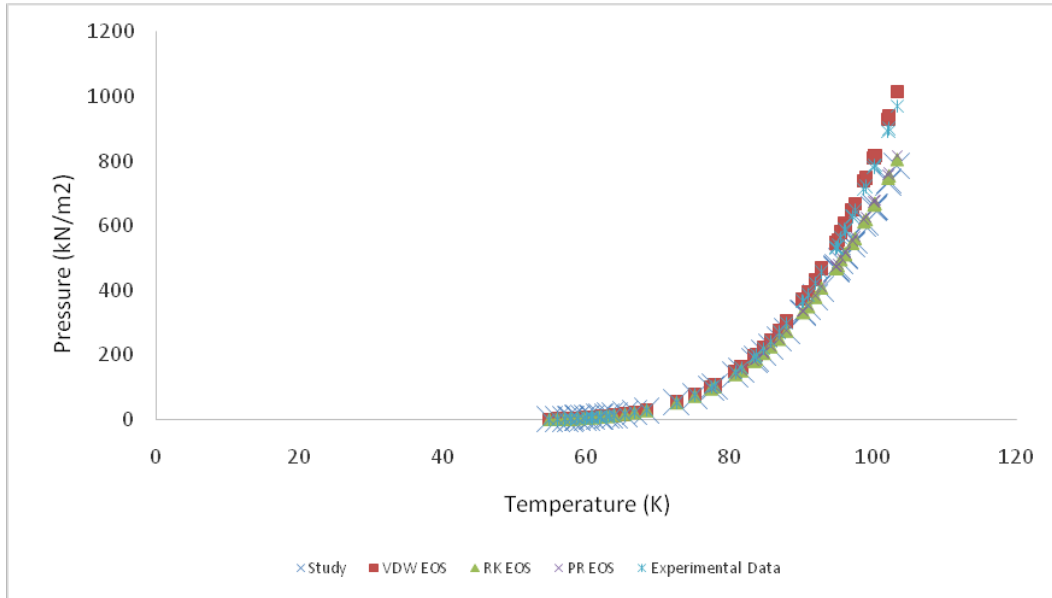
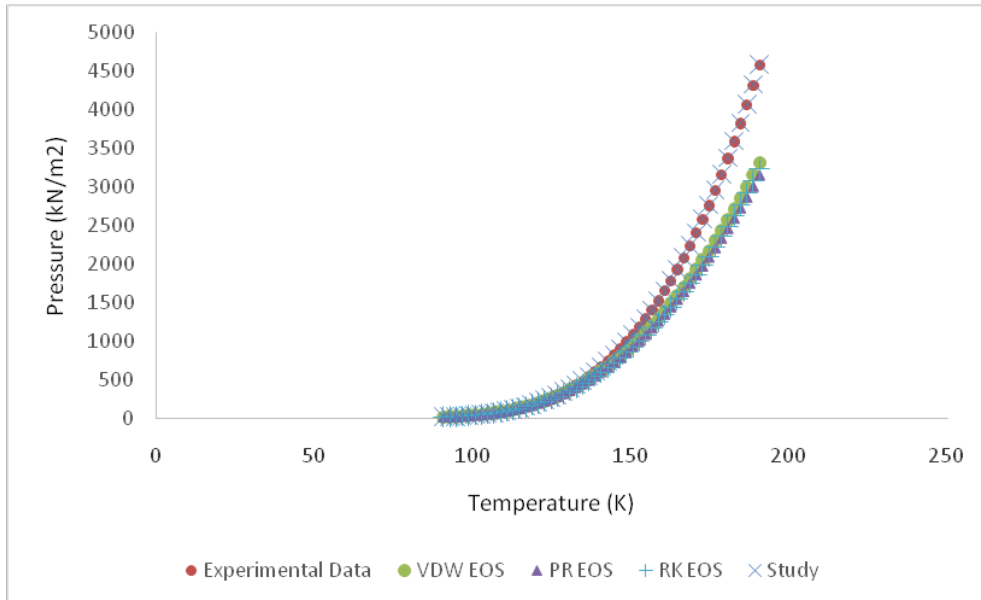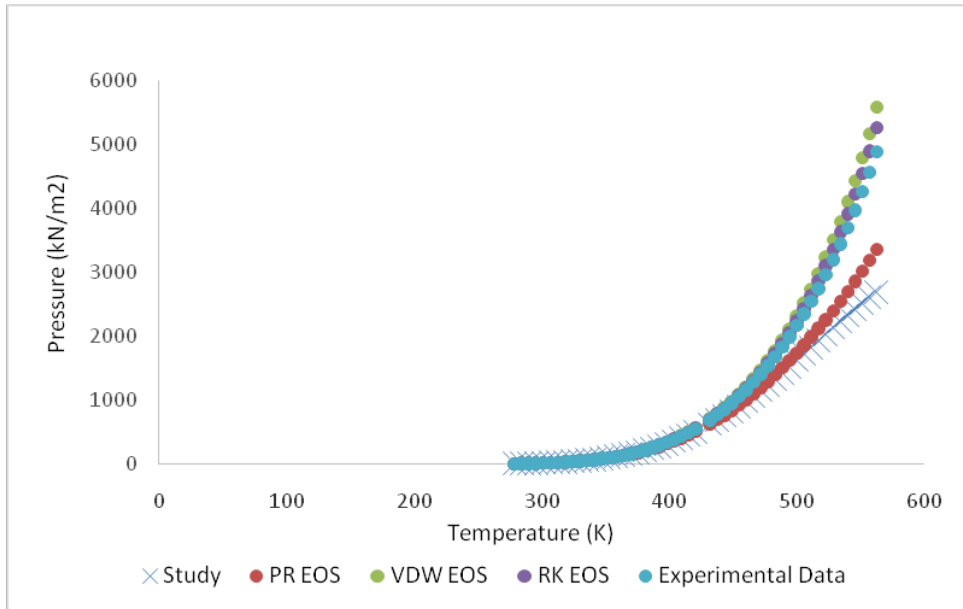Figure 4.10: Pressure Temperature diagram for benzene comparing the suggested equation of state with PR EOS, VDW EOS, RK EOS and experimental data
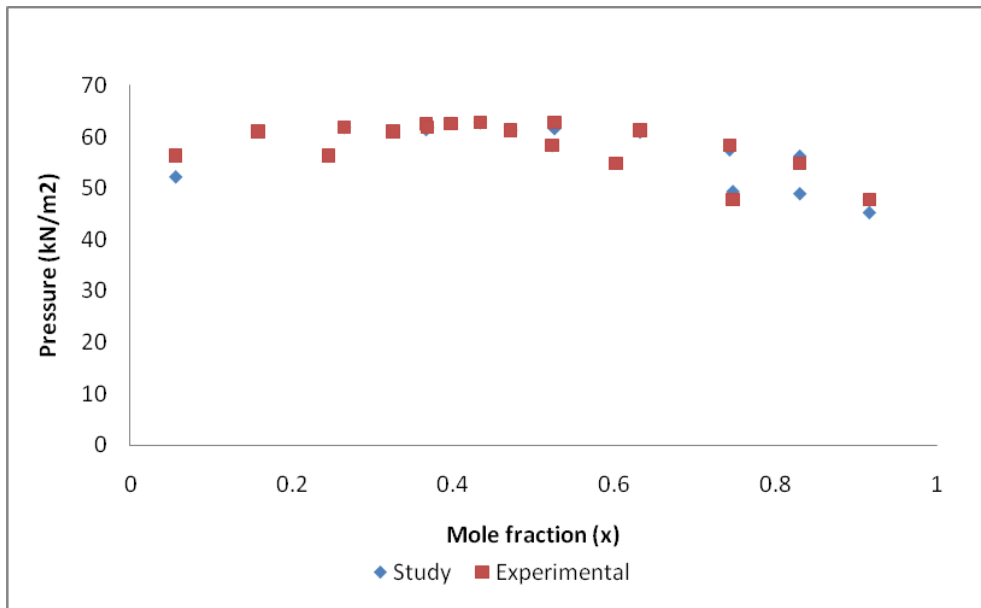
Figure 4.11: P-xy diagram for benzene-ethanol mixture at 328.15K, comparing the suggested Equation of State with experimental data
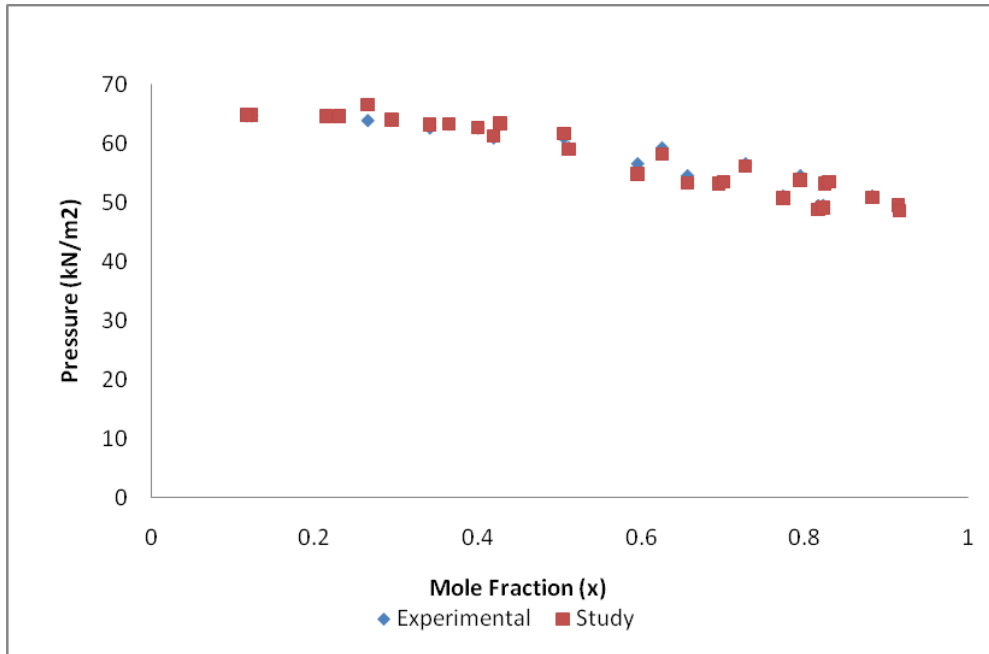
Figure 4.12: P-xy diagram for benzene-hexane mixture at 328.15K, comparing the suggested equation of state with experimental data
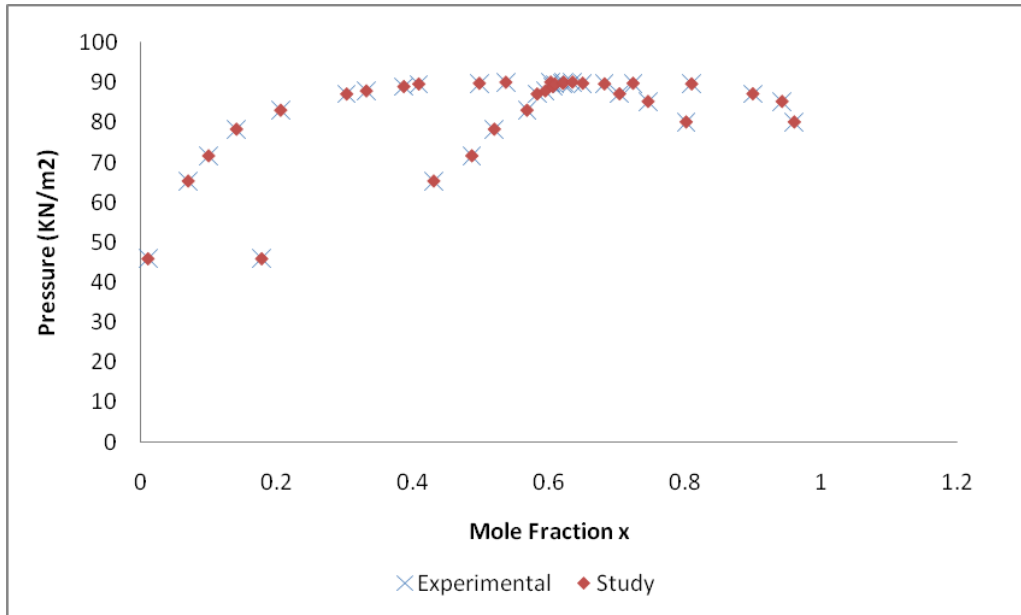
Figure 4.13: P-xy diagram for hexane- ethanol mixture at 328.15K, comparing the suggested

equation of state with experimental data
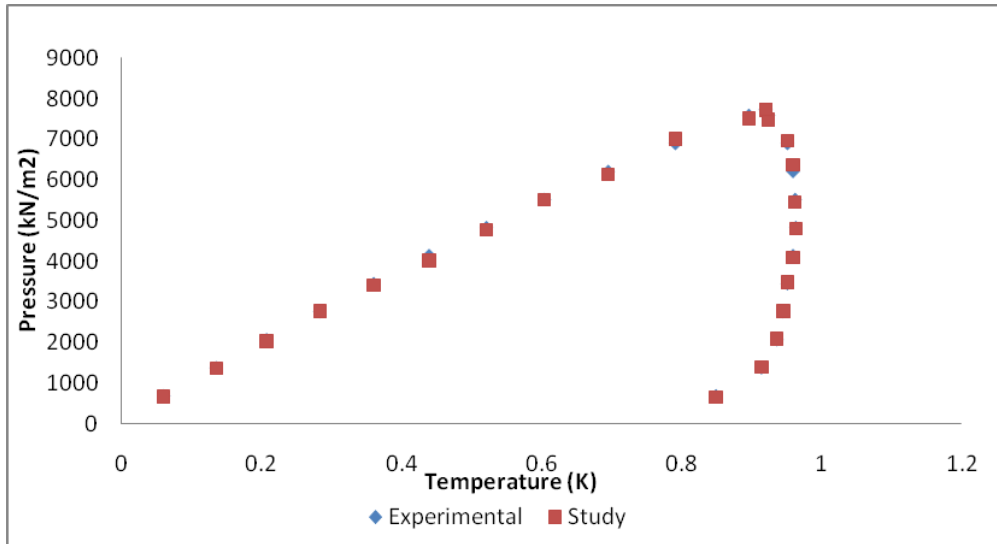
Figure 4.14: P-xy diagram for methane-propane mixture at 226.48K, comparing the suggested equation of state with experimental data
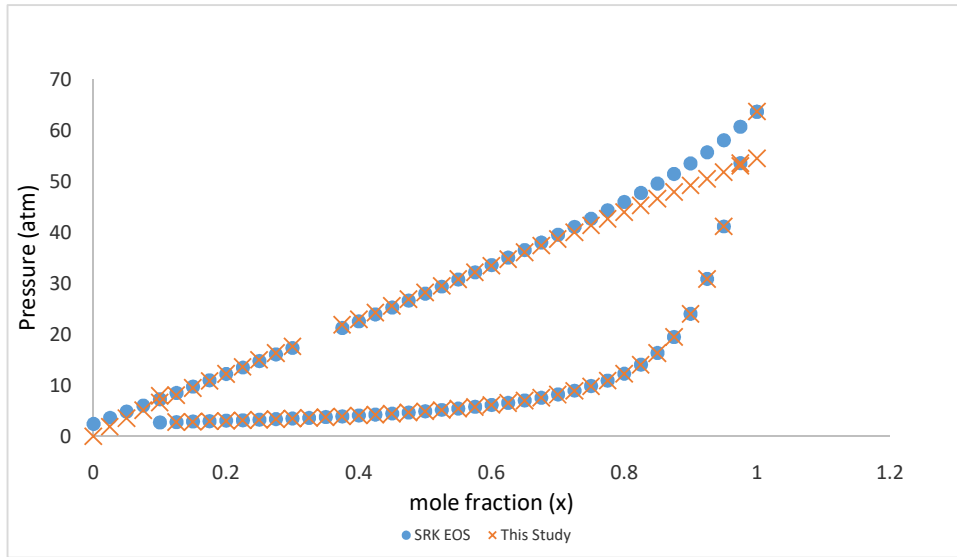
Figure 4.15: P-xy diagram for CO2 + n-hexane mixture at 298.15 K comparing the suggested equation of state with experimental data

4.2 APPLICATION OF EQUATION OF STATE TO CRUDE OIL

4.2.1 Crude Oil Characterisation

In other to characterise the reservoir fluid both the flash gas and the stock thank oil were considered. The flash gas was divided in six components N_2, CO_2, C1, C2, C3 and heavy Gases (C_4-C_7). The composition and PVT data for the different oils studied is shown in table (4.6). The molecular average of the heavy gases is slightly close to the molecular weight of pentane. The molecular weight averaging was done using the equation

$$Z_+ = \sum_{i=c_+}^{C_{max}} Z_i ....(4.2)$$

$$M_+ = \frac{\sum_{i=c}^{C_{max}} Z_i M_i}{\sum_{i=c}^{C_{max}} Z_i} ....(4.3)$$

Where C_{max} represents the heaviest carbon number considered and Z represents the mole fraction of different carbon numbers contained in the mixture. N_2 and CO_2 are modelled separately rather than as a pseudo component because they are non-hydrocarbon gases light gases.

Table 4.6: Composition and PVT Data for Cases Studied

Component	Case A	Case B	Case C
N2	0.0038	0.0003	0.0012
Co2	0.0064	0.002	0.0249
C1	0.7581	0.4183	0.7643
C2	0.1066	0.0351	0.0746
C3	0.0792	0.0540	0.0312
Heavy Gas	0.0459	0.1078	0.0362
C7+	0.5703	0.3825	0.0676
Fluid Mw	207.23	-	195.40
GOR		-	-
Oil Vicosity @ 40°C (sq mm/sec	4.99	-	0.60
Oil Vicosity @ 50°C (sq mm/sec	4.05	--	0.55
Specific Gravity @15°C	0.86	-	0.72
API Gravity	32.9	-	62.5
Fluid Type	Light Crude	-	Condensate
MW of Flashed Gas	22.15 g/mol	-	-
Separator Liquid	117.83 g/mol	-	-

TABLE: 4.7: PC SAFT Parameter for Characterised Separator Gas Components of Reservoir Fluid ABURA 9L

Component	MW (g/mol)	Mol Fraction	Number of Segment per Chain (m)	Diameter of Segment (σ)	Dispersion Energy (e/k)
N_2	28.04	0.0038	1.210	3.310	90.96
CO_2	44.01	0.0064	2.070	2.780	169.21
CH_4	16.04	0.7581	1.000	3.704	150.03
C_2H_6	30.07	0.1066	1.607	3.521	191.42
C_3H_6	44.10	0.0792	2.002	3.618	208.11
Heavy gas	63.10	0.0459	2.520	3.700	216.40

Table: 4.8: CHARACTERISED ABURA 9L CRUDE OIL

Component	MW	Separator Gas Component	STO Component	Number of Moles In Oil	M	σ	ϵ/k
N2	28.04	1.193	0	1.193	1.21	3.31	90.96
CO2	44.01	4.252	0	4.252	2.07	2.78	169.21
C1	16.04	16.265	0	16.265	1.00	3.70	150.03
C2	30.07	12.004	0	12.004	1.61	3.52	191.42
C3	44.10	9.360	0	9.360	2.00	3.62	208.11
Heavy Gas	63.1	14.243	0	14.243	2.52	3.70	216.4
Saturates	164.882	0	24.048	24.048	5.10	3.87	246.41
A+R	346.1	0	10.796	10.796	8.43	4.03	285.44
Asphaltenes	718.9	0	7.840	7.840	29.5	4.30	395.00

TABLE 4.9: PROPERTIES OF RESERVOIR FLUID ABURA 9L

Gas to Oil Ratio (scf/stb)	-
MW of Reservoir Fluid (g/mol)	67.25
MW of Flashed gas (g/mol)	22.15 g/mol
MW of Separator Liquid (g/mol)	117.83 g/mol
Density of Reservoir Fluid (g/cm^3)	0.764
Saturates wt%	47.3
Aromatics wt%	28.3
Resins wt%	17.5
Asphaltenes wt%	0.89
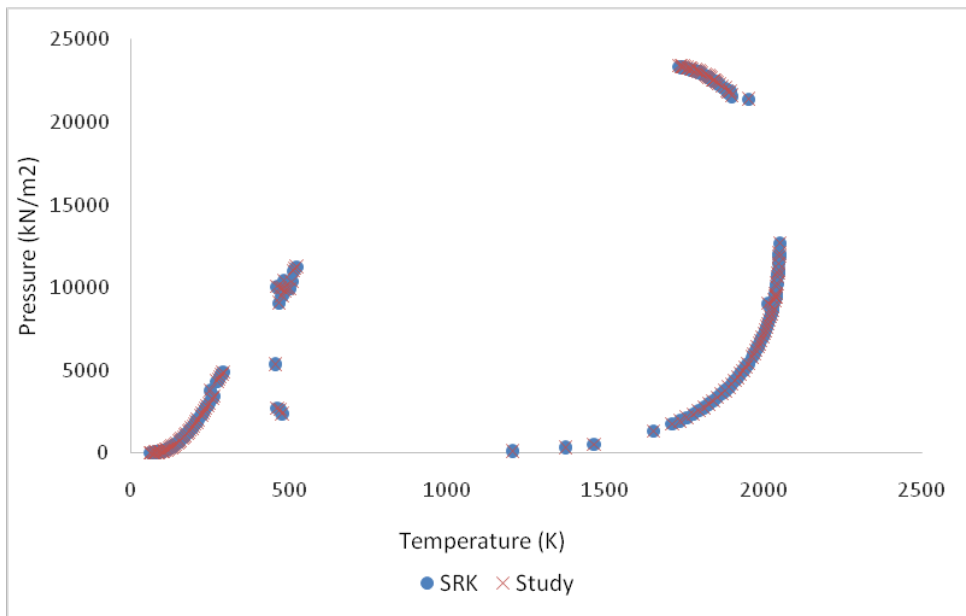
Figure 4.16: Pressure Temperature Diagram for Characterised Crude Oil Abura 9L at 273K Comparing the suggested model equation with SRK EOS.
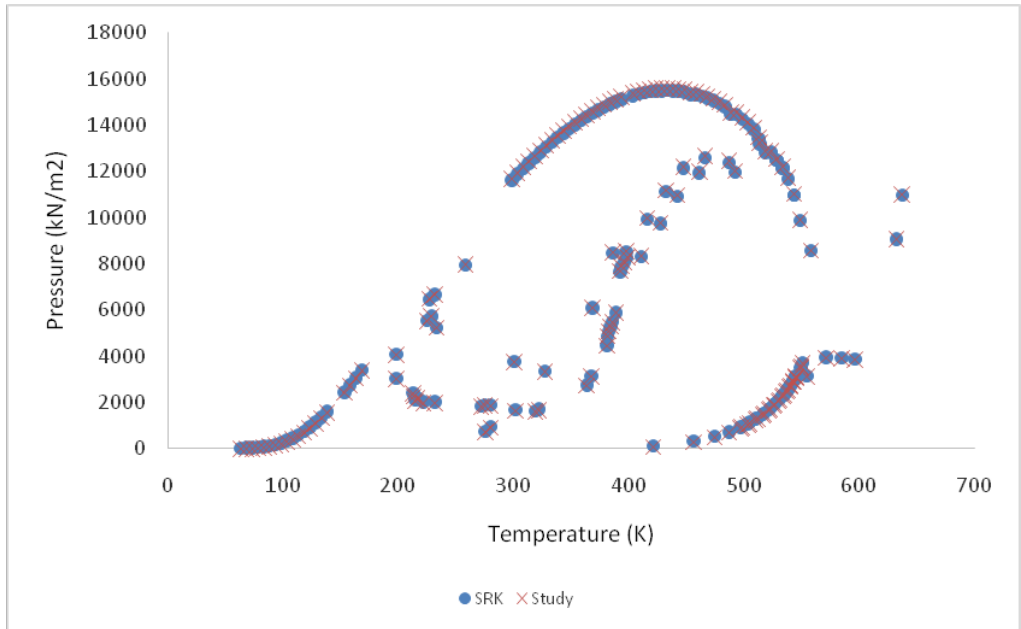
Figure 4.17: Pressure Temperature Diagram for Characterised Crude Oil B at 333K comparing the suggested model equation with SRK EOS.
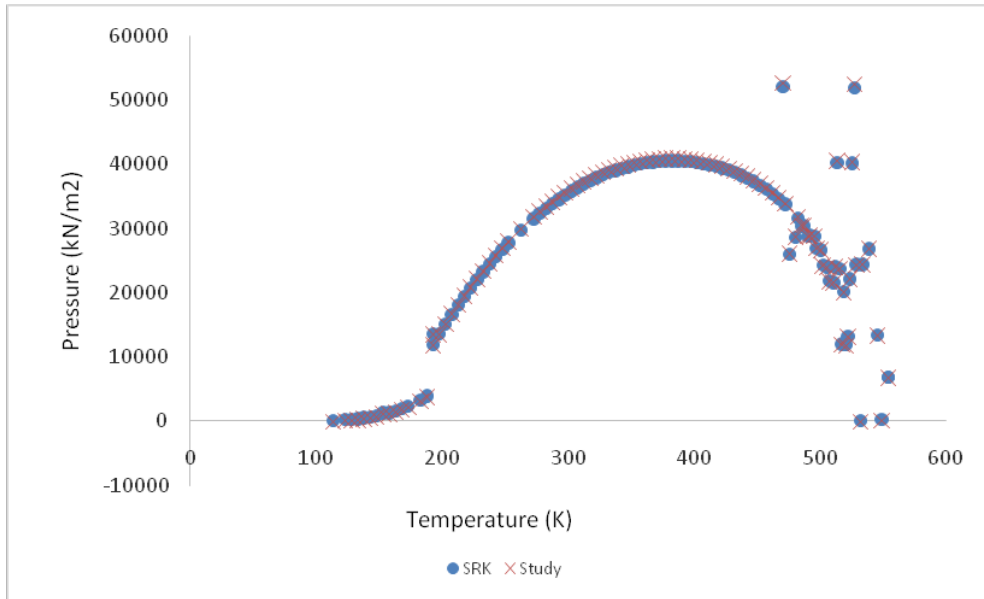
Figure 4.18: Pressure Temperature Diagram for Characterised Crude Oil C. At 333K comparing the suggested model equation with SRK EOS.
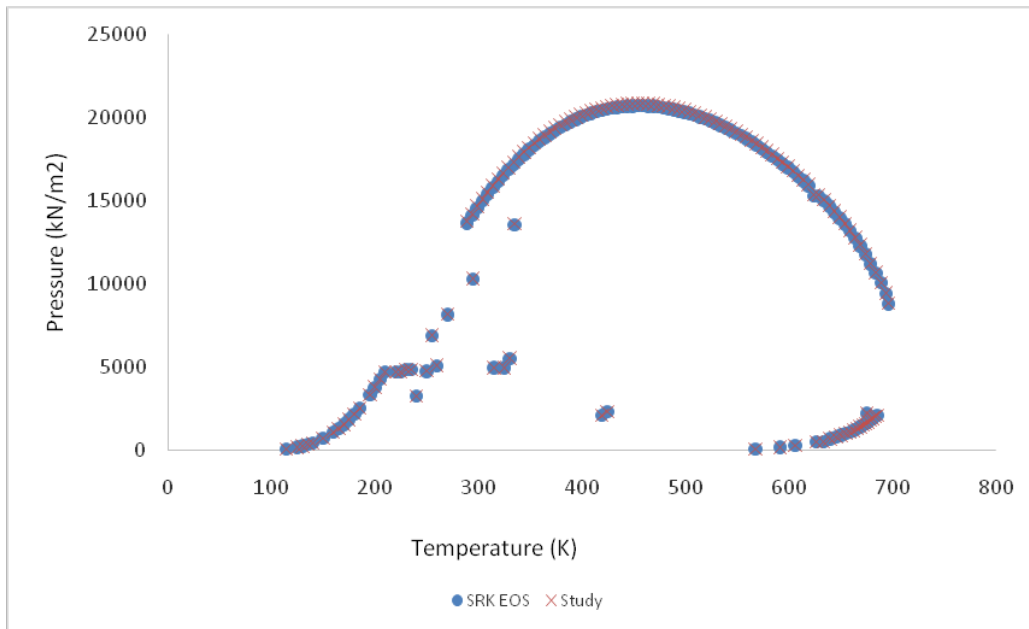
Figure 4.19: Pressure Temperature Diagram for Characterised Crude Oil D at 473.15K comparing the suggested model equation with SRK EOS.
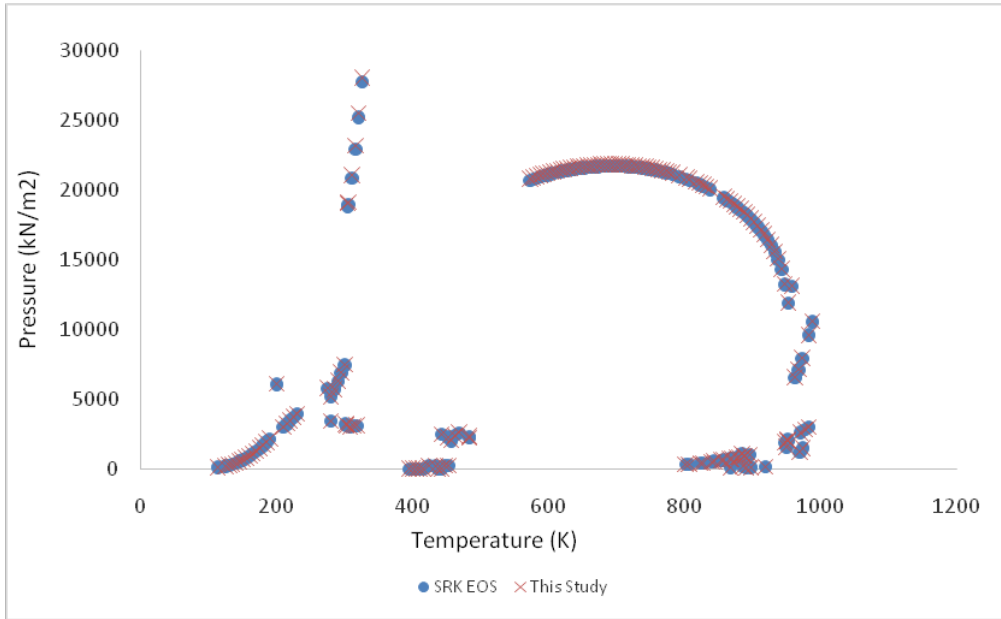
Figure 4.20: Pressure Temperature Diagram for Characterised Crude Oil D at 300.15K comparing the suggested model equation with SRK EOS.
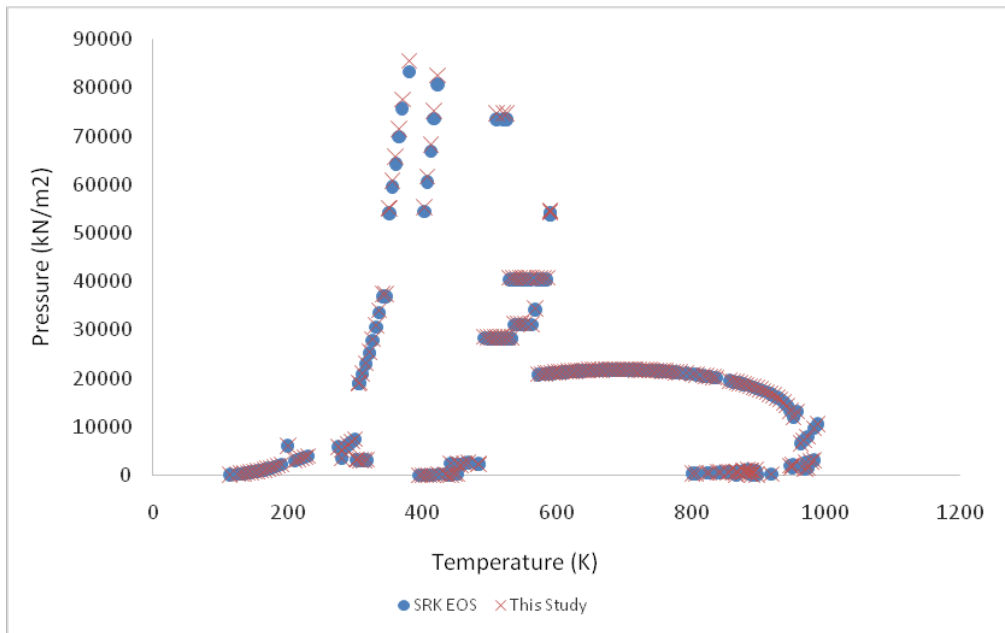
Figure 4.21: Asphaltene Precipitation Envelope for Characterised Crude Oil D at 300.15K comparing the suggested model equation with SRK EOS.

4.10. Pressure and Temperature properties of Reservoir fluids studied

Crude Oil	Critical Temperature (K)		Critical Pressure (kN/m2)		Cricondentherm (K)		Cricondenbar (kN/m2)	
	SRK	Study	SRK	Study	SRK	Study	SRK	Study
Abura 9L	544.5	544.5	3141.0	3143.1	636.8	636.8	15516.5	15583.5
Crude B	192.34	192.34	11883.6	11869.8	554.1	554.1	40566.6	40969.66
Crude C	689	689	10071.5	10089.1	685.4	685.4	20736.5	20850.4
Crude D	-	-	-	-	987.8	987.8	27749.0	28034.8

4.3 Asphaltene Stability in Pentane-Violanthrone 97 and Pentane-Octaethylpropline Mixtures

The Asphaltene stability plot show the bubble point line in model crude oil mixture as conditions of the physical conditions changes. Figure 4.22 shows the Pressure-mole fraction phase stability of simulated oil mixture consisting of Pentane and 0.3% coal based Asphaltene Violanthrone-97 determined at temperatures of 298K and 338K using SRK EOS, and compared with the model equation developed in this study. Similarly, model live oil system consisting of Pentane and Octaethylpropline was further characterised using the SRK EOS to determine the phase behaviour. Comparison between PC-SAFT, SRK EOS predictions and prediction from studies showed an agreement. The Violanthrone-97 - Pentane mixture interaction parameter (Kij) was set at 1, a molecular weight of 700 amu was used for Asphaltene, as was determined by Groenzin and Mullins (2007). While model equation predicts the correct pressure dependence of n-pentane- Octaethylporphyrin mixture, at both 298K and 350K, the model equation accurately predicted the behaviour of Violanthrone 97 at 338K but failed predict the behaviour at a 298K. The study indicated that Violanthrone-97 phase remains stable below the bubble point possibly due low pressures and an increase in the concentration of the solvent (Pentane) phase. The two-phase region occurs faster at a lower temperature, pressure and low n- pentane fractions while at a higher temperature it will occur at a higher pressure and increasing mole fractions of n-pentane
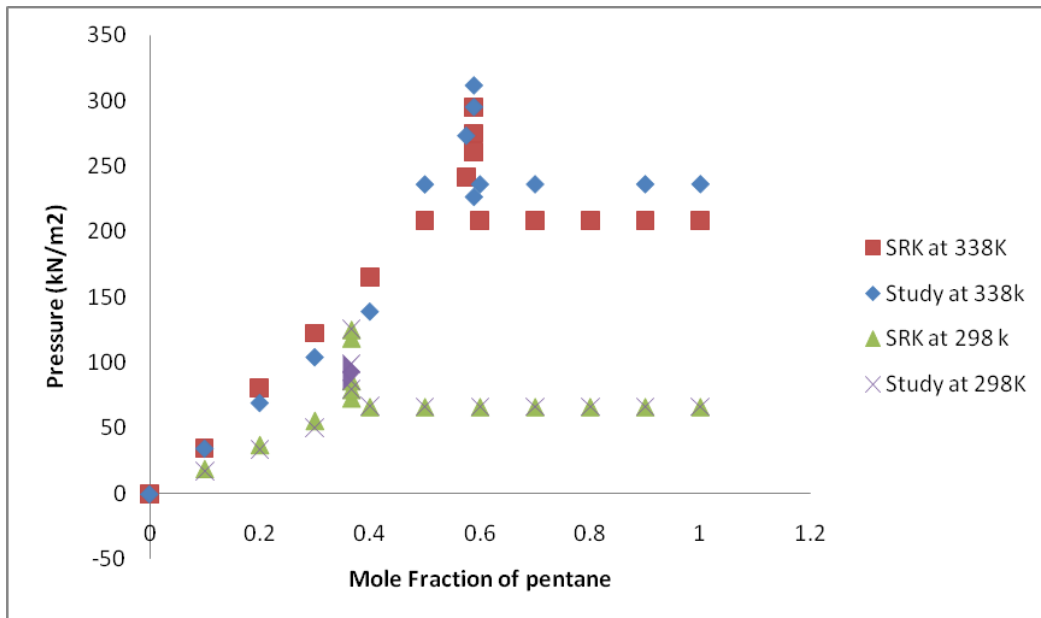
Figure 4.22: Phase Behaviour of Pentane + Violanthrone-97 Mixture at 298K and 338K using PC-SAFT EOS and This Study. At a higher temperature, the mixture separates into violanthrone-97 rich phase and the pentane rich phase at higher pressure.
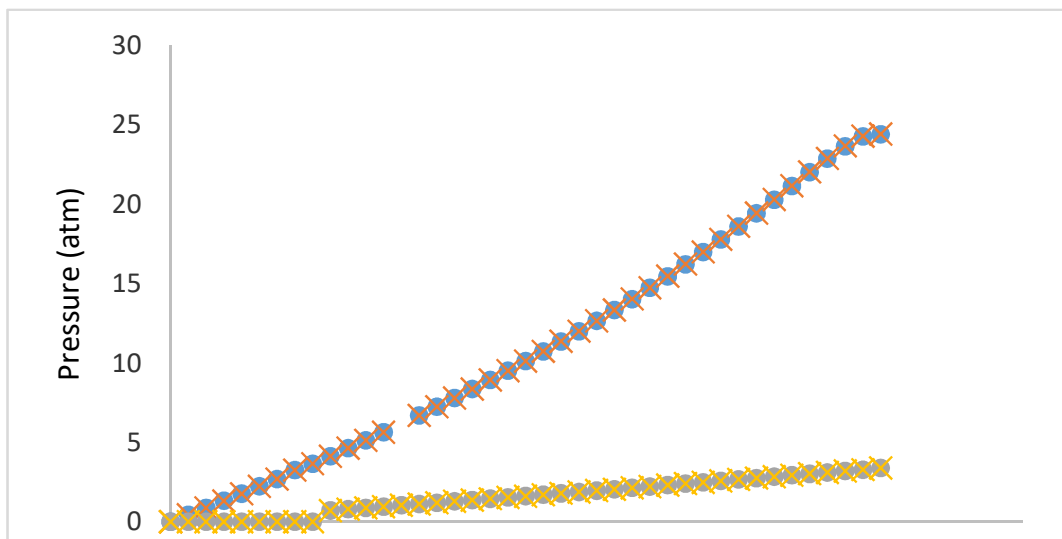
Figure 4.23: Phase Behaviour of Pentane + Octaethylporphyrin Mixture at 298K and 350K using SRK EOS and This Study

4.4 Application of Model Equation to Asphaltene phase behaviour modelling

Four reservoir fluid Data from the studies done by Al-Hammadi et al, (2015); Jamaluddin et al, (2002); Kabir and Jamaluddin (2002); Memon et al, (2012); and a model oil mixture developed by Marcano et al (2013); designated as Fluid-1, Fluid-2, Fluid-3, Fluid-4 and Fluid-5, respectively were investigated. In order to model Asphaltene precipitation in the test petroleum fluid samples, two assumptions were made for the liquid volumes. (1) Liquid volume changes with the pressure and (2) The liquid volume remains constant even at change in pressure. For case (1) the model prediction when compared to experimental data and PC SAFT prediction for Asphaltene onset pressures and bubble point pressures at 0wt% and 5wt% gas injection, showed a percentage error of ±12% when compared to both experimental data and PC SAFT predictions. The study also showed that Asphaltene precipitation pressure increased as gas injection increased from 0 wt% to 30wt%., the model also showed an increase in Asphaltene instability with increased amount of injected gas. Figures 4.29 – 4.39 summaries the Asphaltene precipitation phase envelope for the five reservoir fluids studied, the study predicted the UAOP and saturation pressures. For case (2), the molar volume was determined using an adjustment procedure. The model result showed agreement with experimental data and PC-SAFT data for the bubble point pressures and UOP at different values of pressure and temperature.

4.4.1 Fluid-1

Al-Hammadi et al, (2015) and Arya et al, (2016), have studied fluid-1. The PC SAFT results was obtained by an approach similar to Panuganti, (2012). Figure (4.30-4.32) shows the result of some comparison between the PC SAFT model and this study with respect to experimental model, for the gas injection scenarios of 0, 15, and 30 wt% the model result showed agreement with experimental data and PC-SAFT data for the bubble point pressures and UAOP at

different values of pressure and temperature. The model predicted both the Saturation pressures and Upper Asphaltene onset pressure (UAOP) of the reservoir fluids sho wn in Tables 4.15 and 4.16. The deviations between the PC SAFT and this study was less pronounced for the saturation pressure especially at lower temperature, while the deviation for UAOP was more pronounced at higher pressures. The result also showed an increase in the gap between the saturation pressure line and the upper Asphaltene onset UAOP as injection increased from 0 to 30wt. %. This may be due to an increase in interaction between Asphaltene and STO and increased precipitation as a result of change in fluid composition during gas injection.

4.4.2 Fluid-2

Fluid-2 has been studied (Jamaluddin et al, 2002), under nitrogen gas injections of 5, 10 and 20wt. %. Figures (4.33-4.36) shows the comparison between the model equations developed for this study and the simulated PC-SAFT predicted results for the fluid under CO_2 gas injection by Arya et al, (2016) when compared with the model equation under injections of 0, 10 and 20 wt. %. The model prediction shows agreement with the experimental data and PC SAFT results, at 0wt. % gas injection and noticeable deviations was observed at 10 wt. % and 20wt. % Co_2 gas injections, this indicates an increase in the difference between UAOP and the saturation pressure with increase in amount of injected gas. This agrees with the findings of Gonzalez et al, (2005). The a and c parameter for the model equation were obtained by a parameter fitting procedure while a temperature based correlation was used to obtain the b parameter as shown in table 4.17. Generally, the study showed slight deviations in the UAOP as the injected gas increased from 0 wt% to 30 wt% natural gas injection for Fluid-1; 10 and 10 wt% to 20 wt% CO_2 gas Injection for Fluid-2, this shows that changes in the composition of crude oil will affect the Asphaltene behaviour. These deviations were also proportional to the changes in the values of the liquids volume used in the model equation. The liquid volume also

141

decreased with an increase in gas injection for Fluid-1, Fluid-2. This may be due to the formation of Asphaltene precipitation in the petroleum fluids.

4.4.3 Fluid-3

Fluid-3 was studied by Kabir and Jamaluddin, (2002) and utilized for Asphaltene studies by Zhang et al, (2011). In fluid-3 case the study equation and PC-SAFT parameters give prediction for both UAOP and saturation pressures. The results show that the study equation gave a better prediction for the UAOP while PC-SAFT parameter gave a better prediction for the saturation pressures. As shown in figure 4.37, the prediction was made at 0wt% gas injection, but both models are capable of further predicting the effect of asphaltene precipitation due to Nitrogen, CO_2 or Natural Gas injection.

4.4.4 Fluid-4

This Fluid was studied by Memon et al, (2012) and was also used by Arya et al, (2016) for Asphaltene studies. Figure 4.38 shows that PC-SAFT and Model equation are capable of predicting both UAOP and saturation pressure for Fluid-4 and both models also agree with experimental data. The model equation parameters were obtained by fitting equation to experimental data. Due to lack of experimental data for gas injections for fluid-4, the fluid was studied at only 0 wt.% GI.

4.4.5 Fluid-5

Fluid-5 is a model oil prepared by Marcano et al, (2013), it consists of a mixture of 0.04wt% heptane insoluble Asphaltene solution in 60mol% toluene and 40mol% n-heptane. For this study, the model parameters were determined using both 10wt% and 20wt% scenarios as shown in table 4.17. The asphaltene onset pressure were studied at 10 and 20wt% CO2 injection. The model equation predictions for the UAOP and saturation pressures, were compared with both experimental and PC-SAFT results. Both the model equation gave

accurate prediction for the UAOP when compared with the experimental and PC SAFT data, but when compared PC SAFT results gave a better prediction when compared with experimental data for the saturation pressures. The model equation gave a slightly poor prediction for saturation pressures at 10wt% CO2 injections and also over predicts the UAOP at 10wt% CO2 injection.

Generally, predicted results for both the Saturation pressures and Upper Asphaltene onset pressure (UAOP) of the four reservoir fluids and the model live oil shown in Tables 4.15 and 4.16 the results show in figures 4.30 to 4.40 indicated an increase in the difference between UAOP and the saturation pressure with increase in amount of injected gas. This agrees with the findings of Gonzalez et. al, 2005. The study showed slight deviations in the UAOP as the injected gas increased from 0 wt% to 30 wt% Natural gas injection for F1; 0 wt% to 20 wt% 0CO2 gas injection for F2 and 10 wt% to 20 wt% CO2 gas Injection for F5, this shows that changes in the composition of crude oil will affect the Asphaltene behaviour. These deviations were also proportional to the changes in the values of the liquids volume used in the model equation. The liquid volume also decreased with an increase in gas injection for F1, F2, and F5. This may be due to the formation of Asphaltene precipitation in the petroleum fluids.

Table 4.11: Crude oil Composition For this Study

Component	F1 (Mol %)	F2 (Mol %)	F3 (Mol %)	F4 (Mol %)
N_2	0.163	0.490	0.088	0.390
H_2S	1.944	3.220	1.022	0.840
CO_2	0.000	11.370	0.048	0.000
Methane	33.600	27.360	42.420	36.63
Ethane	7.673	9.410	10.800	8.630
Propane	7.282	6.700	6.918	6.660
Iso-butane	1.885	0.810	0.957	1.210
n-Butane	5.671	3.710	3.518	3.690
Iso-pentane	2.993	1.220	1.213	1.550
n-pentane	2.980	1.980	2.086	2.250
C6+	38.236	34.280	30.390	38.150

Table 4.12. Crude oil properties used for This Study (Kontogeorgis 2016)

Properties	F1	F2	F3	F4
Saturates (wt. %)	66.26	57.4	63.3	-
Aromatics (wt. %)	25.29	30.8	24.9	-
Resins (wt. %)	5.25	10.4	11.5	-
Asphaltenes (wt. %)	2.80	1.40	0.50	**-**
MW of C6+	208.08	-	204.3	**-**
Res. Fluid MW (g/mol)	97.50	102.04	81.7	102.6
STO Density (g/cm^3)	0.823	0.906	0.840	0.863
GOR (scf/stb)	787	900	-	786.04

Table 4.13. Fitted and Calculated Values of the Model Parameters Used for this Study.

Fluid	a	b	c
Fluid-1	0.999	$0.0025T^2-2.291T+582.15$	0.778
Fluid-2	0.999	$0.0036T^2-3.760T+1002.9$	0.964
Fluid-3	0.999	$0.002T^2-1.830T+528.72$	0.860
Fluid-4	0.999	$0.0969T^2-68.534T+12133$	0.915
Fluid-5	0.999	$0.0725T^2-51.796T+9018.3$	0.740
Fluid-5	0.998	$0.0128T^2-9.118T+1588.0$	0.918
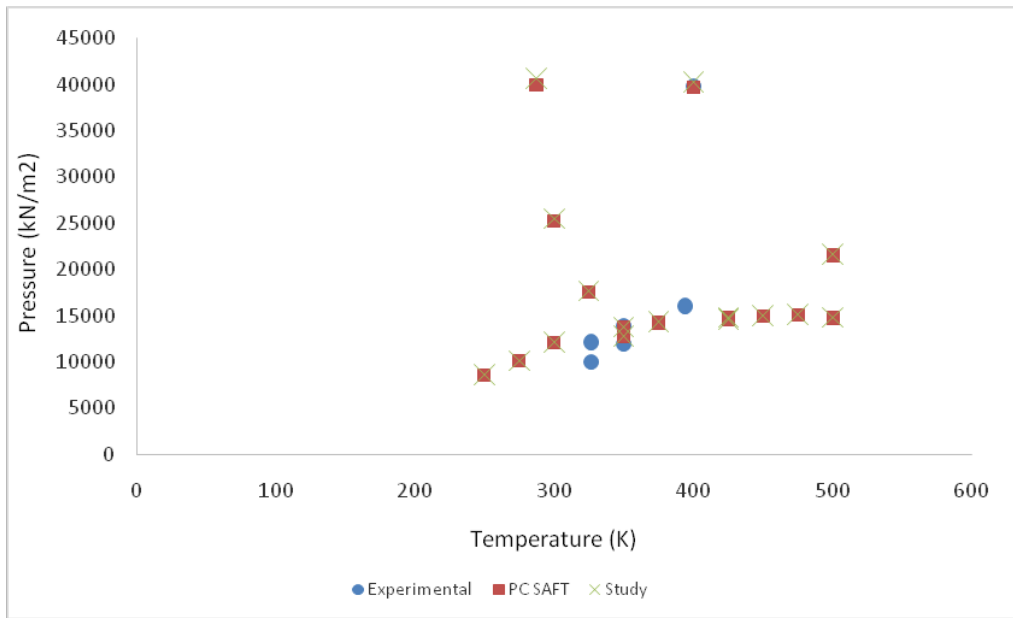
Figure 4.24. Asphaltene Precipitation envelope for F1 at 0wt% gas Natural Injection using
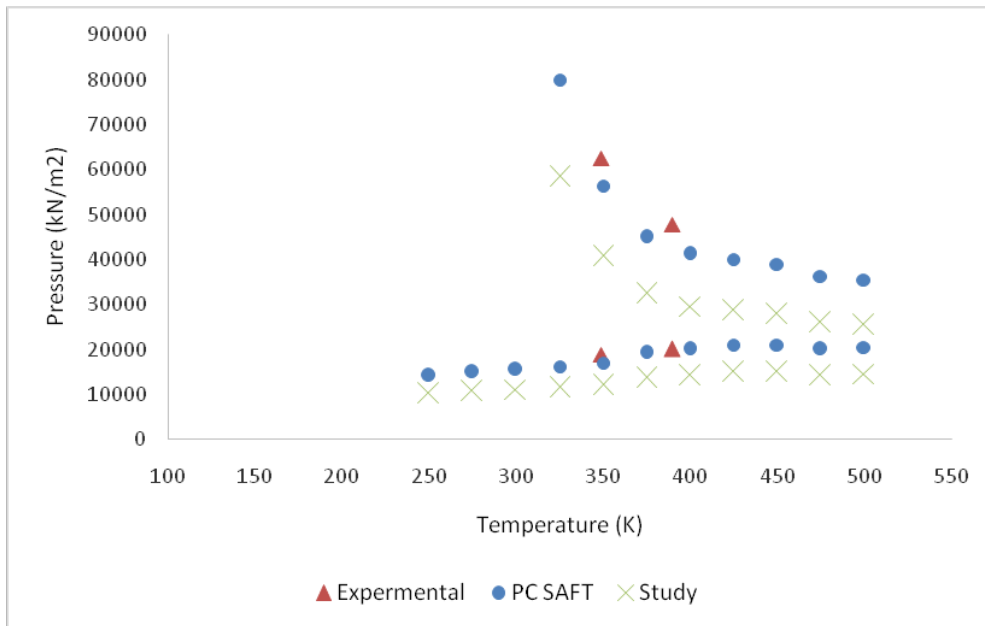
Method 1

Figure 4.25. Asphaltene Precipitation envelope and bubble point line for F1 at 15wt% gas

Natural Injection using Method 1
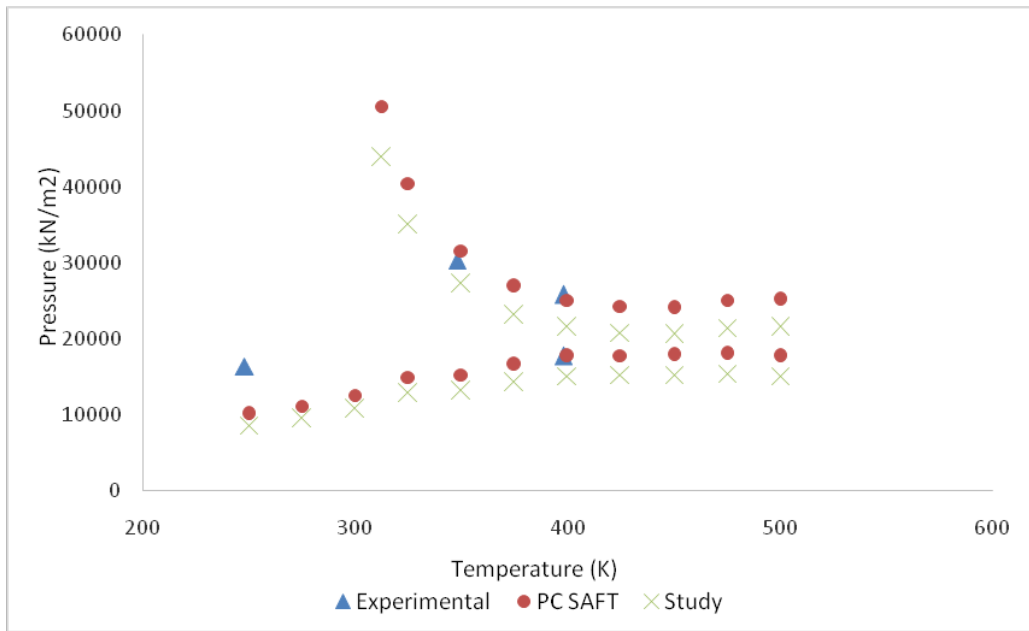
Figure 4.26. Asphaltene precipitation envelope and bubble point line for F1 at 15wt% gas injection using method 1
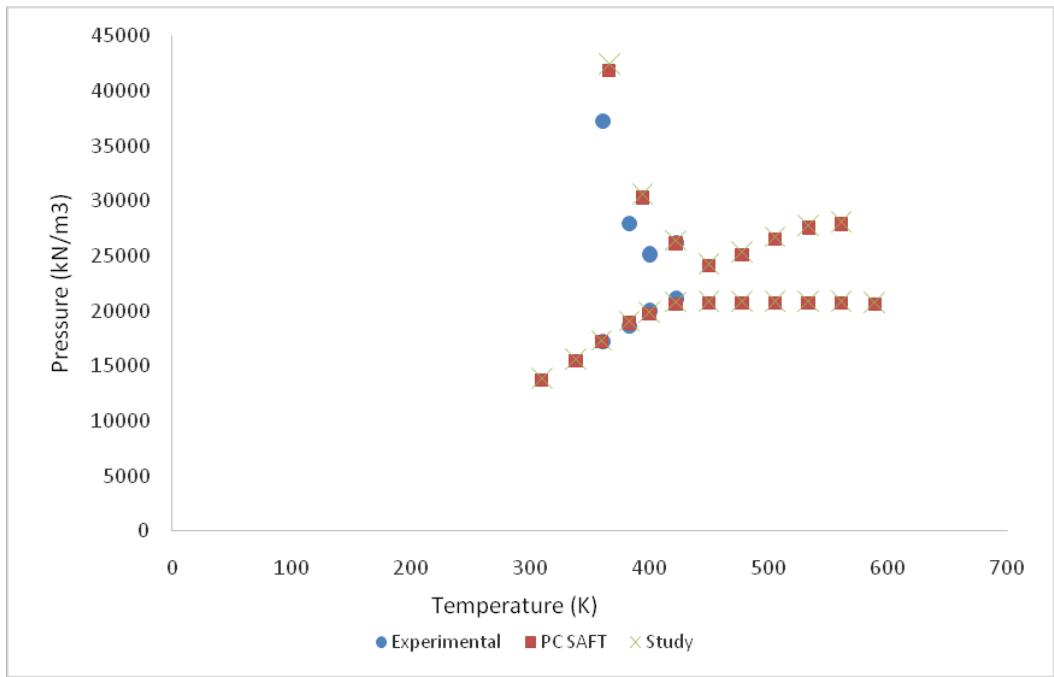
Figure 4.27. Asphaltene precipitation envelope and bubble point line for F2 at 5wt% nitrogen gas injection using method 1
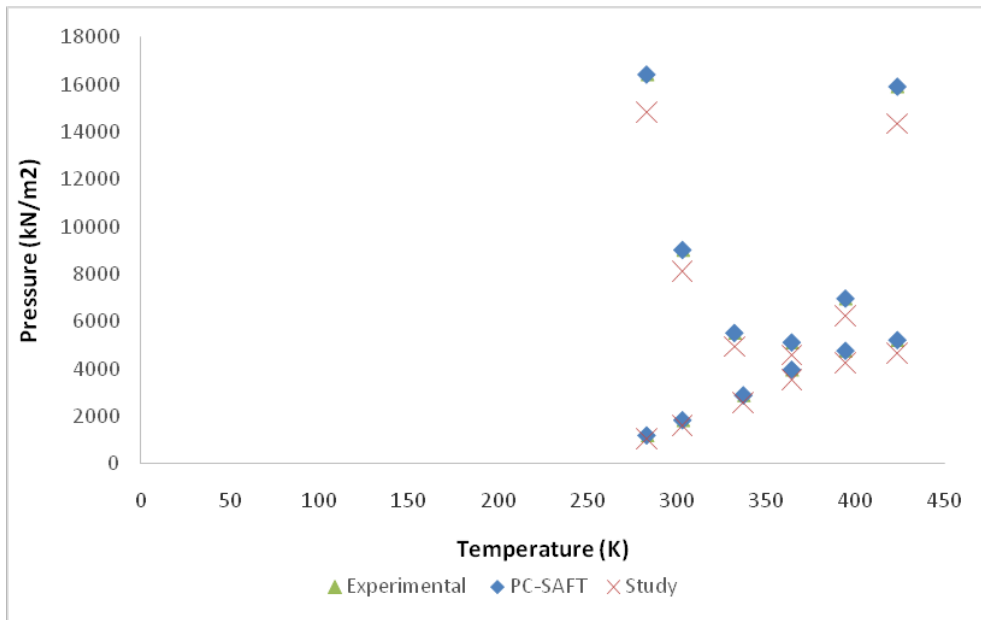
Figure 4.28. Asphaltene precipitation and bubble point line envelope for F5 at 10wt% CO_2 gas injection using method 1.
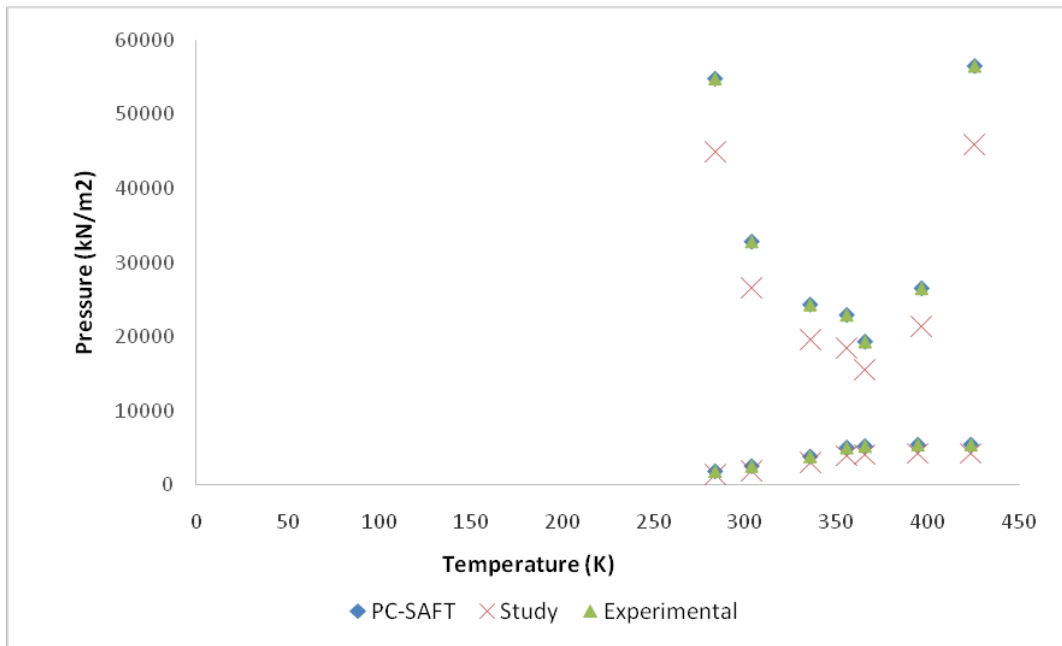
Figure 4.29. Asphaltene precipitation envelope and bubble point line for F5 at 20wt% CO_2 gas injection using method 1.
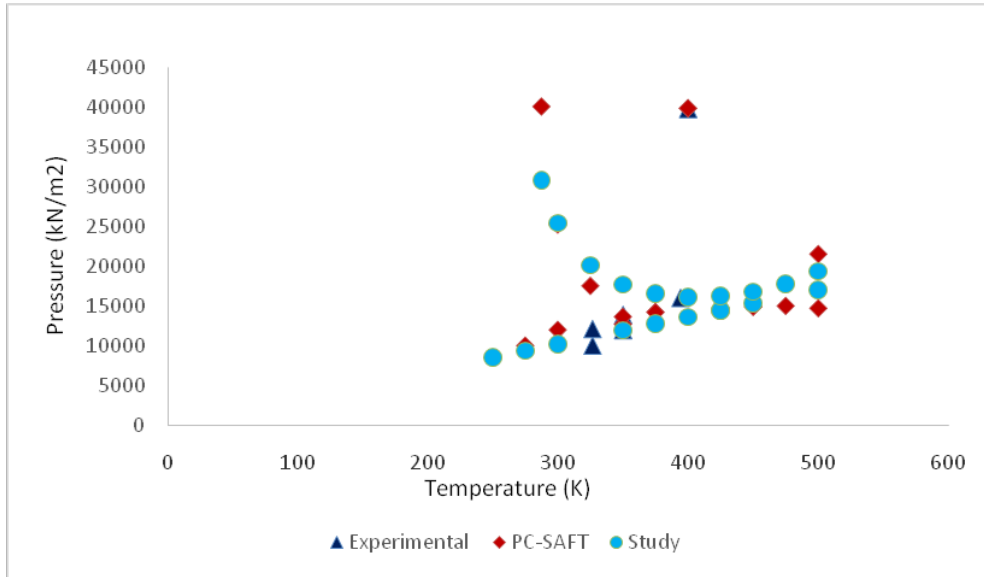
Figure 4.30. Asphaltene precipitation envelope and bubble point line for F1 at 0wt% natural gas injection using method 2 parameter a=0.997, $b = 0.0025T^2 - 2.291T + 582.15$, c=0.778.
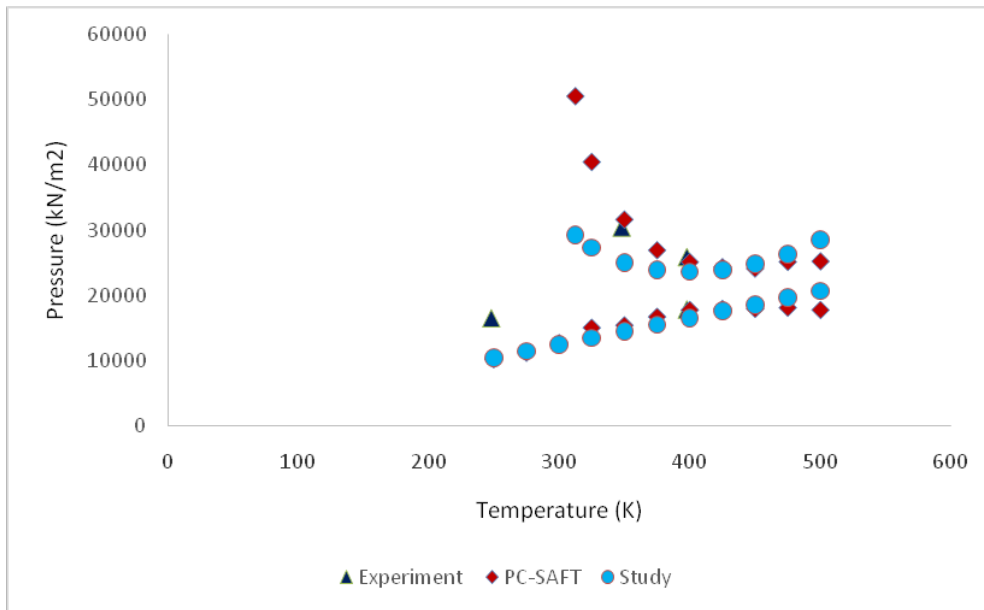
Figure 4.31: Asphaltene precipitation envelope and bubble point line for F1 at 15wt. % natural gas injection using method 2 with parameter a=0.994 $b = 0.0025T^2 - 2.291T + 582.15$, c=0.05.
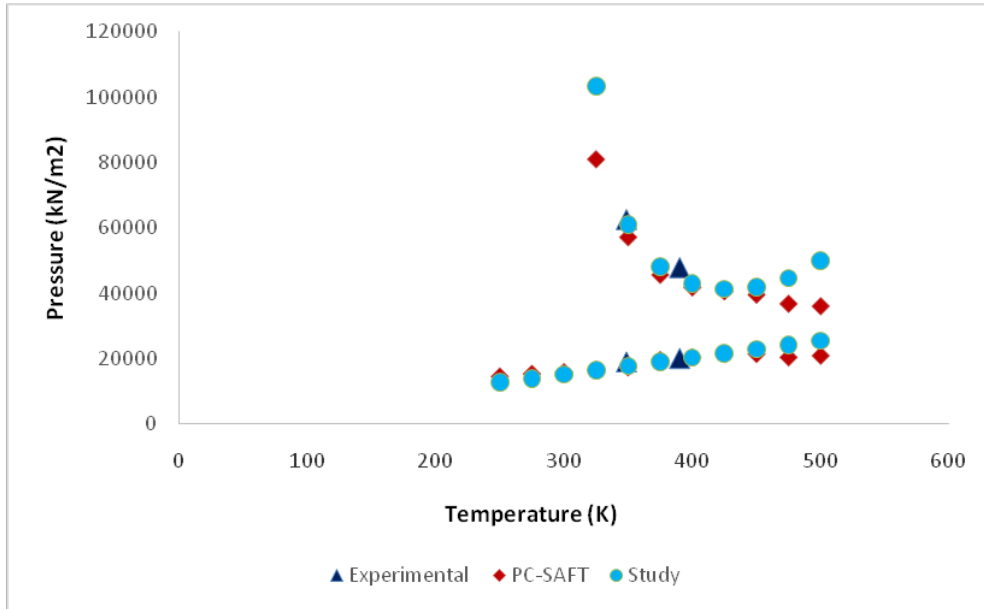
Figure 4.32 Asphaltene precipitation envelope and bubble point line for F1 at 30 wt. % natural gas injection using method 2 with parameter a=0.999, $b = 0.0025T^2 - 2.291T + 582.15$, c=0.999.
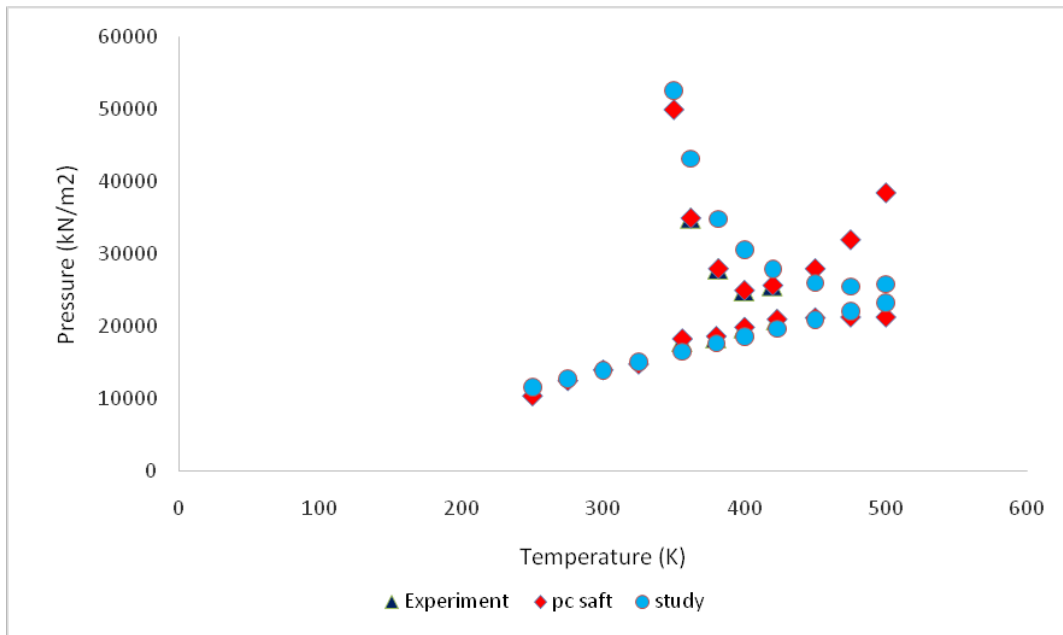
Figure 4.33. Asphaltene precipitation envelope and bubble point line for F2 at 0wt. % CO_2 gas injection using method 2 parameter a=0.999, $b = 0.0036T^2 - 3.7604T + 1002.9$, c=0.976
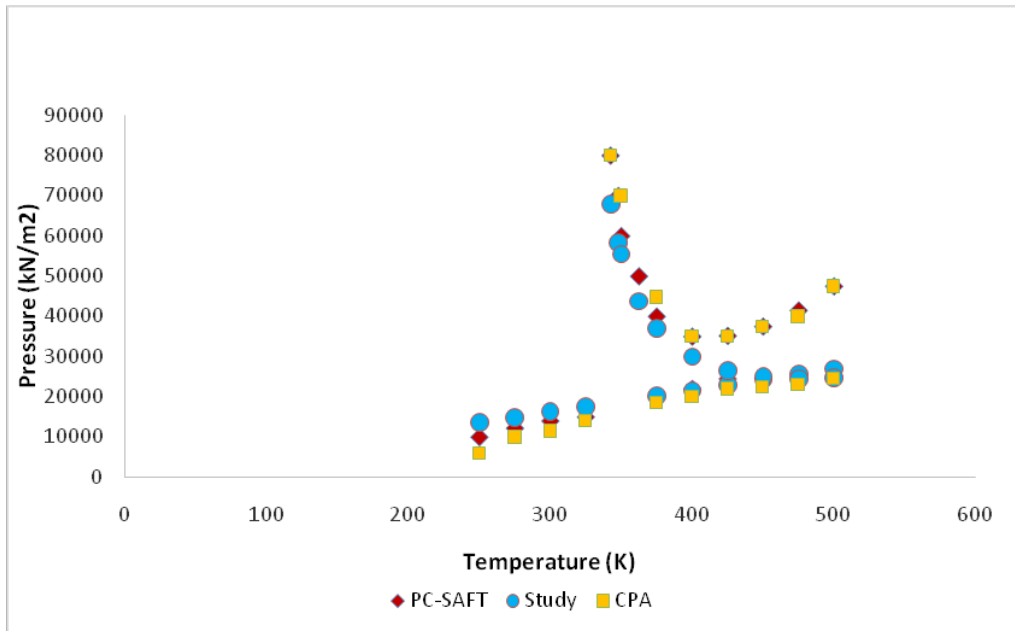
Figure 4.34. Asphaltene precipitation envelope and bubble point line for F2 at 10wt% CO_2 gas injection using method 2 with parameter a=0.998, $b = 0.0036T^2 - 3.7604T + 1002.9$, c=0.803
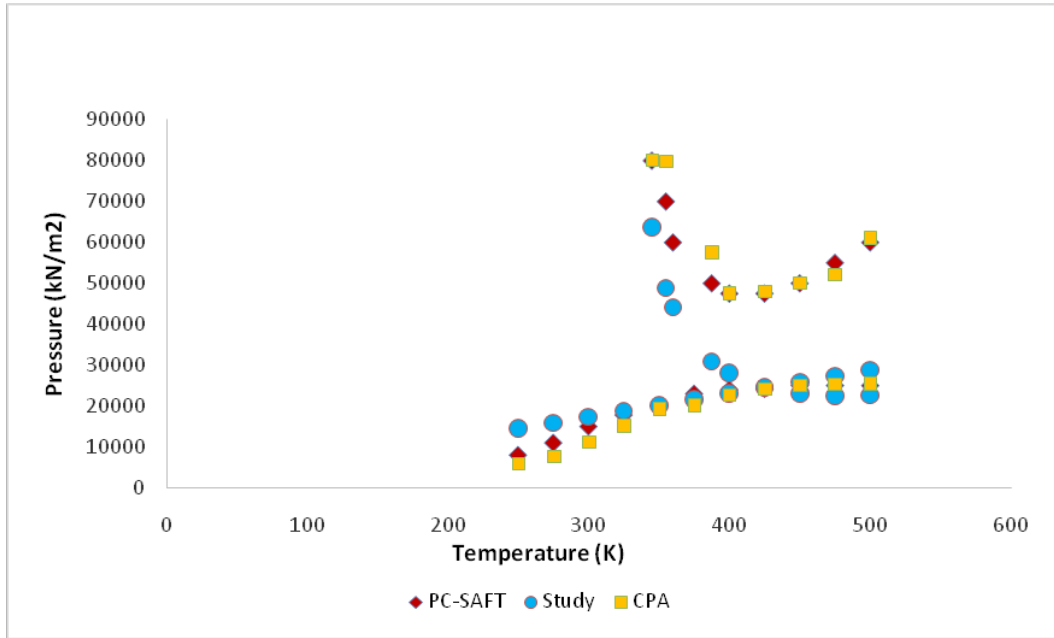
Figure 4.35. Asphaltene precipitation envelope and bubble point line for F2 at 20wt. % CO_2 gas injection using method 2 with parameter a=0.998, $b = 0.0036T^2 - 3.7604T + 1002.9$, c=0.699
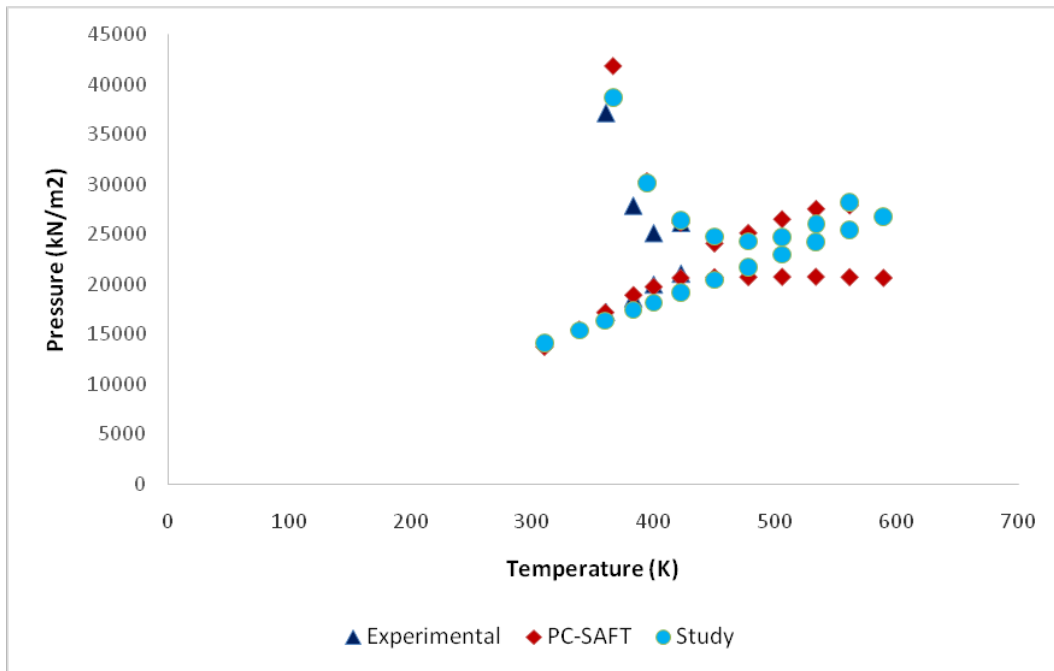
Figure 4.36. Asphaltene precipitation envelope and bubble point line for F2 at 5wt.% nitrogen gas injection using method 2 with parameter a=0.998, $b = 0.0036T^2 - 3.7604T + 1002.9$, c=0.964
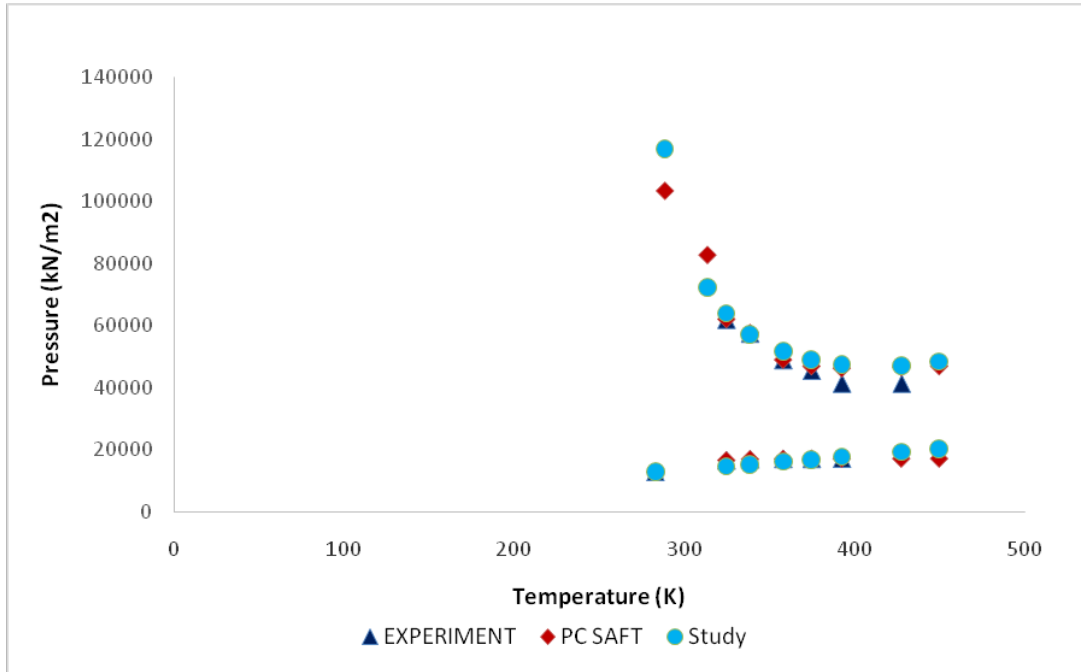
Figure 4.37. Asphaltene precipitation envelope and bubble point line for F3 at 0wt% Gas injection using method 2 with parameter $b = 0.002T^2 - 1.8303T + 528.72$.
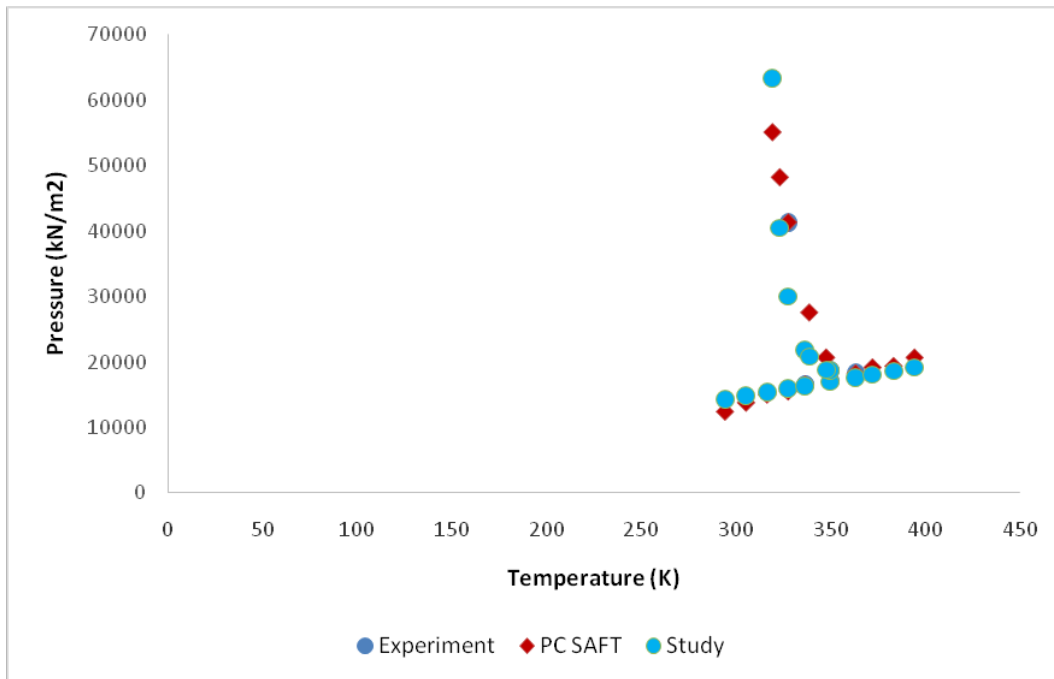
Figure 4.38. Asphaltene precipitation envelope and bubble point line for F4 at 0wt% natural Gas injection using method 2 parameter a=1.000, $b = 0.0969T^2 - 68.534T + 12133$, c=1.000.
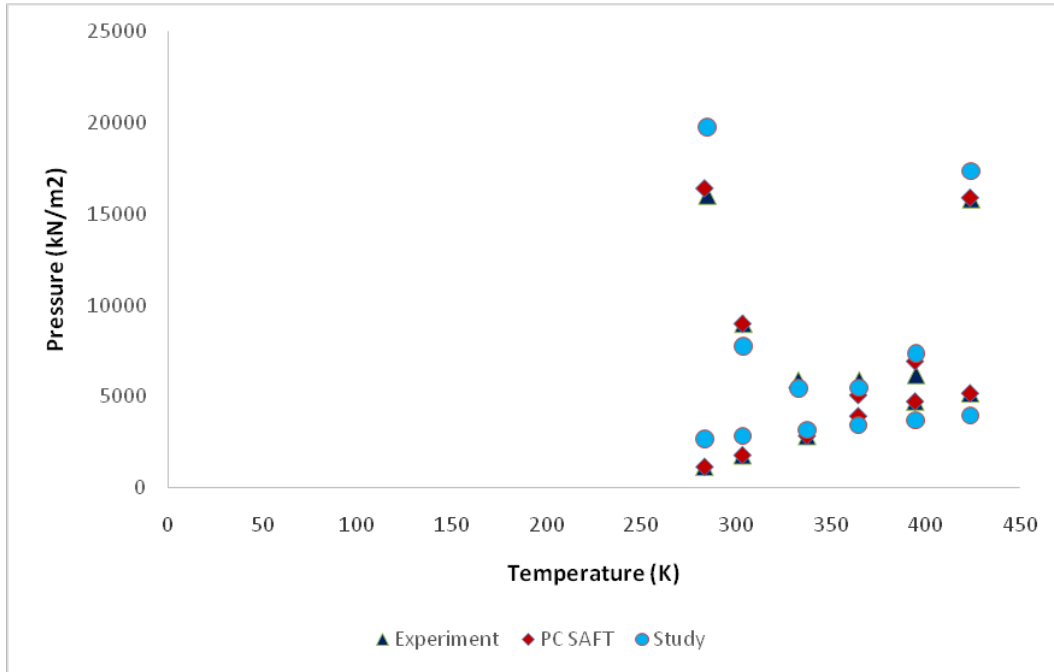
Figure 4.39.   Asphaltene precipitation envelope and bubble point line for F5 at 10wt% CO2 gas injection using method 2 parameter a=1.000, $b = 0.0725T^2 - 51.796T + 9018.3$, c=1.000.
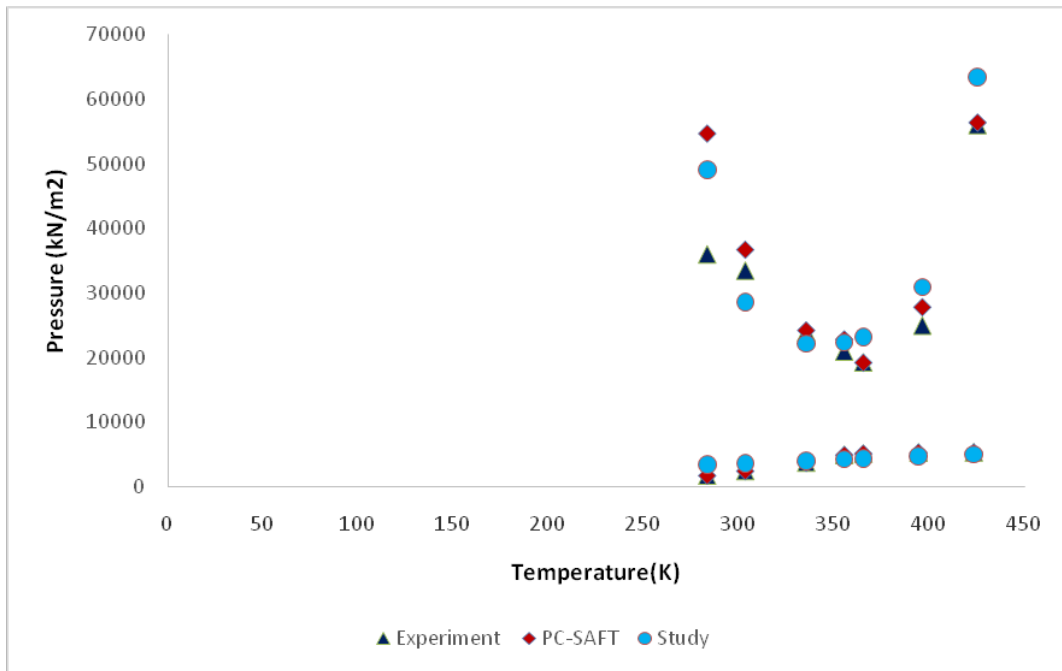
Figure 4.40. Asphaltene precipitation envelope and bubble point line for F5 at 20 wt%. CO2 gas injection using method 2 parameters a=1.001, $b = 0.0128T^2 - 9.1183T + 1588$, c=1.000.

CHAPTER FIVE

CONCLUSION AND RECOMMENDATIONS

5.1 Conclusion

The following conclusions were drawn from the study:

1. Asphaltene precipitation can occur in oil systems during injection of natural gas, CO2 or Nitrogen.

2. Simplified model for predicting Phase Behaviour and Asphaltene precipitation in oil during gas injection was developed

3. The model achieved faster and better control of Asphaltene precipitation during gas injection operations in oil reservoirs.

4. The model equation predicted the upper Asphaltene onset pressures and bubble point pressure of petroleum fluids.

5. Changes in the composition of crude oil affect the Asphaltene behaviour

6. UAOP increased with increasing proportion of injected gases, and varied with reservoir fluid and type of injected fluid.

5.2 Recommendations

1. This study was carried out under gas injection; it is possible to investigate asphaltene precipitation during water injection or water alternating gas injections.

2. It is possible to investigate how viscosity of oil can affect asphaltene precipitation during gas injection.

3. The effect of bottom hole equipment and well angle on asphaltene phase behavior can be further investigated.

4. The study was carried out under limited availability of data; therefore, more studies can be carried out using additional data

REFERENCES

Agrawala, M. 2001. Mesurement *and modelling of asphaltene association.* Diss. Chemical and Petroleum, Engineering. University of Calgary.

Ahmed, T. 2007. *Equation of state and pvt analysis: applications for improved reservoir modelling.* Texas: Gulf Publishing Company.

Al- Hammadi, A.A., Vargas, F.M. and Chapman, W.G. 2015. Comparison of cubic plus association and perturbed-chain statistical associating fluid theory methods for modelling asphaltene phase behaviour and pressure-volume temperature properties. *Energy Fuels 29. 5: 2864-2875*

Al- Jarrah, M.M.H. and Al- Dujaili, A.H. 1989. Characterization of some Iraqi asphalts II: new findings on the physical nature of asphaltenes. *Fuel Science and Technology International 7.1: 69-88.*

Ali, L.H. and Al- Ghannam, K.A. 1981. Investigation into asphaltenes in heavy crude oils: I. effect of temperature on precipitation by alkane solvents. *Fuel 60.11:1043-1045.*

Ameli, F., Abdolhossein H.S., Bahram, D. and Amir, H.M. 2016. Determination of asphaltene precipitation conditions during natural depletion of oil reservoirs: a robust compositional approach. *Fluid Phase Equilibria 412: 235-248.*

Andersen, S. I. and Birdi, K. S. 1991. Aggregation of asphaltene as determined by calorimetery. *Journal of Colloidal and Interface Science 142: 497-502.*

Andersen, S. I. and J. Speight, J. G. 1993. Observations on the critical micelle concentration of asphaltenes. *Fuel 72. 9: 1343*-1344.

Andersen, S.I. 1994. Dissolution of solid boscan asphaltene in mixed solvent. *Fuel Science and Technology International 12: 11-12.*

Andersen, S.I. and Christensen S. D. 2000. The critical micelle concentration of asphaltene as measured by calorimetry. *Energy and Fuels 14. 1: 38-42.*

Anisimov, M.A., Ganeeva, M.Y., Gorodetskil, E.E., Deshabo, V.A., Kosov, V.I. Kuryakov, V.N., Yudin, D.I. and Yudin, I.K. 2014. Effects of resin on aggregation and stability of asphaltene. *Energy and Fuels 28. 10: 6200-6209.*

Aquino-Olivos, M. A., Andersen, S. I. and Lira Galeana, C. 2003. Comparisons between asphaltenes from the dead and live oil samples of the same crude oils. *Petroleum. Science. and Technology 21. 3-4: 1017-1041.*

Aske, N., Kallevik, H., Johnsen, E. E. and Sjoblom, J. 2002. Asphaltene aggregation from crude oil and model system studied by high pressure spectroscopy. *Energy and Fuels 16: 1287-1295.*

Badre, S., Goncalves, C.C., Norinaga, K., Gustavso, G. amd Mullins, O.C. 2006. Molecular Size and weight of asphaltene and asphaltene solubility fractions from coal, crude oils and bitumen. *Fuel 85.1*

Bartholdy, J. and Andersen, S.I. 2000. Changes in asphaltene stability during hydro treating. *Energy Fuels 14: 52-55.*

Barton, F.M. 1991. Handbook of solubility parameters and other cohesion parameters. Boca Raton: CRC Press.

Bauget, F., Langevin, D. and Lenormand, R. 2001. Dynamic surface properties of asphaltenes and resins at the oil- air interface. *Journal of Colloid and Interface Science 239.2:*

501-508.

Blas, F.J. and Veja, L.F. 1998. Prediction of binary and ternary diagrams using the statistical associating fluid theory (saft) equation of state. *Industrial and Engineering Chemistry Research* 37: 660-674.

Brandt, H.C.A., Hendriks, E.M., Michels, M.AJ. and Visser, F. 1995. Thermodynamic modelling of asphaltene stacking. *Journal of Physical Chemistry* 99. 26: 10430 10432.

Broseta, D., Robin, M., Savvidis, T., Fejean, C., Durandeau, M. and Zhou, H. 2000. Detection of asphaltene deposition by capillary flow measurement. *Society of Petroleum Engineers.* . Retrieved Jun. 5, 2019, from http://www.onepetro.org/journal-paper/SPE-59294-MS.

Buckley, J.S., Hirasaki, G.J., Liu, Y., Von Drasek, S. Wang, J.X. and Gill, B.S. 1998. Asphaltene precipitation and solvent properties of crude oils. *Petroleum Science and Technology* 16. 3-4: 251-285.

Buenrostro-Eduardo, E., Lira- Galeana, C., Gil-Villegas, A. and Wu, J. 2004. Asphaltene precipitation in crude oil: theory and experiments. *American Institute of Chemical Engineers Journal* 5: 2552-2570.

Burke, N. E., Hobbs, R.E., and Kashou, S.F. 1990. Measurement and modelling of asphaltene precipitation. *Journal of Petroleum Technology. Society of Petroleum Engineers* 289:1440-1446.

Carbognani, L., 2003. Solid petroleum asphaltenes seems surrounded by alkyl layers. *Petroleum Science and Technology* 21: 537-556.

Carnahan, N. F., and Starling, K.E. 1972. Intermolecular repulsions and the equation of state for fluids. *American Institute of Chemical Engineers Journal* 18. 6: 1184-1189.

Carpentier, B., Wilheims, A. and Mansoori, G.A. 1997. Reservoir organic geochemistry: processes and application. *Journal of Petroleum Science and Engineering* 56: 341-343.

Chakma, A., Islam, M.R., and Berruti, F. 1994. Asphaltene-viscosity relationship of processed and unprocessed bitumen. *Asphaltene particles in fossil fuel exploration, recovery and production processes.* M.K. Sharma, and T.F. Yen. Eds. Boston: Springer. 1-22.

Chapman, N.G., Gubbins, K.E., Jackson, G. and Radosz, M. 1990. New reference equation of state for associating fluids. *Fluid Phase Equlibria* 52: 31-38.

Chapman, N.G., Gubbins, K.E., Jackson, G. and Radosz, M. 1989. SAFT: Equation of states solution model for associating fluids. *Fluid Phase Equilibria* 52: 31 35.

Cimino, R., Correra, S., Del Bianco, A. and Lockhart, T.P., 1995. Solubility and phase behaviour of asphaltene in hydrocarbon media, asphltenes: fundamentals and application. NewYork: Plenum Press. 97-130.

Danesh, A. 1998. PVT and phase behaviour of petroleum reservoir fluids: developments in petroleum science. 1st ed. Amsterdam: Elsevier.

De Boer, R.K., Leerlooyer, M., Eigner, M. and Van Bergen, A. 1995. Screening of crude oils for asphalt precipitation: theory, practice, and the selection of inhibitors. *Society of Petroleum Engineers.* Retrieved Jun. 4, 2019, from http://www.onepetro.org/journal-paper/SPE-24987-PA.

De Pedroza, T.M., Calderon, G.G., and Rico, P.A. 1996. Impact of asphaltene presence in some rock properties. *Society of Petroleum Engineers.* Retrieved Jun. 4, 2019, from http://www.onepetro.org/journal-paper/SPE-27069-PA.

Dickie, J.P, and Yen, T.F. 1967. Macrostructures of asphaltic fractions by various instrumental methods. *Analytical Chemistry* 39: 1847 – 1852.

Dwinggins, C.W. 1965. A small angle x-ray scattering study of the colloid nature of petroleum. *Journal of Physical Chemistry* 69: 3500-3506.

Ekulu, G., Magri, P. and Rogaski, M. 2004. Sanning aggregation phenomenon in crude oil with density measurements. *Journal of Dispersion Science and Technology* 25: 321-331.

Eliassi, A., Modarres, H. and Mansoori, G.A. 2003. Extension of Flory Huggins theory to satisfy the hard sphere limit. *Iranian Polymer Journal* 12.5:357-366.

Elliot, J. R., Jayaraman S. S. and Donohue, M. D. 1990. A simple equation of state for non-spherical and associating molecules. *Industrial and Engineering Chemical Research* 29.7:1476-1485.

Escobedo, J and Mansoori, G.A. 1995. Solid particle deposition during turbulent flow production operations. *Society of Petroleum Engineers.* Retrieved Jun. 5, 2019, from http://www.onepetro.org/conference-paper/SPE-29488-MS.

_____. 2009. Heavy- organic particle deposition from petroleum fluid flow in oil well and pipelines. *Petroleum Science* 7: 502-508.

Eskin, D., Ratalowski, J. Akbarzadeh, K. and Pan, S. 2011. Modelling asphaltene deposition in turbulent pipeline flows. *Canadian Journal of Chemical Engineering* 89: 421- 441.

Eyring, H., Ma, S., Youn, Y.H. and Lee, S.T. 1977. Single partition function for three phases. *Proceedings of the National Academy of Sciences* 74.7: 2598-2601.

Fotland, P., Anfinsen, H., Foerdedal, H. and Hjermstad, H.P. 1997. The phase diagram of asphaltene: experimental technique, results and modelling of some north sea crude oils. *OALib Journal.* Retrieved Jun. 4, 2019, from http://www.oalib.com/references/14440449

Fuhr, B.J., and Cathrea, C., Coates, L., Kalya, H. and Majeed, A.I. 1991. Properties of asphaltene from from waxy crude. *Fuel* 70.11:1293-1297.

Galtsev, E. V., Ametov, I. M. and Grinberg, I. O. 1995. Asphaltene association in crude oil as Studied by ENDOR. *Fuel* 74: 670-673.

Ganguly, J. 2001. Thermodynamic modelling of solid solutions. *EMU Notes in Mineralogy* 3.3: 37-69.

Gharagheizi, F., Mehrpooya, M. and Vatani, A. 2006. Modification of sako-wu parusnitz equation for fluids phase equilibria in polyethylene- ethylene system at high pressures. *Brazilian Journal of Chemical Engineering* 23.3: 383-394.

Gmachowski, L. and Paczuski, 2015. Modelling asphaltene aggregates structure and deposition; colloids and surfaces. *A Physicochemical and Engineering Aspect* 484: 402 - 407.

Gonzalez, G. and Louvisse, A.M.T. 1991. The Absorption of asphaltene and its effect on oil production. *Society of Petroleum Engineers.* Retrieved Jun. 4, 2019, from http://www.onepetro.org

Goual, L. and Firoozabadi, A. 2002. Measuring asphaltenes and resins and dipole moment in petroleum fluids. *American Institute of Chemical Engineers Journal* 48:2646-2663.

Griffith, M.G. and Siegmund, C.W. 1985. Controlling compatibility of residual fuel oils. *Marine Fuels* 227-247.

Groenzin, H., and Mullins, O.C. 2000. Molecular size and structure of asphaltene from various sources. *Energy Fuels* 14.3: 677.

Gross, J. and Sadowski, G. 2002. Application of the perturbed- chain saft equation of state to associating systems. *Industrial and Engineering Chemical. Research* 4:5510-5515.

Guerrier, Y., Pontes, K.V., Costa, G.M.N., Embirucu, M., 2012. A survey of equation of state for polymers. *Polymerization.* Ed. A. D. Gomes. Intech Open. Retrieved Jun. 4, 2019, from http://www.semanticscholar.org/paper/A-survey-of-Equations-of-State-for-polymers-Gurrieri-Pontes/7d3304047242827a6f69bcb4ede90c39c0654eb. 357-391.

Guggenheim, E.A. 1937. Theoretical basis of Raoult Law. *Transactions of the Faraday Society* 33: 151-159.

Gupta, A.K., 1986. Model for asphaltene flocculation using an equation of state. *Thesis. Chemical and Petroleum Enginnering, Engineering. University of Calgary.*

Hammami, A., Phelps, C.H., Monger-Mc Clure, T. and Little, T.M. 2000. Asphaltene precipitation from live crude oils; an experimental investigation of onset conditions and reversibility. *Energy Fuels* 14.1: 14-18.

Hasanvand, M. Z., Ahmadi, M. A. and Behbahani, R. M. 2015. Solving asphaltene precipitation issue in vertical wells via redesigning of production facilities. *Petroleum* 1. 2: 139-145.

Hirschberg, A., DeJong, L.N.J., Schipper, B.A. and Meijers, J.G. 1984. Influence of temperature and pressure on asphaltene flocculation. *Society of Petroleum Engineers* 24.5: 283-293.

Ho, B. and Briggs, D.E. 1982. Small Angle X-ray Scattering from coal derived liquids. *Colloids Surfaces* 4.3: 271-284.

Huang, S.H., Radosz, M. 1990. Equation of states for small, large polydisperse and associating molecules. *Industrial and Engineering Chemical Research* 29: 2284-2294.

Isehunwa, O.S. and Falade, G.K. 2007. Improved characterisation of heptane-plus fractions of light crudes. *Society Petroleum Engineers*. Retrieved Jun. 4, 2019, from http://www.onepetro.org/conference-paper/SPE-111918-MS.

Jamaluddin, A. K. M., Joshi, N., Iwere, F., and Gurpina, O. 2002. An investigation of asphaltene instability under nitrogen injection. *Society of Petroleum Engineers.* Retrieved Jun. 4, 2019, from http://www.onepetro.org/conference-paper/SPE-74393-MS.

Janier, J.B., Razali, R.B., Afza, S. and Samir, B.B. 2013. Mathematical modelling of sphaltene precipitation, a review. *International Journal of Chemical, Materials Science and Engineering* 7:184-187.

Kabir, C.S. and Jamaluddin, A.K.M. 2002. Asphaltene characterisation and mitigation in South Kuwait's Marrat Reservoir. *Society of Petroleum Engineers Production and Facilities* 17.4:251-258.

Katz, D.L. and Beu, K. E. 1945. Nature of asphaltic substance. *Industrial and Engineering Chemistry* 37: 195-203.

Kawanaka, S., Park, S. J. and Mansoori, G. A. 1991. Organic deposition from reservoir fluids: a thermodynamic predictive technique. *Society of Petroleum Engineering Reservoir Engineering* 6.2: 185-192.

Kilpatrick, K.P., Speicker, M. P. and Gawrys, K.L., 2003. The Role of asphaltene solubility and chemical composition on asphaltene aggregation. *Petroleum Science and Technology* 2.3:461-489.

Klein, G.C., Rodgers, P.R. and Marshall, A.G., 2006. Identification of hydrotreatment resistant heteroatomic species in a crude oil distillation cut by Electrospray Ionization FT-ICR Mass Spectrometry. Fuel 85: 14-15.

Kokal, S. L., Najman, J., Sayegh, S. G. and George, A. E. 1992. Measurement and correlation of asphaltene precipitation from heavy oils by gas injection. *Journal. of Canadian Petroleum Technology* 31.4:1-8.

Kokal, S.L. and Sayegh, S.G. 1995. Asphaltenes the cholesterol of petroleum. *Society of Petroleum Engineers*. Retrieved Jun. 4, 2019, from http://www.onepetro.org/conference-paper/SPE-29787-MS.

Kontogeorgis, G. 2005. Intermolecular forces and hydrogen bonding. Notes. Chemical Engineering, Engineering Technical University of Denmark.

_____, Folas, G. K. 2010. Thermodynamic models for industrial applications: from classical and advanced mixing rules to association theories. West Sussex: John Wiley& Sons. 41-47.

_____, Voutsas, C. M., Yakoumis, V. I. and Tassios, D. P. 1996. An Equation of State for Associating Fluids. *Industrial and Engineering Chemistry* 35.11: 4310-4318.

_____, Arya, A., Liang, X. and von Solms, N. 2016. Modelling of asphaltene onset precipitation conditions with Cubic Plus Association (CPA) and Perturbed Chain Statistical Associating Fluid Theory (PC SAFT) equation of state. *Energy and Fuels* 30.8:6835-6852.

_____, Harismiadis, V.I., Fredeslund, A. and Tassios, D.P. 1994.   Application of the Van der waals equation of states to polymers I: Correlation. *Fluid Phase Equilib* 96: 65- 92.

Koots, J.A. and Speight, J.G. 1975. Relation of petroleum resin to asphaltene. *Fuel*   54.3: 179-184.

Lalit, S. and Achala, D. 2012. Environmentally acceptable emulsion system: an   effective approach for removal of asphaltene deposits. *Society of Petroleum Engineers.* Retrieved Jun. 4, 2019, from http://www.onepetro.org/conference-paper/SPE-160877-MS

Lawal, K.A., Crawshaw, J.P., Boek, E.S. and Vesovic, V. 2012. Experimental   investigation of asphaltene deposition in capillary flow. *Energy and Fuels 26:*   1245-2153.

Leon, A.Y., Guzman, A., Laverde, D., Chaudhari, R., Subramaniam, B. and Bravo Suarez, J.J. 2017. Thermal cracking and catalytic hydrocracking of a Colombian vacuum residue and its maltenes and asphaltenes fractions in toluene. *Energy Fuels* 31.4: 3868-3877.

Leon, O., Rogel, E., Espidel, J. and Torres, G. 2000.Asphaltenes: Structural characterisation, self-association and stability behavior. *Energy and Fuels* 14.1:6-10.

Leontaritis K. 1998. Asphaltene near- wellbore formation damage modelling. *Society of Petroleum   Engineers.*   Retrieved   Jun.   4,   2019,   from http://www.onepetro.org/conference-paper/SPE-39446-MS.

Leontaritis, K.J. and Mansoori, G.A. 1989. Fast crude- oil heavy component characterisation using combination of ASTM, HPLC and GPC Method.   *Journal   of Petroleum Science and Engineering* 2:1-12.

Lian, H., Lin, J.R. and Mansoori, A.G. 1994. Peptization studies of asphaltene andsolubility parameters spectra. *Fuel* 73.3:423-428.

Lin, C.S., Moulton, R.W. and Putnam, G. L. 1953. Mass transfer between solid wall   and fluid streams. *Industrial and Engineering Chemistry* 45.3: 636-646.

Lira-Galeana, C., Buenrostro-Gonzalez, E., Gill-Villegas, A. and Wu, J., 2004.   Asphaltene precipitation in crude oils: theory and experiments. *American   Institute of chemical Engineers Journal* 50.10: 2552-2570.

Loh, W., Mohammed, R.S., and Ramos, A.C. 1999. Aggregation of asphaltene   obtained from Brazilian crude oil in aromatic solvents. *Petroleum Science and   Technology* 17:147-163

Long, R.B. 1981. The concept of asphaltene. *Chemistry of Asphaltenes.* Eds. J.W.Bunger and N.C. Li *Washington DC: ACS.* 17-27

Luo, P. and Gu, Y. 2005. Effect of asphaltene content and solvent concentration on heavy oil viscosity. *Society of Petroleum Engineers.* Retrieved Jun. 4, 2019, from http://www.onepetro.org/conference-paper/SPE-97778-MS.

_____. 2007. Effects of asphaltene content on the heavy oil viscosity at different temperature. *Fuel* 86.7: 1069-1078.

Maini, B.B., Sarma, H.K., George, A.E. 1993. Significance of foamy- oil behaviour in primary production of heavy oils. *Journal of Canadian Petroleum   Technology* 32:9: 1-6.

Mansoori, G.A. 1997. Modelling of asphaltenes and other heavy organic depositions. *Petroleum Science and Engineering* 17.1-2: 101-111.

_____. 1998. Asphaltene deposition: an economic challenge in heavy petroleum crude utilization and processing. *OPEC Review* 12.1:103-113.

_____. 2018. Arterial blocakge in the petroleum and natural gas industries-heavy organics (Asphaltene/Bitumen, Resins, Organometallics, Paraffin, wax, Diamondoids, etc.) Depositions from Petroleum Fluids Retrieved on Jan. 25, 2018 from http://www.uic.edu/~mansoori/HOD.html.

_____, Canahan, N.F., Starling, K.E., and Leland, T.W. 1971. Equilibrum thermodynamic properties of the mixture of hard spheres. *Journal of Chemical Physics* 54.4: 1523.

Marcano, F., Ranaudo, A.M., Chirinos, J., Daridon, J.L. and Carrier, H. 2013. Study of asphaltene aggregation in toluene/n-haptane/co2 mixtures under high pressure conditions. *Energy& Fuels* 27.8: 4598-4603.

Margues, C.C.L., Pereira, J.O. Bueno, A.D., Margues, S.V., Lucas, E.F. Mansur, C.R.E, Machado, A.L.C. and Gonzalez, G. 2012. Astudy of asphaltene resin interactions. *Journal of Brazilian Chemical Society* 23.10:1880-1888.

Maruska, H.P. and Rao, B.M.L. 1987. The Role of polar species in the aggregation of asphaltene. *Fuel Science and Technology International* 5.2: 119-168.

Mclean, J. D. and Kilpatrick, P. K. 1997. Effects of Asphaltene aggregation in model heptane toluene mixture on stability of oil- in- water emulsion. *Journal of Colloidal and Interface Science* 196: 23-34.

Mehta, A.P. and Sloan, E.D. 1996. Structure H. Hydrates: Implication for the petroleum industry. *Society of Petroleum Engineers.* Retrieved Jun. 4, 2019, from http://www.onepetro.org/conference-paper/SPE-36742-MS.

Memon, A., Qassim, B., Al-Ajmi, M., Tharanivasan, A.K., Gao, J., et. al. 2012. Miscible gas injection and asphaltene flow assurance fluid characterisation: a laboratory case study for black oil reservoir. *Society of Petroleum Engineers.* Retrieved Jun. 3, 2019, from http://www.onepetro.org/conference-paper/SPE-150938-MS.

Merino-Garcia, D. 2004. Calorimetric investigation of asphaltene self association and interaction with resins. Thesis. *Chemical Engineering, Engineering. Technical Univsersity of Denmark.*

Minssieux, L. 1997. Core damage from crude asphaltene deposition. Retrieved Jun. 3, 2019, from http://www.onepetro.org/conference-paper/SPE-37250-MS

Mirzayi, B., Mousavi- Dehghani, S.A. and Chakan M. 2013. Modelling of asphaltene deposition in pipelines. *Journal of Petroleum Science and Technology* 3.2: 15-23.

Mirzayi, B., Mousavi- Dehghani, S.A. and Sohbi, G.A. 2012. Prediction of solvent effect on asphaltene precipitation at reservoir conditions. *Journal of Petroleum Science and Engineering* 2.2: 17-24.

Mirzayi, B., Vafaie-Sefti, M., Mousavi- Dehghani, S.A. Fasih, M. and Mansoori, G. A. 2008. Effects of asphaltene deposition on unconsolidated porous media properties during miscible natural gas flooding. *Petroleum Science and Technology* 26: 231-243

Mohammadi, A.H., and Richon, D. 2008. The Scott-Maggat Polymer Theory for determining onset of precipitation of dissolved asphaltene in solvent + precipitant solution. *Open Thermodynamic Journal* 2: 82-88

Mohammed, R.S., Loh, W. and Ramos, A.C. 1999. Aggregation Behaviour of Two Asphalenic Fractions in Aromatic Solvents. *Energy and Fuels* 13.2: 323-327

Monger, T.G. and Fu, J.C. 1987. The nature of CO_2 Induced organic deposition. *Society of Petroleum Engineers.* Retrieved Jun. 3, 2019, from http://www.onepetro.org/conference-paper/SPE-16713-MS

Monger, T.G. and Trujillo, D.E. 1991. Organic deposition during CO_2 and rich gas flooding. *Society of Petroleum Engineering Reservoir. Engineering* 6.1: 17-24.

Moschopedis, S.E. and Speight, J.G. 1976. Oxygen functions in asphaltenes. *Fuel* 55.4:334-336

Mousavi- Dehghani S. A., Riazi, M., Vafaie- Sefti, M. and Mansoori, G.A. 2004. An analysis of method for determination of onsets of asphaltene phase separation. *Journal of Petroleum Science and Engineering* 42:145-156.

Mukhametzyanov, I. Z. and Kuzeev, I.R. 1991. Fractal structure of paramagnetic aggregates of petroleum pitches. *Colloid. Journal of USSR* 53.4: 644-648.

Mullins, O.C. 2010. The modified Yen model. *Energy and Fuels* 24.4 2179 2207

Nabzer, L. and Aguilera, M. E. 2008. The colloidal approach: a promising route for asphaltene deposition modelling. *Oil and Gas Technology- Review. IFP* 63.1: 21-35.

Nalwaya, V., Tangtayakom, V., Piumsomboon, P. and Fogler, S. 1999. Studies on asphaltenes through analysis of polar fractions. *Industrial and Engineeering Chemistry Research* 38.3:964-972.

Nazmul, N. H. G., Tadeusz, D. and Masliyah, J. H. 2005. Fractal structure of asphaltene aggregates. *Journal of Colloid and Interface Science* 285.2: 599-608.

Nellensteyn, F. J. 1924. The constitution of asphalt. *Journal of the Institute of Petroleum Technology* 10, 311.

Neumann, H.J. 1965. Investigations regarding the separation of crude oil emulsions. *Petrochemie* 18:776.

Newberry, M. E., and Baker, K. M. 1985. Formation damage prevention through the control of paraffin and asphaltene deposition. *Society of Petroleum Engineers*. Retrieved Jun. 3, 2019 from http://www.onepetro.org/conference-paper/SPE-13796-MS.

Nghiem, L.X., Hassam, N.S., Nutakki, R. and George, A.E.D. 1993. Efficient modelling of aspahltene precipitation. *Society of Petroleum Engineers.*Retrieved Jun. 3, 2019 from http://www.onepetro.org/conference-paper/SPE-26642-MS.

Nomura, M., Artok, L., Murata, S., Yammoto, A., Hama, H., Gao, H.and Kidena, K. 1998. Structural evaluation of zao zhuang coal. *Energy Fuels* 12.3:512-523

Nomura, M., Murata, S., Kidena, K., Ookawa, T. and Komoda, O. 2003. Consideration on the density evaluation of the model of heavy hydrocarbon by computer simulation. *Fuel Chemical Division* 48.1: 47.

Okafor, H.E., Ismail, M.S. and Rasidah, M.P. 2014. Organic deposit remediation using environmentally benign solvent: A review. *ARPN. Journal of Engineering and Applied Science* 9.10:1930-1935

Pan, H. and Faroozabadi, A. 2004. Thermodynamic micellization model for asphlatene precipitation inhibition. *AIChE Journal* 46.2:416-426.

_____. 2000. Thermodynamic micellization model for asphlatene precipitation from reservoir crudes at high pressure and temperature. SPE. Production. and Facilities 15.1: 58-65.

Panuganti, S.R. 2013. Asphaltene behaviour in crude oil system. Thesis. *Chemical Engineering, Enginnering. Rice University.*

Park, S.J. and Masoori, G.A. 1998. Aggregation and deposition of heavy organics in petroleum crudes. *Journal of Energy Sources.* 10.2: 109-125.

Pfeiffer, J. Ph. and Saal, R. N. J. 1940. Asphaltic bitumen as colloid system. *The Journal of Physical Chemistry* 44.2: 139-149.

Pineda-Flores, G., Mesta-Howard, A.M. 2001. petroleum asphaltene: generated problematic and possible biodegradation mechanism. *Revista, Latino americana Microbiologia* 43.3: 143-150.

Porte, G., Zhou, H. and Lazzeri, V. 2003. Reversible description of asphaltene colloidal association and precipitation. *Langmuir* 19: 40-47.

Wu, J., Prausnitz, J.M., Firoozabadi, A. 1998. Molecular thermodynamics framework from waxy crude. *American Institute of Chemical Engineers Journal* 44.5: 1188-1199.

Prausnitz, J.M., Lichtenthaler, R.N. and Gomes de Azevedo, E. 1999. Molecular thermodynamics of fluid- phase equilibria. 3rd Ed. *Prentice Hall International Series. N.J: Prentice Hall PTR.*

Priyanto, S., Mansoori, G.A and Suwono, A. 2001. Measurement of property relationships of nano- structure micelles and coacervates of asphaltene in pure solvent. *Chemical Engineering Science* 56: 6933-6939.

Ramirez-Jaramillo, E., Manero-Brito, O and Lira, G.C.. 2006. Modelling of asphaltene deposition in production pipelines. *Energy and Fuels* 20.3: 1184 1196.

Ramos, A.C., Haraguchi, L., Nostripe, F.R., Loh, W. and Mohammed, R.S. 2001. Interface and colloidal behaviour of asphaltene obtained from Brazilian crude oils. *Journal of Petroleum Science and Engineering* 32:201-216.

Rayes, B.H., Pernyeszi, T., and Lakatos, I. 2003. Comparative study of asphaltene adsorption on formation rock under static and dynamic conditions. *Society of Petrolem Engineers.* Retrieved Jun. 3, 2019, from http://www.onepetro.org/conference-paper/SPE-80265-MS

Redlich, O. and Kister, A.T. 1948. Thermodynamics of non-electrolyte solutions, x-y-t relation in a binary system. *Industrial and Engineering Chemistry* 40.2: 341-345.

Rogacheva, O.V., Rimaev, R.V., Gubaidullin, V.Z. and Khazimov, D.K. 1980. Investigation of the surface activity of the asphaltenes of petroleum residues. *Colloid Journal USSR* 42:586-589.

Roux, J.N. Brosetta, D. and Demi, B. 2001. SANS Study of Asphaltene aggregation concentration and solvent quality effects. *Langmuir* 17, 5085-5092.

Sachanen, A.N. 1945. The chemical constituents of petroleum. *New.York. Reinhold Pub.Corp.*

Sako, T., Wu, A.H. and Prausnitz, J.M. 1989. A cubic equation of state for the high pressure phase equilibria of mixtures containing polymers and volatile fluids. *Journal of Applied Polymer Science* 38: 1839-1858.

Sane, R. C., Tsotsis, T. T., Webster, I. A. and Ravi-Kumar, V. S. 1994. Studies of asphaltene diffusion: implications for asphaltene structure and optimal upgrading of reactor design. *Development in Petroleum Science 4.* Eds. T. F. Yen and G. V. Chilingarian. Chapter 15: 365-380.

Sardrine, P. and Jean-Francois, A. 2005. Influence of pH on stability and dynamic properties of asphaltenes and other amphiphilic molecules at the oil-water interface. *Energy fuels* 19.4:1337-1341.

Scott, R.L. and Magat, M. 1945. The thermodynamics of high pressure solutions: the free energy of mixing of solvents and polymers of heterogeneous distribution. *Journal of Chemical Physics.* 13: 172 177.

Shah, V .M. 1992. Development of a generalised quartic equation of state for pure fluids. Thesis. Chemical Engineering, Engineering. University of Tennessee.

Shedid, S.A. and Zekri, A. 2004. Formation damage due to simultaneous sulphur and asphaltene deposition. Publication No. SPE-86553-PA. Retrieved May. 30, 2019, from http://www.onepetro.org/journal-paper/SPE-86553-PA.

Sheu, E. Y., De Tar, M. M. Storm, D. A. and De Canio, S.J. 1992a. Aggregation and kinetics of asphaltenes in organic solvents. *Fuel* 71.3:299-302.

Sheu, E.Y., Storm, D.A. and De Tar, M. M. 1991. Asphaltene in polar solvents *Journal of .Non Crystal Solids* 131.133: 341-347.

_____. 1992. Self-association, structure, interaction and dynamics of ratawi asphaltenes in solvents. Retrieved Jun. 5, 2019, from https://www.researchgate.net/publications/267994272.

Speight, J. G. 1994. Chemical and physical studies of petroleum asphaltenes in asphaltenes and asphalts, *Developments in Petroleum Science*. Amsterdam: Elsevier Sciences.

_____.1999. The chemistry and technology of petroleum. 3rd ed. New York: Marcel Dekker.

_____.2014. The chemistry and technology of petroleum. *5th ed. CRC Press*.

Spiecker, P.M., Gawrys, K.L. and Kilpatrick, P.K. 2003. Aggregation and solubility behaviour of asphaltenes and their subfractions. *Journal of Colloid and Interfaction* 267: 178-193.

Srivastava, R.K. and Huang, S.S. 1999. Asphaltene deposition during CO_2 Flooding. *Society of Petroleum Engineers, Production and Facilities.*14.4: 235-246.

Stephenson W.K. 1990. Producing asphaltenic crude oil: problems and solutions. *Petroleum Engineering International* 24-91.

Storm, D.A. and Sheu, E.Y. 1995. Characterisation of asphaltenic colloidal particle in heavy oil. *Fuel* 74.8:1140-1145

Strausz, O.P., Mojelsky, T.W. and Lown, E.M. 1992. The molecular structure of asphaltene: an unfolding story. *Fuel* 71. 12:1355-1363.

Taylor, S.E. 1992. Use of surface tension measurement to evaluate aggregation of sphaltene in organic solvents. *Fuel* 71:1338-1339.

Thomas, F.B., Bennion, D.B., Bennion, D.W. and Hunter, B.E. Experimental and theoretical studies of solid precipitation from reservoir fluid. *Journal of Canadian Petroleum Technology* 31.1: 1-11.

Ting, P. D. 2003. Thermodynamic stability and phase behaviour of asphaltene in oil and otherhigher asymmetric mixtures. Thesis, Department of Chemical   Engineering, Engineering   University of Texas.

Tissot, B.P., and Welste, D.H. 1984. Petroleum formation and occurrence. *2nd ed. Berlin: Springer-Verlaf.*

Torcal- Garcia, V. 2004. Asphaltene phase stability after hydrocarbon and heat treatment of heavy feedstocks. *Thesis.* Chemical   Engineering, Engineering   Technical University of Denmark.

Vafaie-Sefti, M., Mousavi-Dehghani, A. S., and Mohammed-Zadeh, M. 2003. A simple model for asphaltene deposition in petroleum mixtures. *Fluid Phase Equlibria* 206.1-2:1-11.

Vasquez, D. and Mansoori, G.A. 2000. Identification and measurement of petroleum precipitates.   *Journal of Petroleum Science and Engineering.* 26.1: 49-55.

Verdier, S. 2006. Experimental study and modelling of asphaltene precipitation caused by gasinjection. Thesis. Chemical Engineering, Engineering. Technical University of Denmark.

Victorov, A. I., and Firoozabadi, A. 1996. Thermodynamic micellization model for asphaltene precipitation from petroleum fluids. *American Institute of Chemical Engineers Journal* 42. 6: 1753-1764.

Waarden, M. V.D. 1958. Stability of emulsion of water in mineral oils containing asphaltenes. *Kolloid. Z.Z. Polymers* 156.2: 116-122.

Wang, J.X. and Buckley, J.S. 2001. A two-component model of the onset of asphaltene flocculation in crude oils. *Energy and Fuels* 15.5: 1004 1012.

_____ and Creek, J.L. 2004. Asphaltene deposition inmetallic surfaces. *Dispersion Science and Technology* 25: 287-298.

Wattana, P, Wojciechouski, D. J., Bolanos, G. and Fogler, H. S. 2007. Study of asphaltene precipitation, using refractive index measurement, petroleum. *Science and Technology* 21. 3-4. 591-613.

Weast, R.C. 1987. CRC handbook of chemistry and physics. 6th ed. Boca Raton: CRC Press.

Wenzel, H. and Schmidt, G. 1980. A modified Van der Waals equation of state for the representation of phase equilibria between solids liquids and gases. *Fluid Phase Equilibria* 5:13-17.

Wertheim, M.S. 1983. Fluids with highly directional attractive forces. I. Statistical Thermodynamics. *Journal of Statistical Physics* 35.1-2: 19-34.

_____. 1984. Fluids with highly directional attractive forces II. Thermodynamic perturbation theory and integral equations. *Journal of Statistical Physics*

35.1-2:35-74.

_____. 1986a. Fluids with directional attractive forces III. multiple attraction site. *Journal of Statistical Physics* 42.3-4: 459-476.

_____. 1986b. Fluids with directional attractive forces IV. Equilibrium polymerization. *Journal. Statistical. Physics* 42.3-4: 477-492.

Wu, J. and Prausnitz, J. M., Firoozabadi, A. 2000. Molecular thermodynamics of asphaltene precipitation in reservoir fluids. *American Institute of Chemical Engineers Journal* 46.1: 197-209.

Xu, Y, Koga, Y., Strausz, O.P. 1994. Characterisation of Athabasca Asphaltene by small angle X-ray scattering. *Fuel* 74.7: 960-964.

Yarranton, H.W., Hussein, H., and Meliyah, J.H. 2000. Water in hydrocarbon emulsions stabilization by asphaltene at low concentrations. *Journal of Colloids and Interface Science* 228.1:52-63.

Yen, T.F. 1972. Present status of the structure of petroleum heavy ends and its significance Preprints- American Chemical Society F., Reprint 17.14:102-114.

Zuo, P. and Shen, W. 2017. Identification of nitrogen-polyaromatic compounds in asphaltene from co-processing of coal and petroleum residue using chromatography with mass spectrometry. *International Journal of Coal Science and Technology* 4.3: 2095-8293.

APPENDIX I: COMPOSITION OF CRUDE OIL ABURA 9L

(Source: Nigeria Petroleum Development Company)

Component	MW g/mol	Separator Liquid Mol %	Mol Fraction	Separator Gas Mol %	Mol Fraction	Reservoir Fluid Mol %	Mol Fraction
N_2	28.04	0.02	0.0002	0.38	0.0038	0.21	0.0021
CO_2	44.01	0.07	0.0007	0.64	0.0064	0.37	0.0037
C_1	16.04	4.93	0.0493	75.81	0.7581	42.28	0.4228
C_2	30.07	3.3	0.0330	10.66	0.1066	7.18	0.0718
C_3	44.10	8.41	0.0841	7.92	0.0792	8.15	0.0815
iC_4	58.12	4.63	0.0463	1.80	0.0180	3.14	0.0314
nC_4	58.12	6.58	0.0658	1.68	0.0168	4.00	0.04
iC_5	72.15	4.81	0.0481	0.48	0.0048	2.53	0.0253
nC_5	72.15	3.79	0.0379	0.28	0.0028	1.94	0.0194
C_6	86.18	6.43	0.0643	0.18	0.00180	3.14	0.0314
C_7	100.20	9.45	0.0945	0.17	0.00170	4.56	0.0456
C_8	114.23	11.41	0.1141	0	0	5.4	0.054
C_9	128.26	6.51	0.0651	0	0	3.08	0.0308
C_{10}	142.29	5.2	0.0520	0	0	2.46	0.0246
C_{11}	156.31	3.78	0.0378	0	0	1.79	0.0179
C_{12}	170.34	3.01	0.0301	0	0	1.42	0.0142
C_{13}	184.37	2.76	0.0276	0	0	1.3	0.013
C_{14}	198.39	2.3	0.0230	0	0	1.09	0.0109
C_{15}	212.42	2.29	0.0229	0	0	1.08	0.0108
C_{16}	226.45	1.59	0.0159	0	0	0.75	0.0075
C_{17}	240.47	1.89	0.0189	0	0	0.89	0.0089
C_{18}	254.53	0.91	0.0091	0	0	0.43	0.0043
C_{19}	268.53	0.97	0.0097	0	0	0.46	0.0046
C_{20+}	346.1	4.96	0.0496	0	0	2.35	0.0235

APPENDIX II: COMPOSITIONAL DATA FOR CRUDE OIL B (Source: Pedersen and Christensen 2007)

Component	Mole%
N_2	0.03
CO_2	0.2
C_1	41.83
C_2	3.51
C_3	5.4
iC_4	1.84
nC_4	3.36
iC_5	1.69
nC_5	1.65
C_6	2.24
C7+	38.25

APPENDIX III: Oil Composition of Crude B after Characterisation and Lumping.

Component	MW	Mole Fraction
N2	28.04	0.0003
CO2	44.01	0.002
C1	16.04	0.4183
C2	30.07	0.0351
C3	44.1	0.0540
Heavy Gas	68.30	0.1078
C7-C11	124.0	0.24113
C12-C20	210.5	0.1404

APPENDIX IV: Composition of Crude Oil C (Source: Pedersen and Christensen 2007)

Component	Mole Fraction	Molecular weight
N2	0.0012	28.014
CO2	0.0249	44.01
C1	0.7643	16.04
C2	0.0746	30.07
C3	0.0312	44.09
iC4	0.0059	58.12
nC4	0.0121	58.12
iC5	0.005	72.15
nC5	0.0059	72.15
C6	0.0079	86.20
C7	0.0059	95
C8	0.0108	106
C9	0.0078	116
C10	0.0059	133
C11	0.0047	152
C12	0.0035	164
C13	0.0038	179
C14	0.0044	193
C15	0.0024	209
C16	0.0021	218
C17	0.0022	239
C18	0.00169	250
C19	0.0014	264
C20	0.001	275
C21	0.000888	291
C22	0.00078	305
C23	0.000686	318
C24	0.000603	331
C25	0.00053	345
C26	0.000465	359
C27	0.000469	374
C28	0.00359	388
C29	0.000316	402
C30	0.000277	416
C31	0.000244	430
C32	0.000214	444
C33	0.000188	458
C34	0.000165	472
C35	0.000128	486
C36	0.000128	500
C37	0.000112	514
C38	0.0000986	528
C39	0.0000866	542

APPENDIX IV (Contd)

Component	Mole Fraction	Molecular weight
N2	0.0012	28.014
CO2	0.0249	44.01
C1	0.7643	16.04
C2	0.0746	30.07
C3	0.0312	44.09
iC4	0.0059	58.12
nC4	0.0121	58.12
iC5	0.005	72.15
nC5	0.0059	72.15
C6	0.0079	86.20
C7	0.0059	95
C8	0.0108	106
C9	0.0078	116
C10	0.0059	133
C11	0.0047	152
C12	0.0035	164
C13	0.0038	179
C14	0.0044	193
C15	0.0024	209
C16	0.0021	218
C17	0.0022	239
C18	0.00169	250
C19	0.0014	264
C20	0.001	275
C21	0.000888	291
C22	0.00078	305
C23	0.000686	318
C24	0.000603	331
C25	0.00053	345
C26	0.000465	359
C27	0.000469	374
C28	0.00359	388
C29	0.000316	402
C30	0.000277	416
C31	0.000244	430
C32	0.000214	444
C33	0.000188	458
C34	0.000165	472
C35	0.000128	486
C36	0.000128	500
C37	0.000112	514
C38	0.0000986	528
C39	0.0000866	542

APPENDIX V: COMPOSITION OF CRUDE OIL C AFTER LUMPING

Component	Mole Fraction	Molecular Weight
N2	0.0012	28.01
CO2	0.0249	44.01
C1	0.7643	16.043
C2	0.0746	30.07
C3	0.0312	44.10
Heavy Gas	0.0362	68.30
C7-C11	0.0351	117.05
C12-C18	0.01989	119.78
C19-C80	0.00978	360.72

APPENDIX VI: SUMMARY OF UPPER ASPHALTENE PRECIPITATION ENVELOPE (UAOP) FOR FLUIDS AT DIFFERENT INJECTION SCENARIOS

Fluid	UAOP kN/m^2			
	Study	PC SAFT	EXPERIMENTAL	C PA
F 1 at 0 wt% Natural Gas	30812.93	39999.19	39787.98	
F 1 at 15 wt% Natural Gas	38369.75	50596.24	30357.74	
F 1 at 30wt % Natural Gas	84947.83	62501.08	103551.3	
F 2 at 0wt% CO2 Injection	52674.81	34967.25	49953.22	
F 2 at 10 wt% CO2	65919.68	79925.16	-	80000
F2 at 20 wt% CO2	67913.93	75729	-	82922.35
F2 at 5wt% Nitrogen gas	38783.64	41851.31	37231.81	-
F3 at 0 wt% Natural Gas	117094.58	62052.83	48952.90	-
F4 at 0 wt% Natural Gas	63326.02	55158.09	41368.56	-
F5 at 10 wt% CO2 Gas	19788.77	16400.1	16000.44	-
F5 at 20 wt% CO2 gas	49051.43	54799.82	35999.90	

APPENDIX VII: The Flow Chart of the Nonlinear optimization using the generalised reduced gradient method